2023 Fall

"Phase Transformation *in* Materials"

11.13.2023

Eun Soo Park

Office: 33-313
Telephone: 880-7221
Email: espark@snu.ac.kr
Office hours: by an appointment

Solidification of Pure Metal : Thermal gradient dominant

⇕

Solidification of single phase alloy: Solute redistribution dominant

a) Constitutional supercooling

Planar → Cellular growth → cellular dendritic growth → Free dendritic growth

응고계면에 조성적 과냉의 thin zone 형성에 의함
Dome 형태 선단 / 주변에 hexagonal array

T↓ → 조성적 과냉영역 증가
Cell 선단의 피라미드형상/ 가지들의 square array/ Dendrite 성장방향쪽으로 성장방향 변화

성장하는 crystal로 부터 발생한 잠열을 과냉각 액상쪽으로 방출함에 의해 형성
Dendrite 성장 방향/ Branched rod-type dendrite

→ "Nucleation of new crystal in liquid"

성장이 일어나는 interface 보다 높은 온도

b) Segregation

: normal segregation, grain boundary segregation, cellular segregation, dendritic segregation, inversegregation, coring and intercrystalline segregation, gravity segregation

* Constitutional Supercooling

No Diffusion on Solid, Diffusional Mixing in the Liquid ➡ Steady State

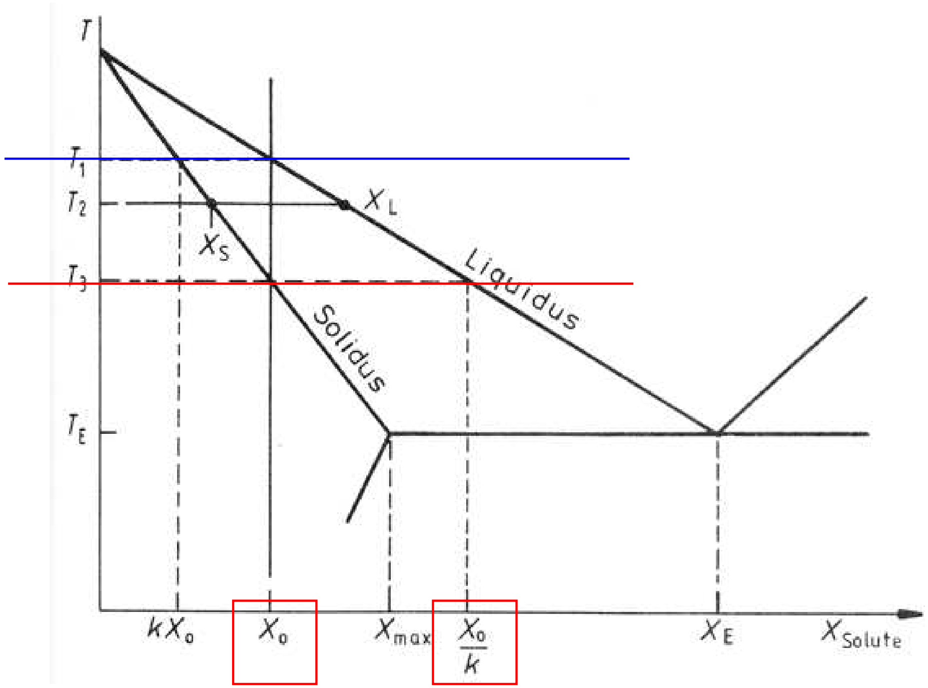

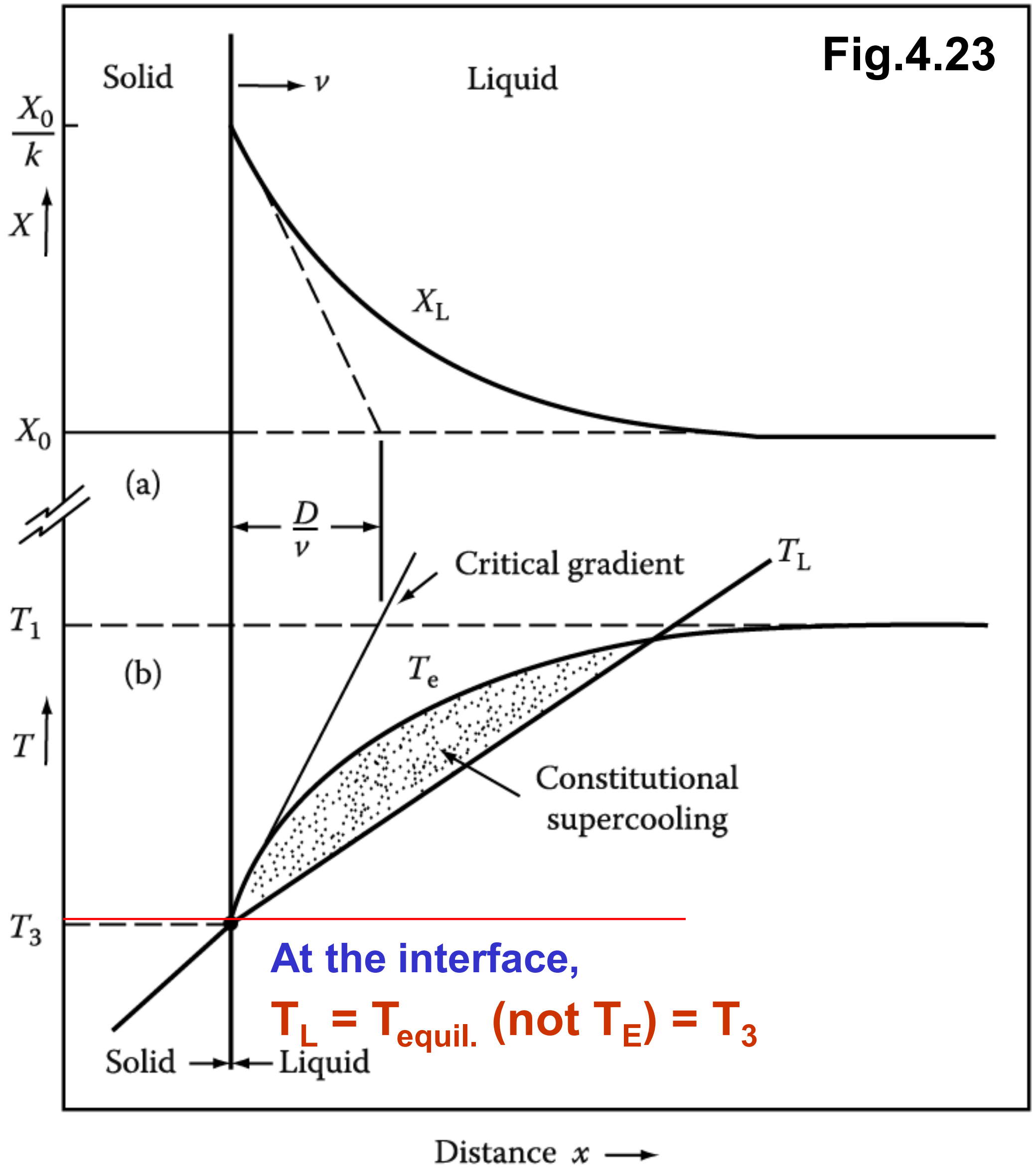

*** Actual temperature gradient in Liquid**

T_L'

*** equilibrium solidification temp. change**

$T_{equil.}$

$T_L' > (T_1-T_3)/(D/v)$: the protrusion melts back ➡ **Planar interface: stable**

$T_L'/v < (T_1-T_3)/D$: Constitutional supercooling → **cellular/ dendritic growth**

Contents for today's class

Solidification: Liquid → Solid

- **Pure Metals** < Nucleation >
  &
  < Growth >
  - Equilibrium Shape and Interface Structure on an Atomic Scale
  - Growth of a pure solid
  - Heat Flow and Interface Stability

4.3 Alloy solidification

- Solidification of single-phase alloys
- **Eutectic solidification**
- **Off-eutectic alloys**
- **Peritectic solidification**

Q: Thermodynamics and Kinetics of eutectic solidification ($L \rightarrow \alpha + \beta$) ?

This section will only be concerned with normal structures, and deal mainly with lamellar morphologies.

2. Eutectic Solidification (Thermodynamics)

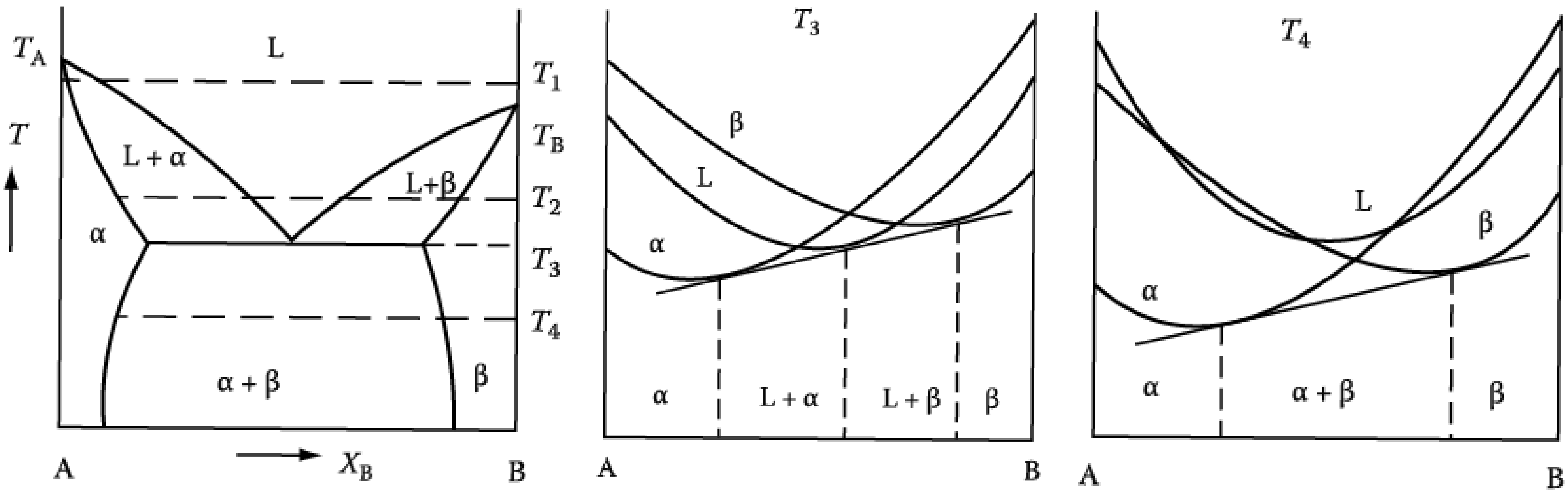

Plot the diagram of Gibbs free energy vs. composition at T_3 and T_4.

What is the driving force for the eutectic reaction ($L \rightarrow \alpha + \beta$) at T_4 at C_{eut}?

What is the driving force for nucleation of α and β? " ΔT "

Eutectic Solidification (Kinetics)

: ΔT→ formation of interface + solute redistribution

If α is nucleated from liquid and starts to grow, what would be the composition at the interface of α/L determined?

→ rough interface (diffusion interface) & local equilibrium

How about at β/L? Nature's choice? Lamellar structure

$$\rightarrow \quad G = G_{bulk} + G_{interface} = G_0 + \gamma A$$

$$\sum A_i \gamma_i + \Delta G_S = minimum$$

Interface energy + Misfit strain energy

Fig. 4.31

interlamellar spacing →

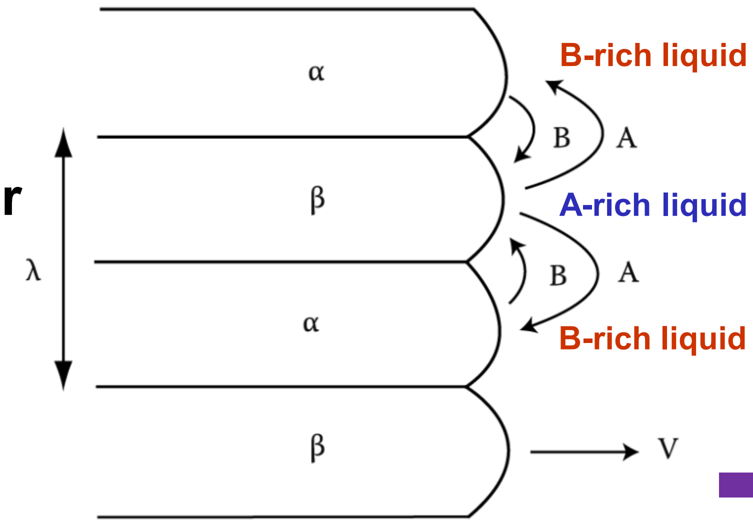

Eutectic solidification

: diffusion controlled process

1) λ ↓ → eutectic growth rate ↑

but 2) λ ↓ → α/β interfacial E, $\gamma_{\alpha\beta}$↑

→ lower limit of λ

➡ fastest growth rate at a certain λ

What would be a role of the curvature at the tip?

→ Gibbs-Thomson Effect

Eutectic Solidification (Kinetics)

: ΔT→ a) formation of interface + b) solute redistribution

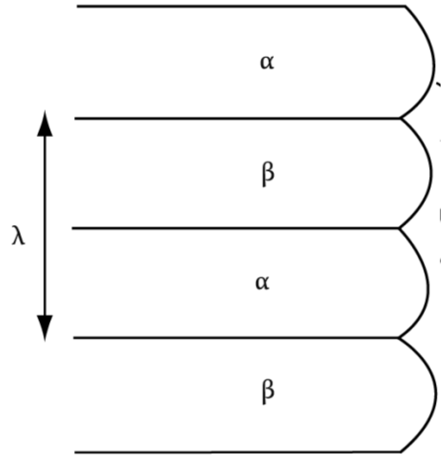

How many α/β interfaces per unit length? $\rightarrow 1/\lambda \times 2$

a) Formation of interface: **ΔG**

For an interlamellar spacing, λ, there is a total of (2/ λ) m² of α/β interface per m³ of eutectic.

$$\Delta G = \Delta \mu \cong \frac{L \Delta T}{T_m}$$

$$\rightarrow \Delta G = \Delta \mu = \frac{2\gamma}{\lambda} \times V_m$$

Molar volume

Driving force for nucleation = Total interfacial E of eutectic phase

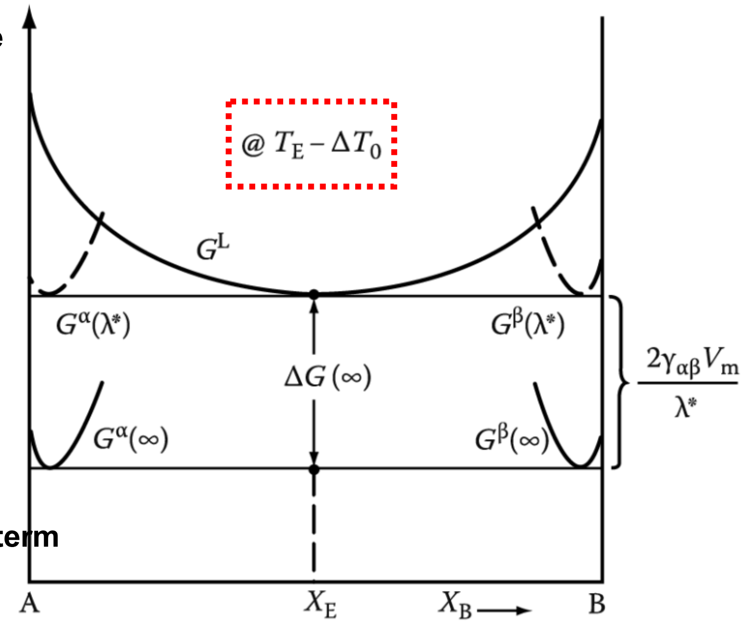

For very large values of λ, interfacial E~ 0

Total undercooling

$$\lambda \rightarrow \infty, \quad \Delta G(\infty) = \Delta \mu = \frac{\Delta H \, \Delta T_0}{T_E}$$

No interface (ideal case)

$$\Delta G(\lambda) = ? = -\Delta G(\infty) + \frac{2\gamma V_m}{\lambda}$$

Interfacial E term

With interface (real case)

Solidification will take place if ΔG is negative (-).

a) All **ΔT→ use for interface formation=** min. **λ**

What would be the minimum λ?

Critical spacing, $\lambda^* : \Delta G(\lambda^*) = 0$

최소 층상 간격

$$\Delta G(\infty) = \frac{2\gamma V_m}{\lambda^*}$$

$$\lambda^* = + \frac{2 T_E \gamma V_m}{\Delta H \, \Delta T_0}$$

$$\lambda^* = -\frac{2T_E\gamma V_m}{\Delta H \Delta T_0} \rightarrow \textit{identical to critical radius of dendrite tip in pure metal}$$

Gibbs-Thomson effect

$$cf)\ r^* = \frac{2\gamma_{SL}}{\Delta G_V} = \left(\frac{2\gamma_{SL}T_m}{L_V}\right)\frac{1}{\Delta T}$$

L_v : *latent heat per unit volume*

$L = \Delta H = H^L - H^S$

* Growth Mechanism: Gibbs-Thomson effect in a ΔG-composition diagram?

1) At λ=λ* (<∞),

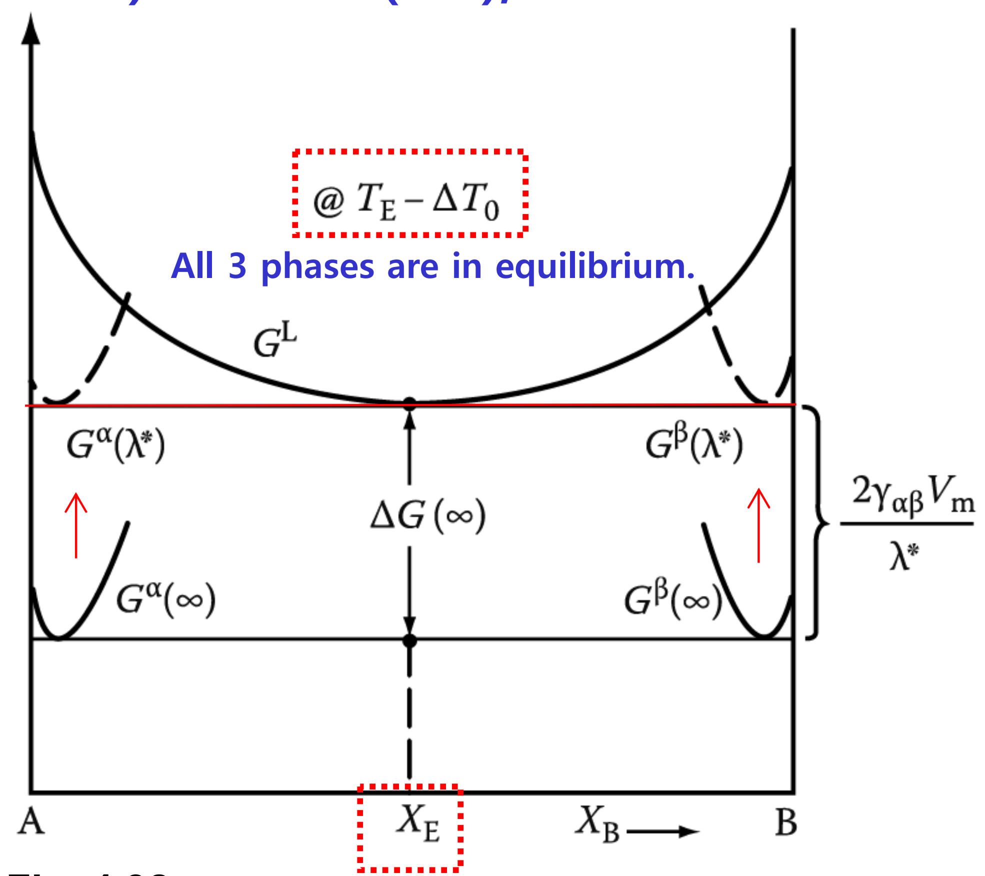

Fig. 4.32

The cause of G increase is the curvature of the α/L and β/L interfaces arising from the need to balance the interfacial tensions at the α/ β/L triple point, therefore the increase will be different for the two phases, but for simple cases it can be shown to be $\frac{2\gamma_{\alpha\beta}V_m}{\lambda}$ for both.

1) If λ=λ*, growth rate will be *infinitely slow* because the liquid in contact with both phases has the same composition, X_E in Figure 4.32.

2) At λ= (∞>) λ (>λ*),

If ∞> λ > λ*, G_α and G_β are correspondingly reduced because less free energy is locked in the interfaces. → $X_B^{L/\alpha} > X_B^{L/\beta}$

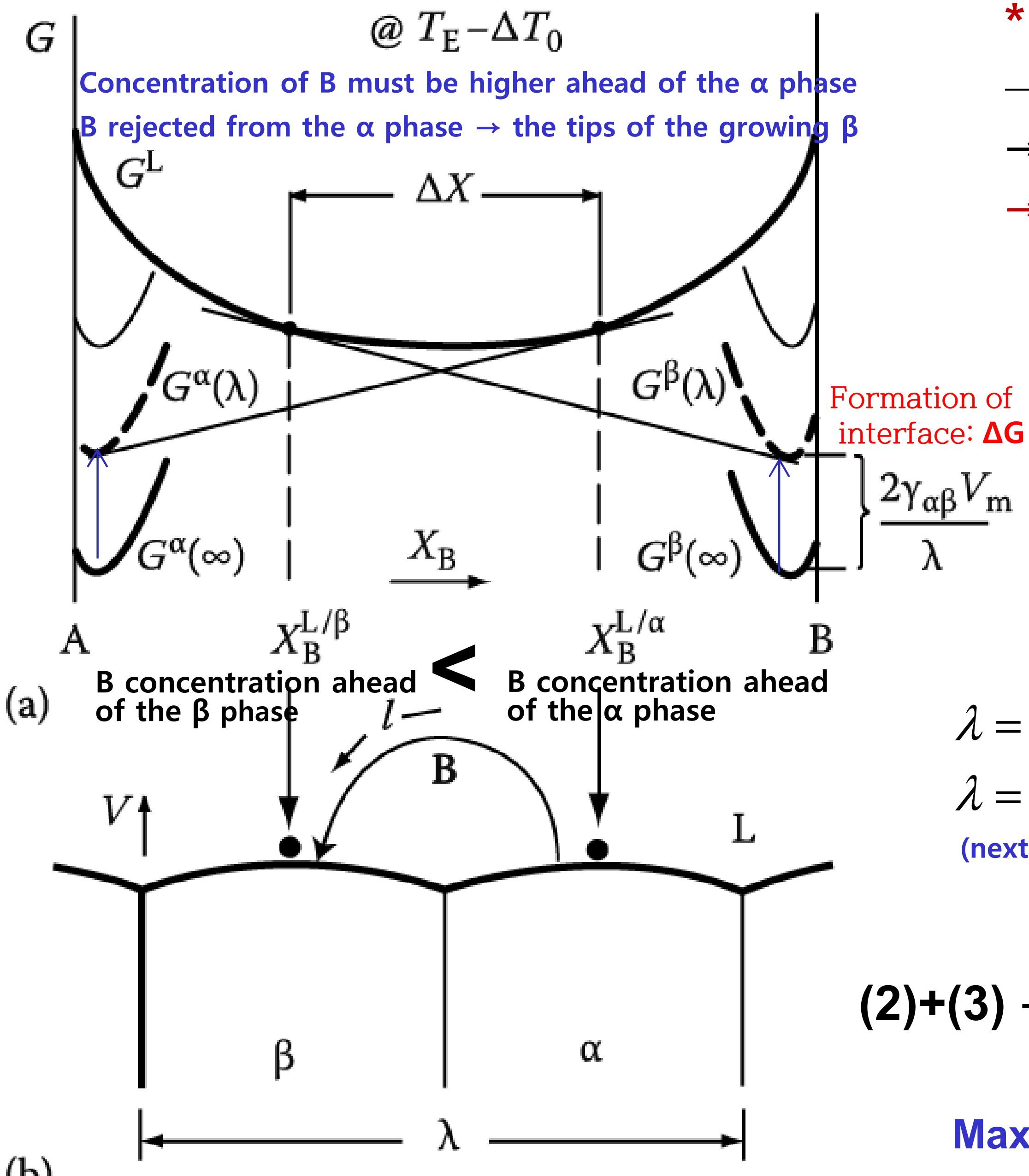

* Eutectic growth rate, v

→ if α/L and β/L interfaces are highly mobile

→ proportional to flux of solute through liquid

→ <u>diffusion controlled process</u>

$$v \propto D\frac{dC}{dl} \propto (X_B^{L/\alpha} - X_B^{L/\beta})$$

∝ 1/effective diffusion distance.. 1/λ

$$v = k_1 D \frac{\Delta X}{\lambda} \quad (1)$$

$\lambda = \lambda^*, \Delta X = 0$

$\lambda = \infty, \Delta X = \Delta X_0$

(next page)

$$\Delta X = \Delta X_0 (1 - \frac{\lambda^*}{\lambda}) \quad (2)$$

$$\Delta X_0 \propto \Delta T_0 \quad (3)$$

(2)+(3) → (1) $$v = k_2 D \frac{\Delta T_0}{\lambda}(1 - \frac{\lambda^*}{\lambda})$$

Maximum growth rate at a fixed ΔT_0 → $\lambda = 2\lambda^*$

Fig. 4.33 (a) Molar free energy diagram at (T_E - ΔT_0) for the case λ* < λ < ∞, showing the composition difference available to drive diffusion through the liquid (ΔX). (b) Model used to calculate the growth rate.

ΔX will it self depend on λ. ~ maximum value, ΔX_0

$$\lambda = \lambda^*, \Delta X = 0$$

$$\lambda = \infty, \Delta X = \Delta X_0$$

$$\Delta X = \Delta X_0 \left(1 - \frac{\lambda^*}{\lambda}\right)$$

If undercooling is small,

$$\Delta X_0 \propto \Delta T_0$$

* **Total Undercooling**

$$\Delta T_0 = \Delta T_r + \Delta T_D$$

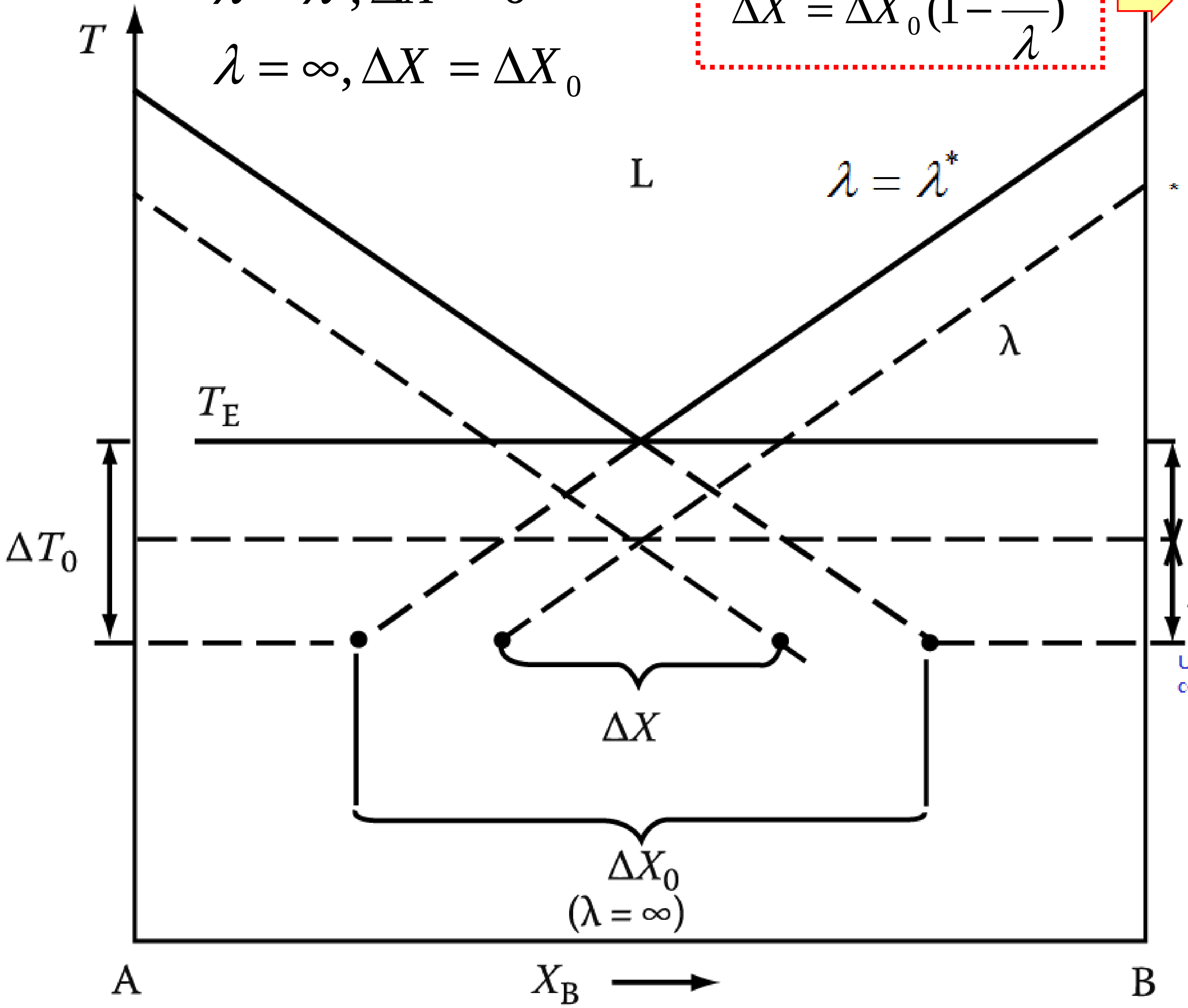

Undercooling required to overcome the interfacial curvature effects

ΔT_r Undercooling for curvature, r

ΔT_D Undercooling for Diffusion

Undercooling required to give a sufficient composition difference to drive the diffusion

Fig. 4.34 Eutectic phase diagram showing the relationship between ΔX and ΔX_0 (exaggerated for clarity)

2) At $\lambda = (\infty >)\ \lambda\ (> \lambda^*)$,

If $\infty > \lambda > \lambda^*$, G_α and G_β are correspondingly reduced because less free energy is locked in the interfaces. → $X_B^{L/\alpha} > X_B^{L/\beta}$

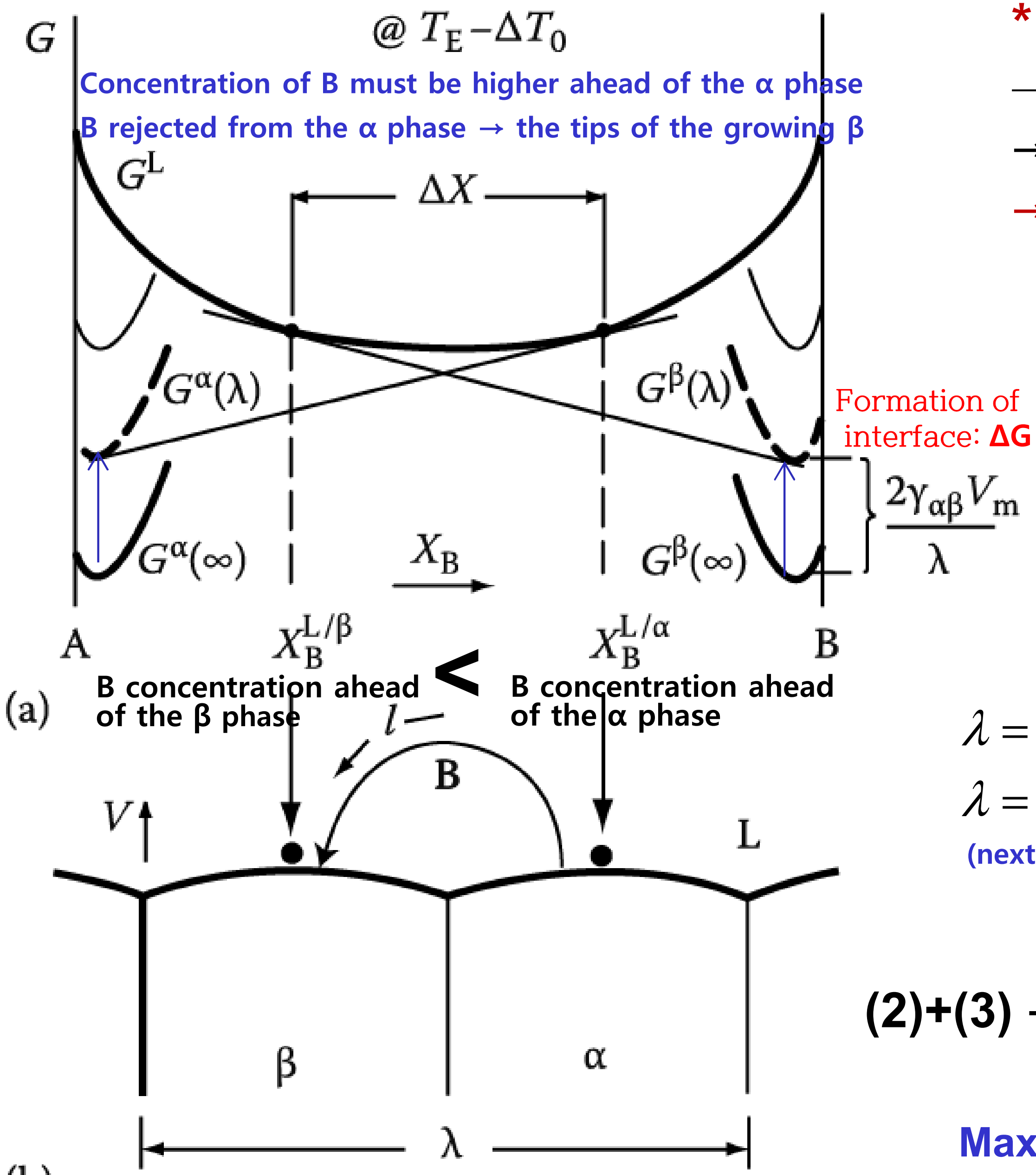

* Eutectic growth rate, v

→ if α/L and β/L interfaces are highly mobile

→ proportional to flux of solute through liquid

→ <u>diffusion controlled process</u>

$$v \propto D\frac{dC}{dl} \propto (X_B^{L/\alpha} - X_B^{L/\beta})$$

$\propto$ 1/effective diffusion distance.. 1/λ

$$v = k_1 D\frac{\Delta X}{\lambda} \quad (1)$$

$\lambda = \lambda^*, \Delta X = 0$

$\lambda = \infty, \Delta X = \Delta X_0$

(next page)

$$\Delta X = \Delta X_0\left(1 - \frac{\lambda^*}{\lambda}\right) \quad (2)$$

$$\Delta X_0 \propto \Delta T_0 \quad (3)$$

(2)+(3) → (1)

$$v = k_2 D\frac{\Delta T_0}{\lambda}\left(1 - \frac{\lambda^*}{\lambda}\right)$$

Maximum growth rate at a fixed ΔT_0 → $\lambda = 2\lambda^*$

Fig. 4.33 (a) Molar free energy diagram at $(T_E - \Delta T_0)$ for the case $\lambda^* < \lambda < \infty$, showing the composition difference available to drive diffusion through the liquid (ΔX). (b) Model used to calculate the growth rate.

Closer look at the tip of a growing dendrite

different from a planar interface because heat can be conducted away from the tip in three dimensions.

Assume the solid is isothermal $(T_S' = 0)$

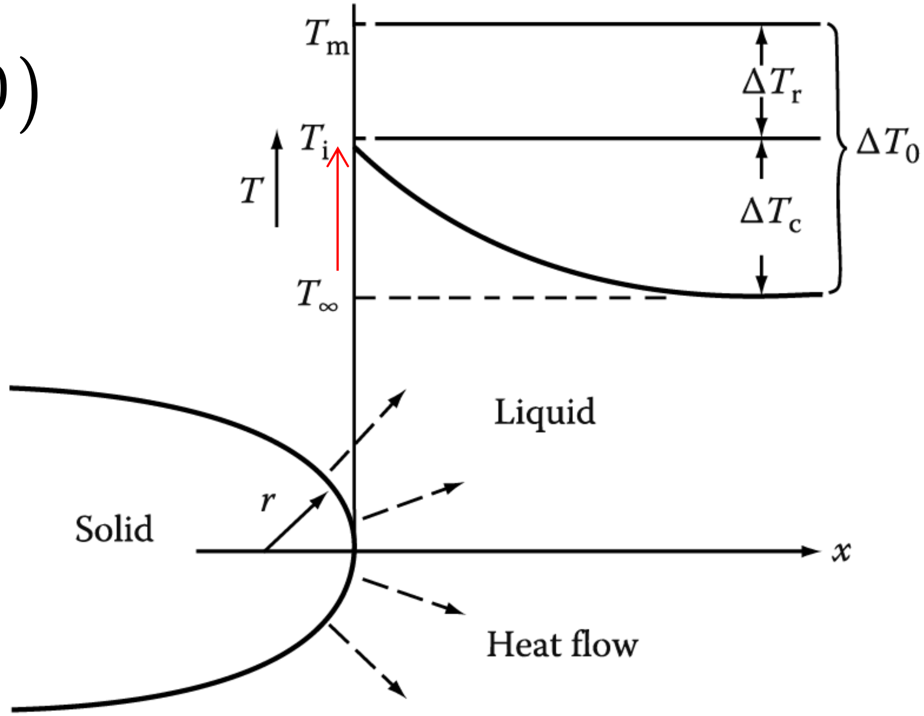

From $$K_S T_S' = K_L T_L' + vL_V$$

$$\text{If } T_S' = 0, \quad v = \frac{-K_L T_L'}{L_V}$$

A solution to the heat-flow equation for a hemispherical tip:

$$T_L'(negative) \cong \frac{\Delta T_C}{r} \qquad \Delta T_C = T_i - T_\infty$$

$$v = \frac{-K_L T_L'}{L_V} \cong \frac{K_L}{L_V} \cdot \frac{\Delta T_C}{r} \qquad v \propto \frac{1}{r}$$

However, ΔT also depends on r. How?

Thermodynamics at the tip?

Gibbs-Thomson effect: melting point depression

$$\Delta G = \frac{L_V}{T_m} \Delta T_r = \frac{2\gamma}{r} \qquad \Delta T_r = \frac{2\gamma T_m}{L_V r}$$

Minimum possible radius (r)?

$$r_{min} : \Delta T_r \rightarrow \Delta T_0 = T_m - T_\infty \rightarrow r^*$$

The crit.nucl.radius

$$r^* = \frac{2\gamma T_m}{L_V \Delta T_o}$$

$$\Delta T_r = \frac{2\gamma T_m}{L_V r}$$

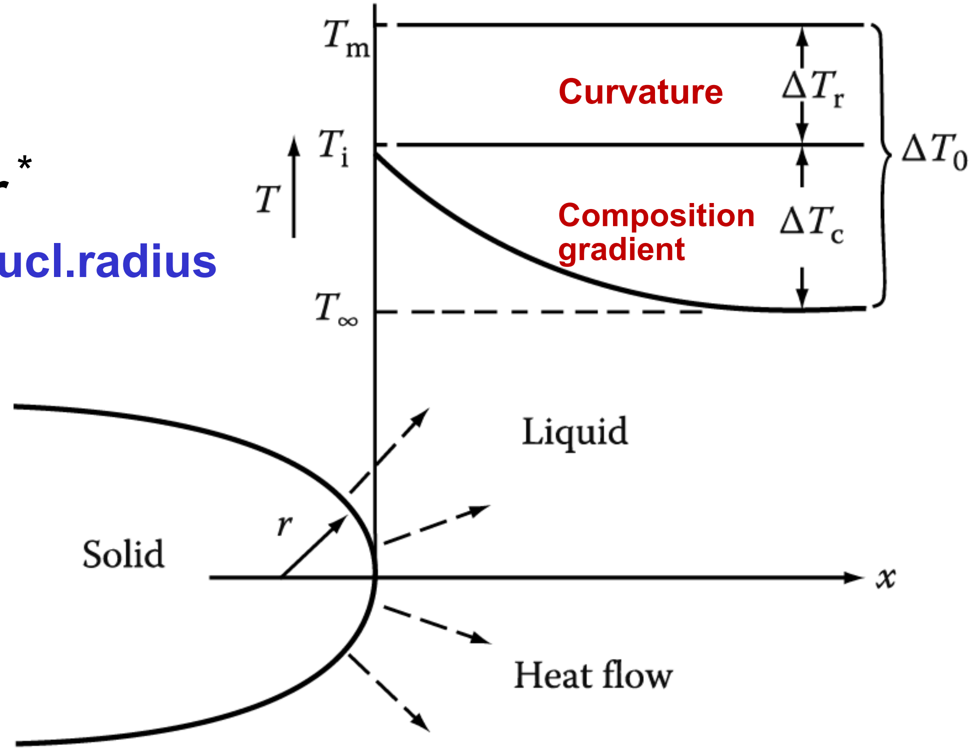

Express ΔT_r by r, r^* and ΔT_o.

$$\Delta T_r = \frac{r^*}{r} \Delta T_o$$

$$v \cong \frac{K_L}{L_V} \cdot \frac{\Delta T_c}{r} = \frac{K_L}{L_V} \cdot \frac{(\Delta T_0 - \Delta T_r)}{r} = \frac{K_L}{L_V} \cdot \frac{\Delta T_0}{r}\left(1 - \frac{r^*}{r}\right)$$

$v \rightarrow 0$ as $r \rightarrow r^*$ due to Gibbs-Thomson effect

as $r \rightarrow \infty$ due to slower heat condution

Maximum velocity? $\rightarrow r = 2r^*$

Undercooling ΔT_0

$$\Delta T_0 = \Delta T_r + \Delta T_D$$

Curvature　Composition gradient

$$\Delta G_{total} = \Delta G_r + \Delta G_D$$

$$v = k_2 D \frac{\Delta T_0}{\lambda}\left(1 - \frac{\lambda^*}{\lambda}\right)$$

$$\Delta G_r = \frac{2\gamma_{\alpha\gamma} V_m}{\lambda}$$

$\rightarrow$ *free energy dissipated in forming α/β interfaces*

$\Delta G_D \rightarrow$ *free energy dissipated in diffusion*

By varying the interface undercooling (ΔT_0) it is possible to vary the growth rate (V) and spacing (λ) independently.

Therefore, it is impossible to predict the spacing that will be observed for a given growth rate. However, controlled growth experiments show that a specific value of λ Is always associated with a given growth rate.

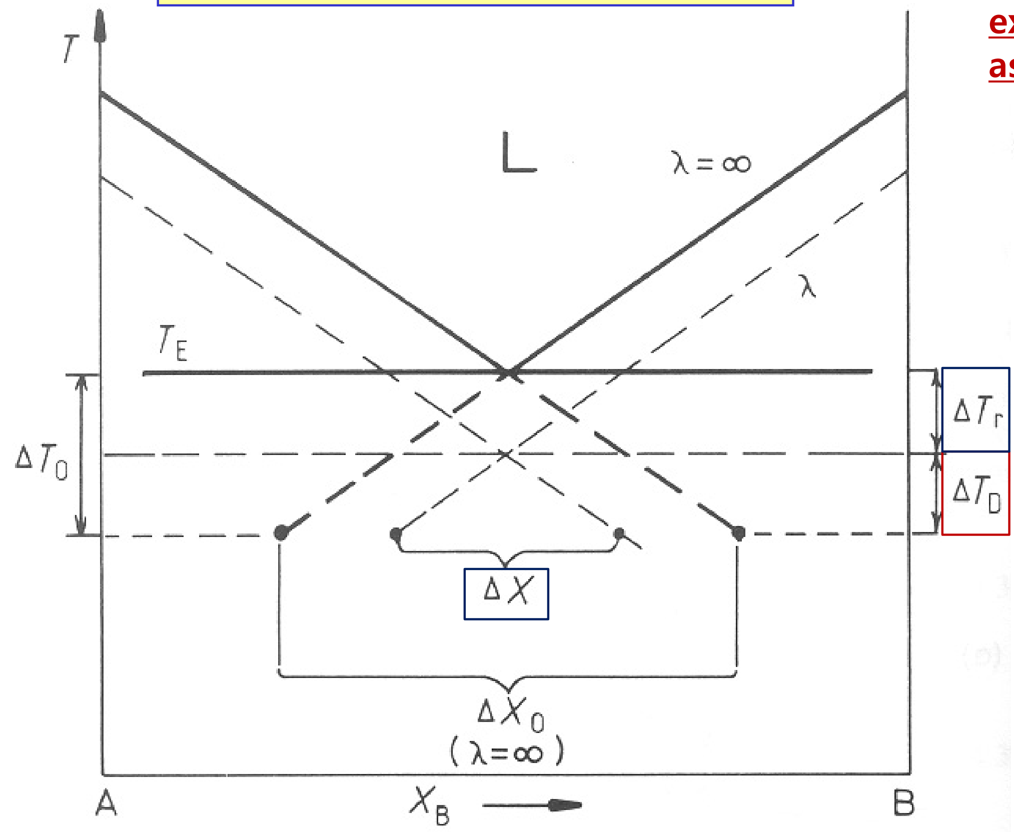

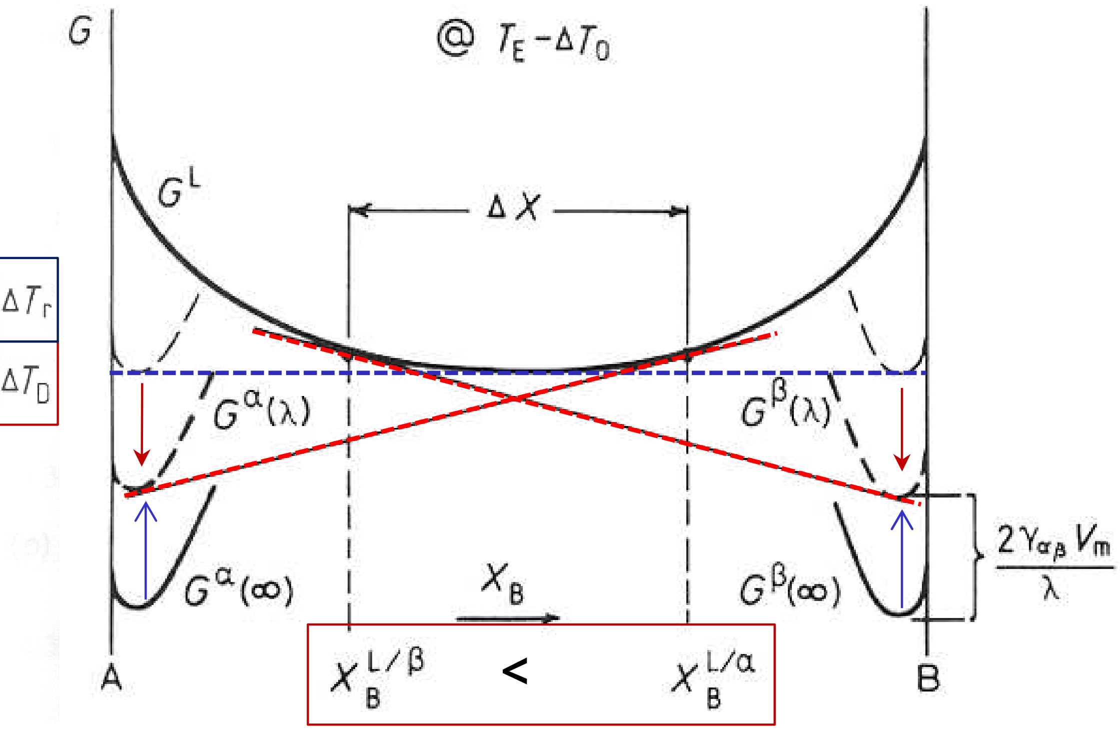

Fig. 4.34 Eutectic phase diagram showing the relationship between ΔX and ΔX_0 (exaggerated for clarity)

Undercooling ΔT_0

$$\Delta T_0 = \Delta T_r + \Delta T_D$$

Curvature | Composition gradient

$$\Delta G_{total} = \Delta G_r + \Delta G_D$$

$$v = k_2 D \frac{\Delta T_0}{\lambda}\left(1 - \frac{\lambda^*}{\lambda}\right)$$

$$\Delta G_r = \frac{2\gamma_{\alpha\gamma} V_m}{\lambda}$$

$\rightarrow$ *free energy dissipated in forming* α/β *interfaces*

$\Delta G_D \rightarrow$ *free energy dissipated in diffusion*

By varying the interface undercooling (ΔT_0) it is possible to vary the growth rate (V) and spacing (λ) independently.

Therefore, it is impossible to predict the spacing that will be observed for a given growth rate. However, controlled growth experiments show that a specific value of λ Is always associated with a given growth rate.

*** For example,**

Maximum growth rate at a fixed ΔT_0 $\rightarrow$ $\lambda_0 = 2\lambda^*$

(4) $$v = k_2 D \frac{\Delta T_0}{\lambda}\left(1 - \frac{\lambda^*}{\lambda}\right) \Rightarrow v_0 = k_2 D \Delta T_0 / 4\lambda^* \quad \textbf{(5)}$$

From Eq. 4.39 $$\lambda^* = +\frac{2T_E \gamma V_m}{\Delta H \Delta T_0} \Rightarrow \Delta T_0 \propto 1/\lambda^* \quad \textbf{(6)}$$

So that the following relationships are predicted:

(5) + (6) $\rightarrow$

$$v_0 \lambda_0^2 = k_3 \ \text{(constant)}$$

$$\frac{v_0}{(\Delta T_0)^2} = k_4$$

Ex) Lamellar eutectic in the Pb-Sn system

k_3~ 33 μm³/s and k_4~ 1 μm/s·K²

$\Rightarrow$ **v = 1 μm/s, λ_0 = 5 μm and ΔT_0 = 1 K**

* Total Undercooling

$$\Delta T_0 = \Delta T_r + \Delta T_D$$

Strictly speaking,

ΔT_i term should be added but, negligible for high mobility interfaces

Driving force for atom migration across the interfaces

ΔT_r: Undercooling required to overcome the interfacial curvature effects

ΔT_D: Undercooling required to give a sufficient composition difference to drive the diffusion

$\Delta T_D \rightarrow$ Vary continuously from the middle of the α to the middle of the β lamellae

$\Delta T_0 = const$ ← Interface is essentially isothermal.

$\Delta T_D \rightarrow \Delta T_r$ The interface curvature will change across the interface.

Should be compensated

* A planar eutectic front is not always stable.

Binary eutectic alloys contains impurities or other alloying elements ➡ "Form a cellular morphology"

analogous to single phase solidification

restrict in a sufficiently high temp. gradient.

➡ The solidification direction changes as the cell walls are approached and the lamellar or rod structure fans out and may even change to an irregular structure.

➡ Impurity elements (here, mainly copper) concentrate at the cell walls.

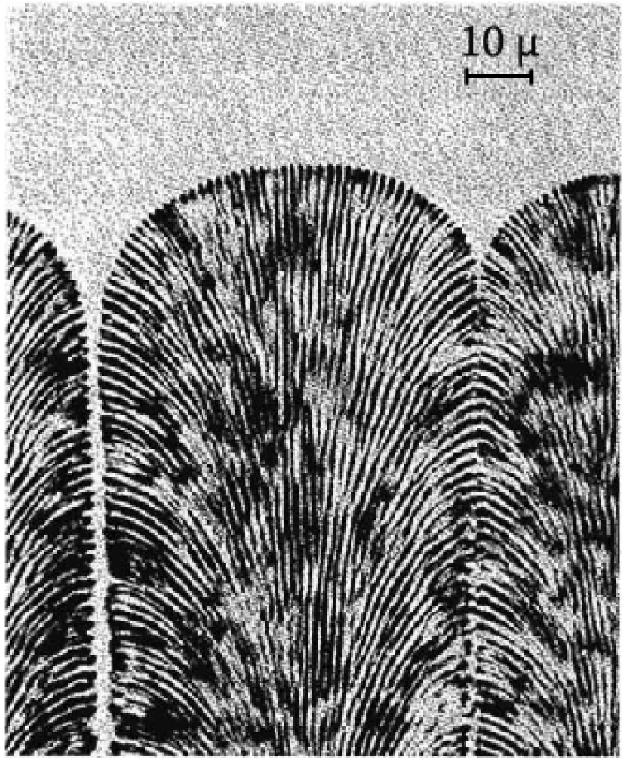

A planar eutectic front is not always stable.

Binary eutectic alloys contains impurities or other alloying elements ➡ "Form a cellular morphology" analogous to single phase solidification restrict in a sufficiently high temp. gradient.

➡ The solidification direction changes as the cell walls are approached and the lamellar or rod structure fans out and may even change to an irregular structure.

➡ Impurity elements (here, mainly copper) concentrate at the cell walls.

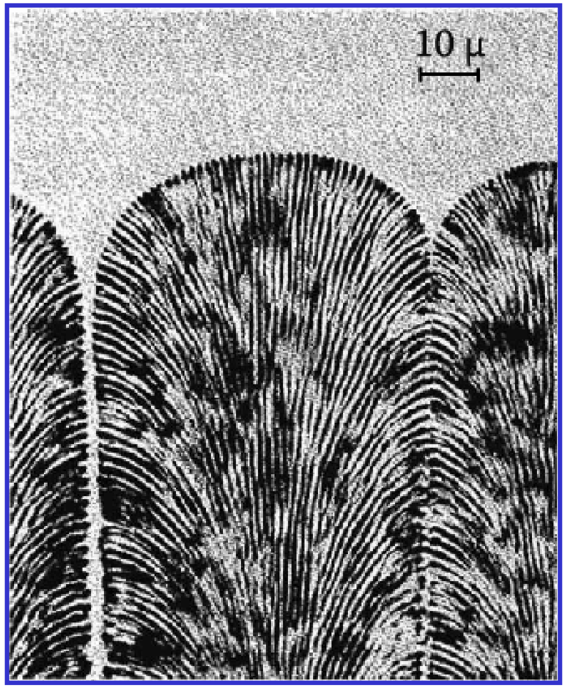

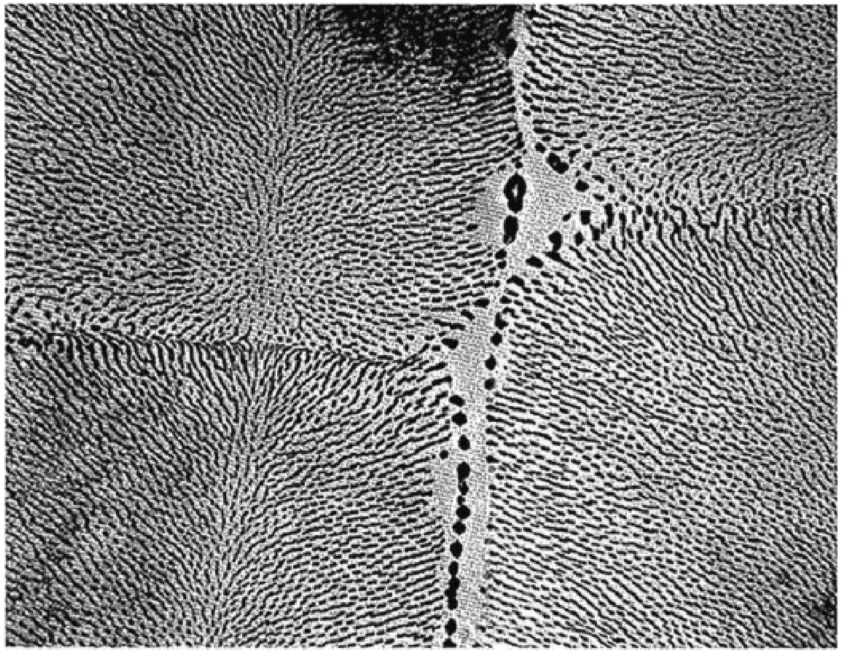

Fig. 4.35 Transverse section through the cellular structure of an Al-Al_6Fe rod eutectic (x3500).

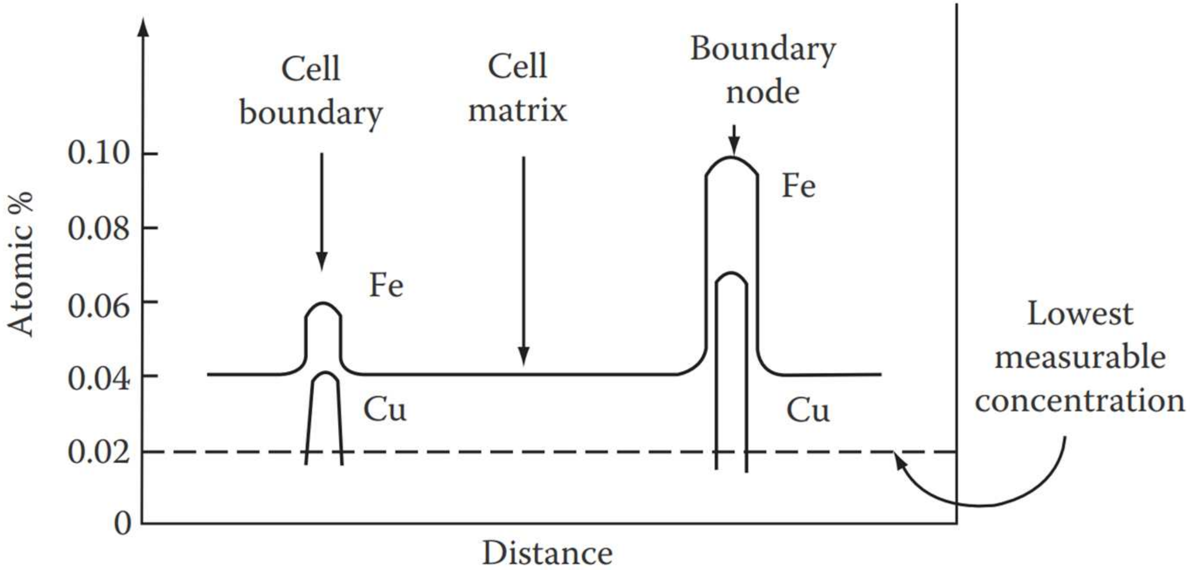

Fig. 4.36 Composition profiles across the cells in Fig. 4.35b.

Q: Off-eutectic Solidification?

4.3.3 Off-eutectic Solidification _Pb-Sn system

(a) Equilibrium solidification

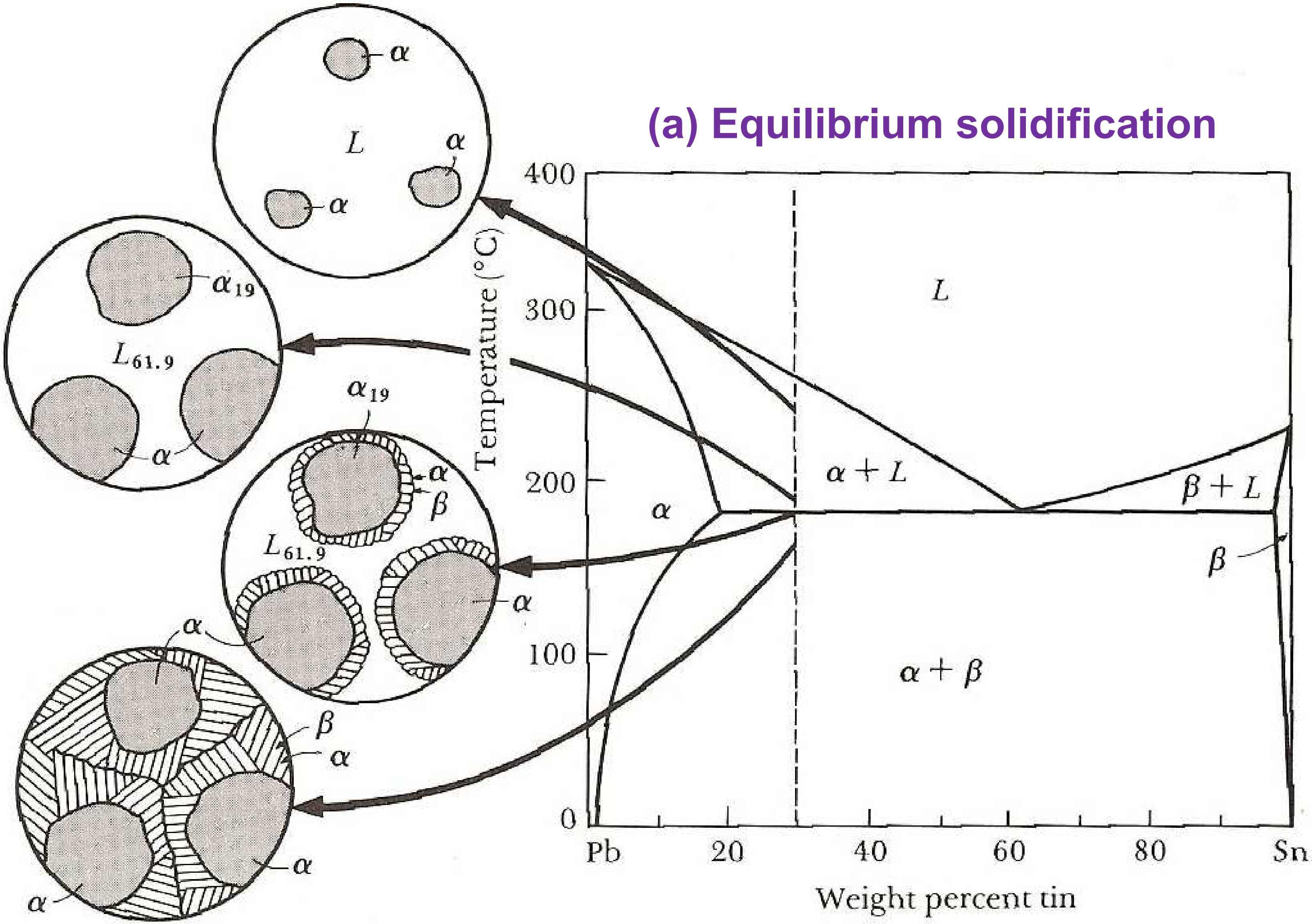

FIGURE 10-12 The solidification and microstructure of a hypoeutectic alloy (Pb-30% Sn).

4.3.3 Off-eutectic Solidification _Pb-Sn system

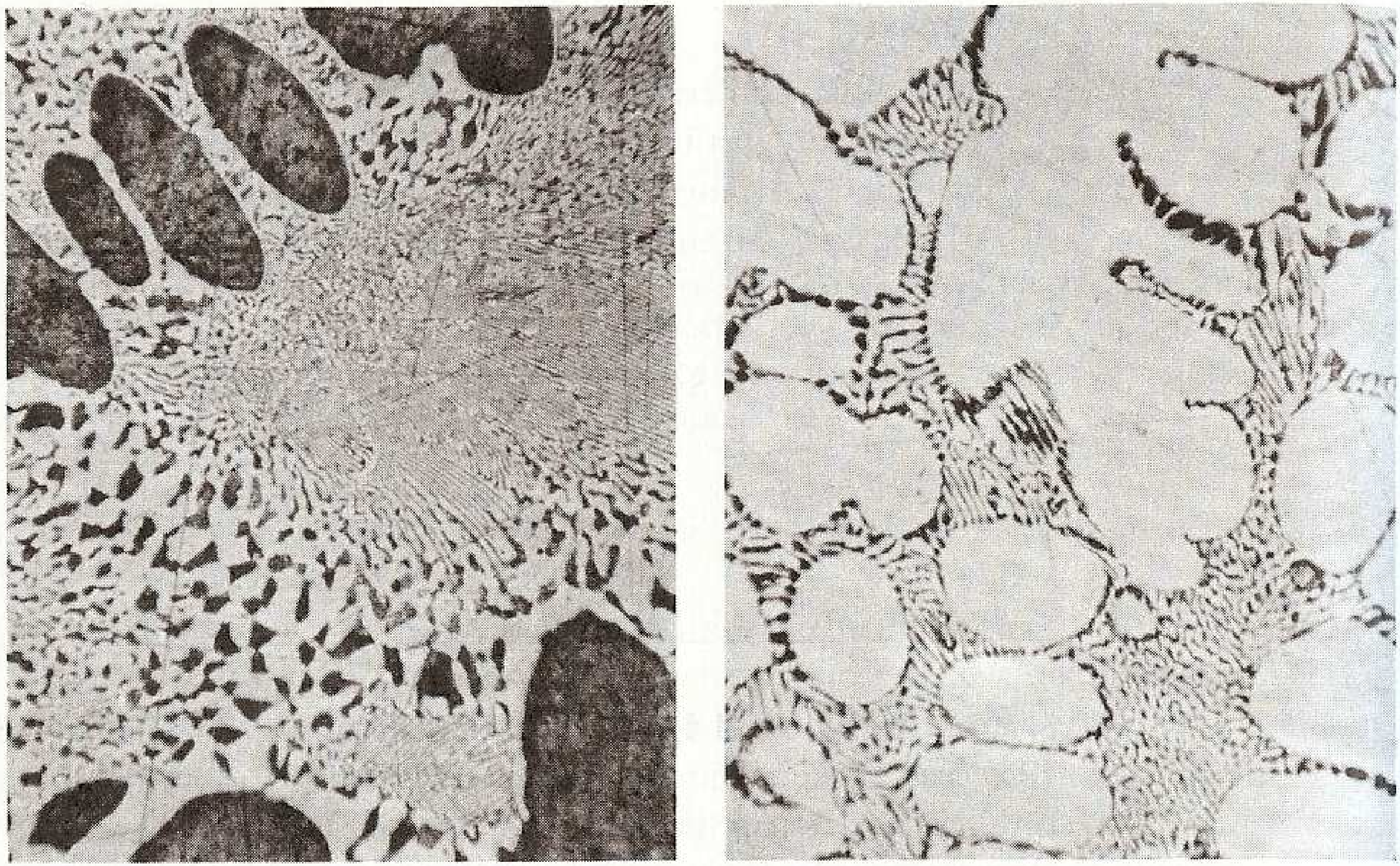

(a) (b)

FIGURE 10-13 (a) A hypoeutectic lead-tin alloy. (b) A hypereutectic lead-tin alloy. The dark constituent is the lead-rich solid α, the light constituent is the tin-rich solid β, and the fine plate structure is the eutectic (× 400).

4.3.3 Off-eutectic Solidification

(b) Non-equilibrium solidification

a. primary α + eutectic lamellar

- **Primary α dendrites form at T_1. Rejected solute increases X_L to X_E; eutectic solidification follows.**
- **Coring: primary α (low solute) at T_1 and the eutectic (high solute) at T_E.**

→ **in-situ composite materials**

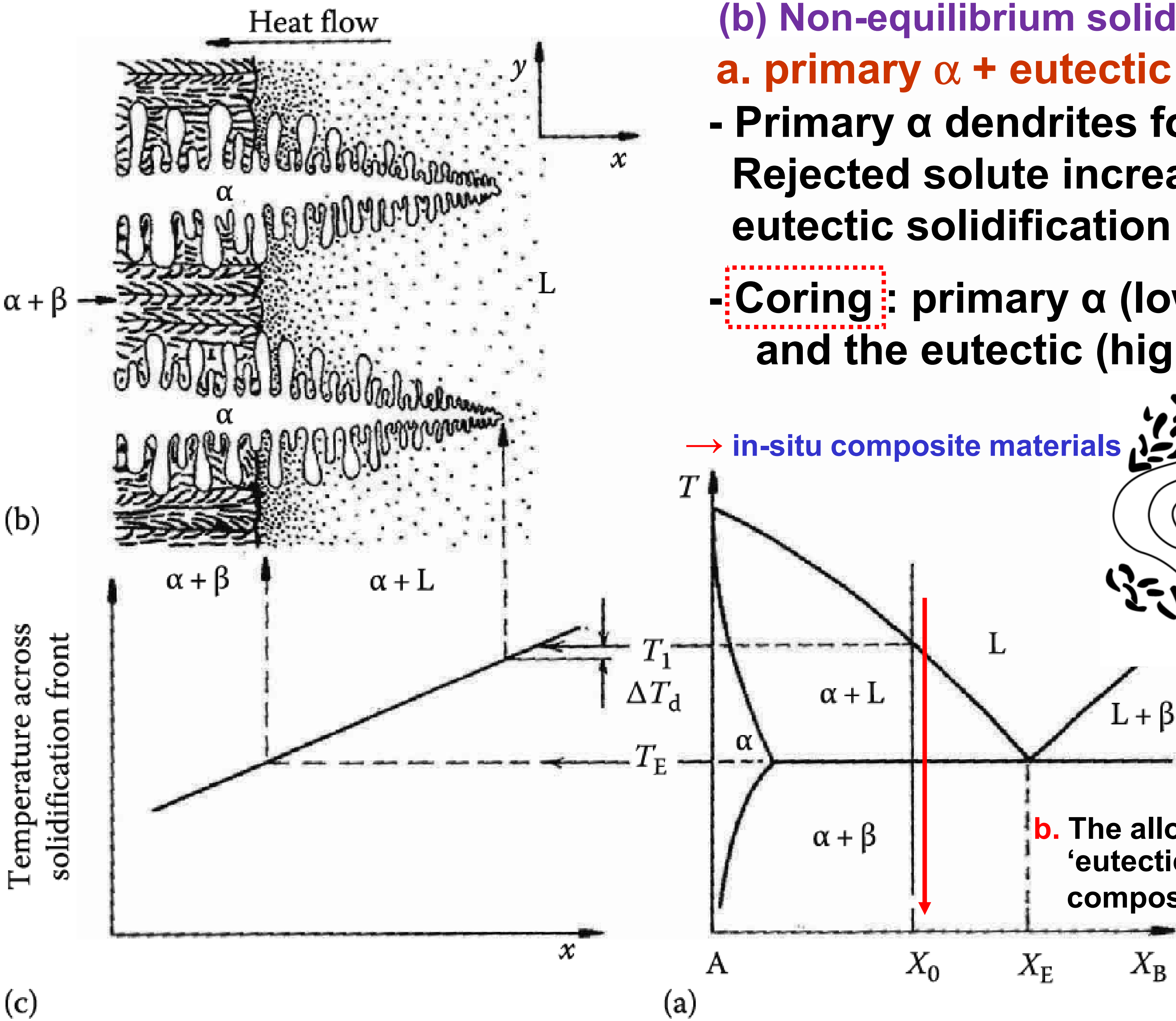

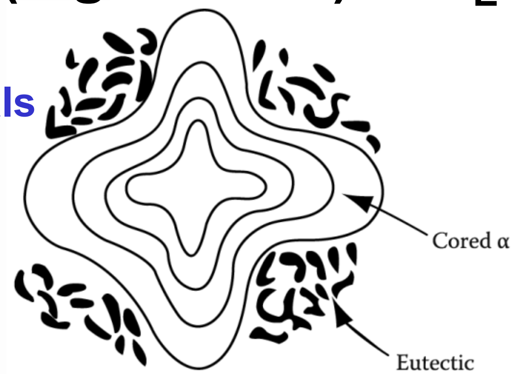

b. The alloy solidifies as 100% 'eutectic' with an overall composition X_0 instead of X_E.

FIG 4.39 Approximate Al–Fe phase diagrams for aluminum-rich compositions. Full lines show the equilibrium state, while the metastable states are indicated by dashed lines (Al6Fe) and dash-dot lines (Al4Fe, generally known as AlmFe). Details of the eutectic regions in Figure 4.40(a).

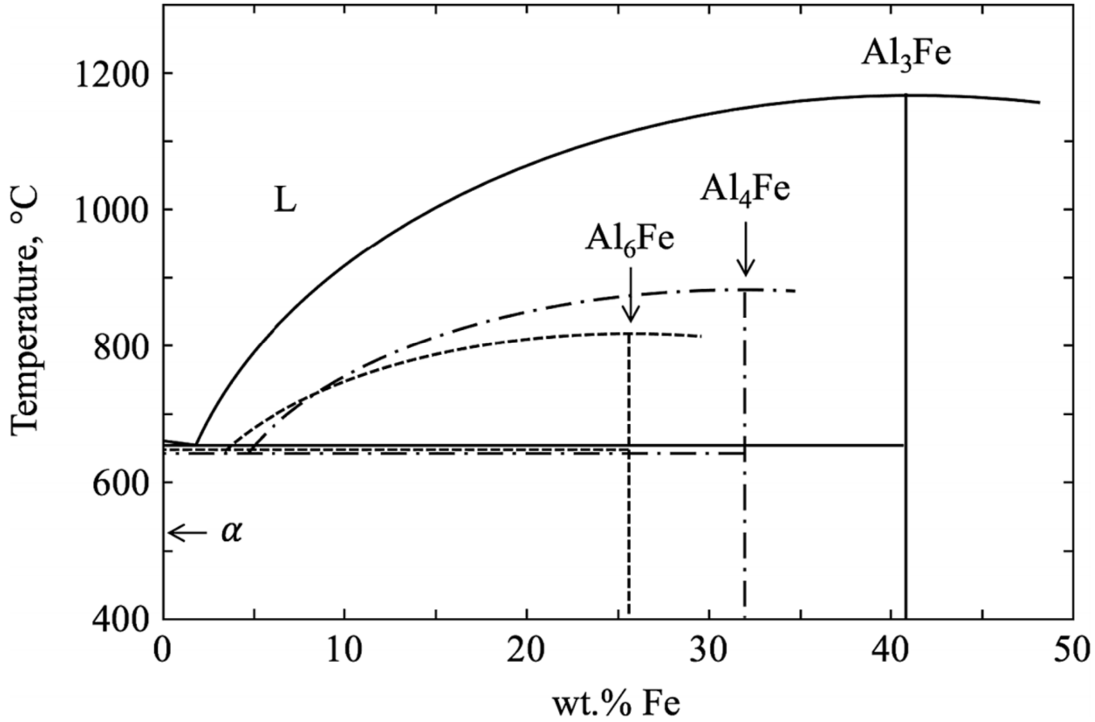

FIG 4.40 (a) Details of the stable and metastable Al–Fe equilibrium diagrams. (b) Schematic diagram illustrating the effect of cooling rate on the undercooling required for the nucleation of Al3Fe, Al6Fe and Al4Fe. (c) Schematic diagram illustrating the effect of growth rate on the growth front temperature for Al3Fe, Al6Fe and Al4Fe. Note that the relative positions of the lines can be affected by the presence of other alloying elements.

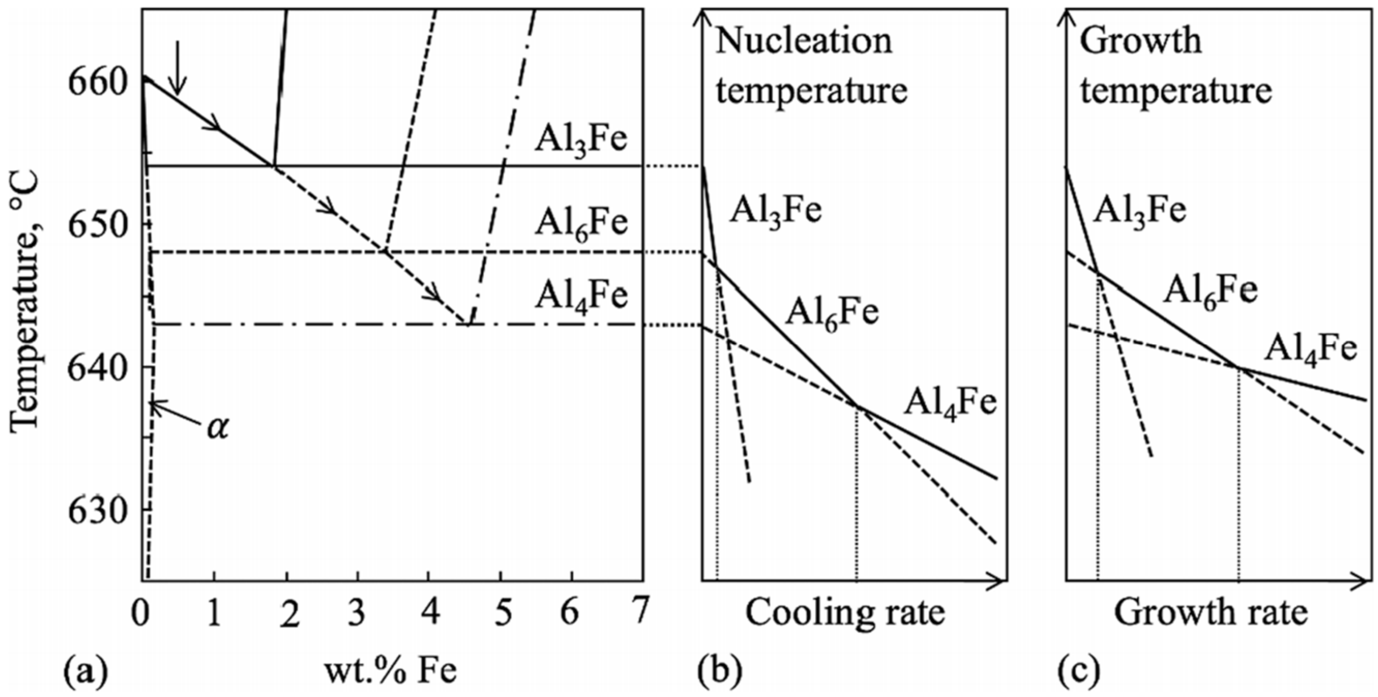

Q: Peritectic Solidification ($L + \alpha \rightarrow \beta$)?

Solidification and microstructure

that develop as a result of the peritectic reaction

(a) Equilibrium solidification

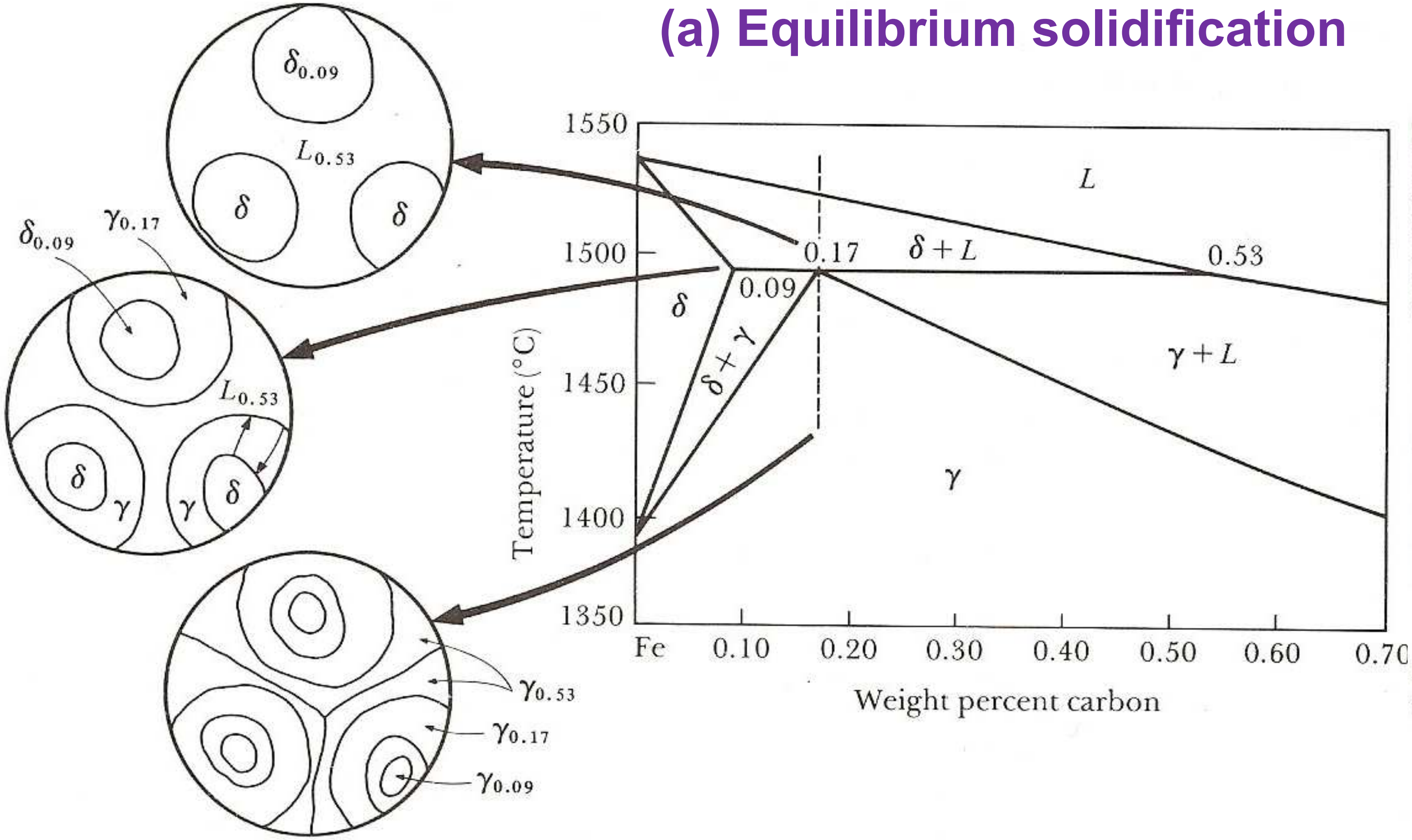

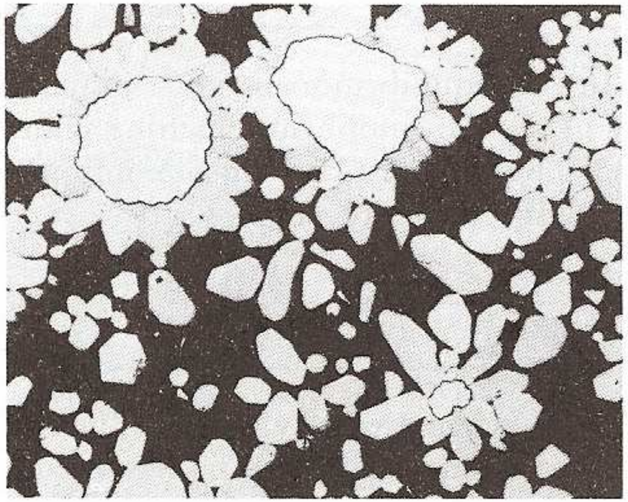

FIGURE 10-24 The peritectic reaction in a Cd-10% Cu alloy begins when rounded

4.3.4 Peritectic Solidification

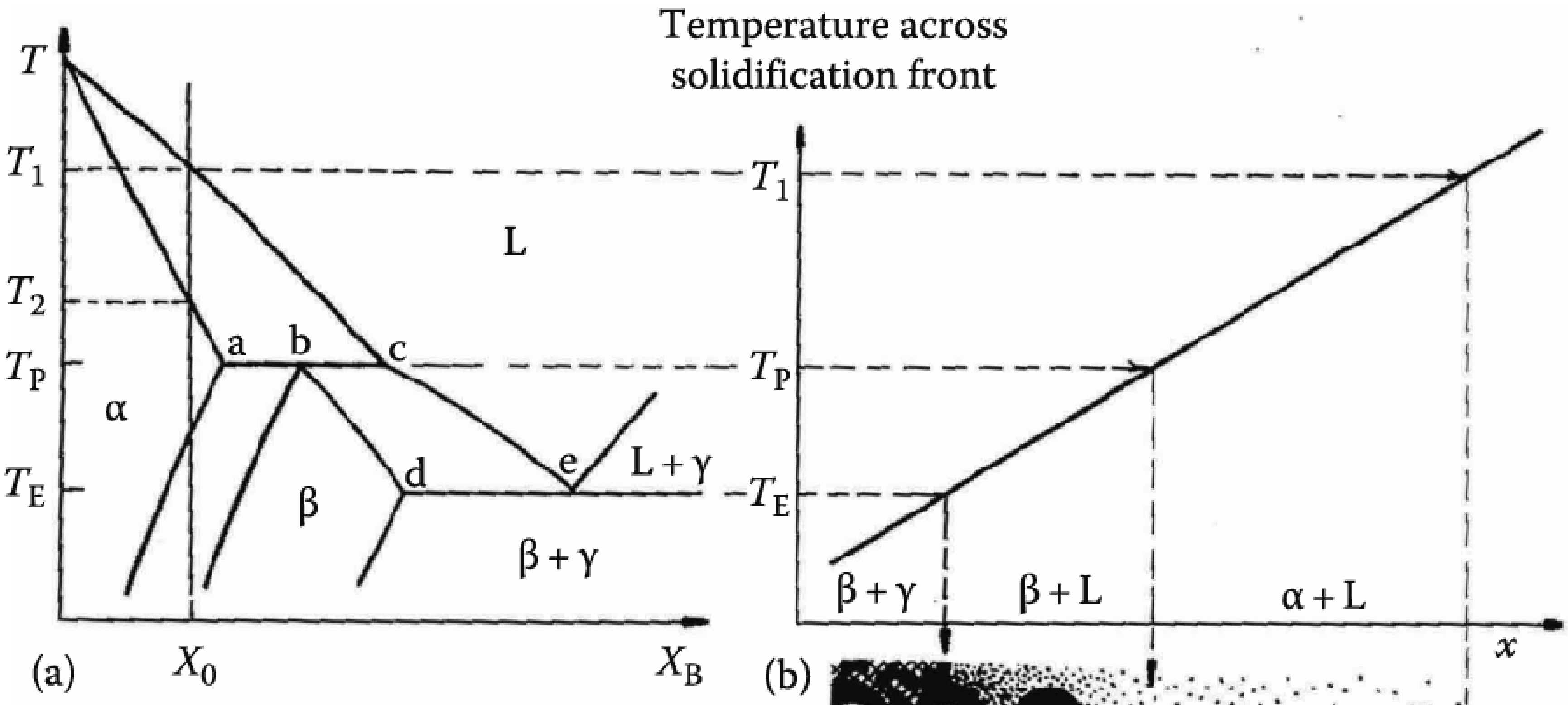

(b) Non-equilibrium solidification

- **L + α → β , difficult to complete.**
  - **α dendrites first form at T_1;**
    Liquid reaches the composition 'c';
    β forms as the result of the peritectic reaction;
    α coring is isolated from further reaction
    finally β + γ eutectic forms.

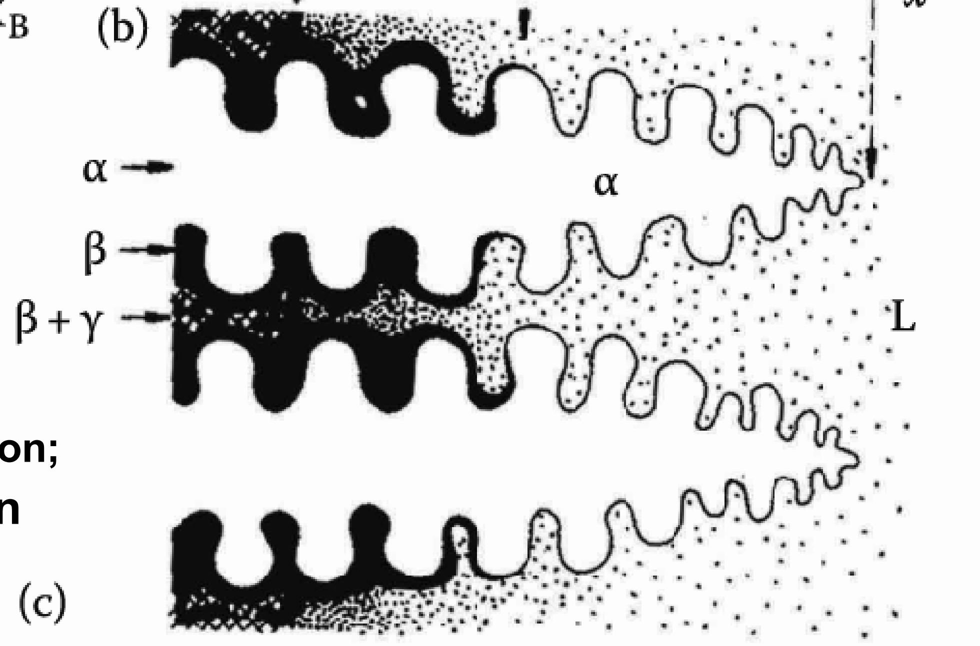

2023 Fall

"Phase Transformation *in* Materials"

11.15.2023

Eun Soo Park

Office: 33-313
Telephone: 880-7221
Email: espark@snu.ac.kr
Office hours: by an appointment

Solidification: Liquid → Solid

4.1 & 4.2 Pure Metals < Nucleation > & < Growth >

4.3 Alloy solidification

- Solidification of single-phase alloys
- Eutectic solidification
- Peritectic solidification

4.4 Solidification of Ingots and Castings

- Ingot Structure
- Segregation in Ingots and Castings
- Continuous Casting

4.6 Solidification during Quenching from the Melt

4.7 Metallic Glasses

Three of the most important application of solidification :
"Casting", "Weld solidification", "Additive manufacturing"

Q: What kinds of ingot structure exist?

Ingot Structure

- **Chill zone**
- **Columnar zone**
- **Equiaxed zone**

4.4 Solidification of Ingots and Castings

a lump of metal, usually shaped like a brick.

Later to be worked, e.g. by rolling, extrusion or forging>> blank (small)

an object or piece of machinery which has been made by pouring a liquid such as hot metal into a container

Permitted to regain their shape afterwards, or reshaped by machining

Ingot Structure

- outer Chill zone
  : equiaxed crystals
- Columnar zone
  : elongated or column-like grains
- central Equiaxed zone

Fig. 4.43

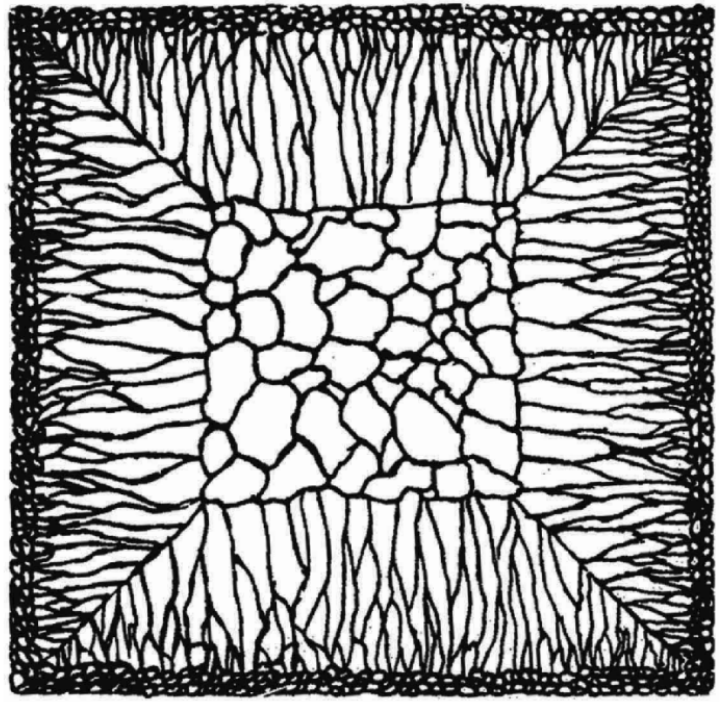

4.4.1 Chill zone

- **Solid nuclei form on the mould wall and begin to grow into the liquid.**

1) **If the pouring temp. is low**: liquid~ rapidly cooled below the liquidus temp. → **big-bang nucleation** → **entirely equiaxed ingot structure**, no columnar zone
2) **If the pouring temp. is high**: liquid~remain above the liquidus temp. for a long time → **majority of crystals~remelt under influence of the turbulent melt ("convection current")** → **form the chill zone**

4.4.2 Columnar zone

After pouring the temperature gradient at the mould walls decreases and the crystals in the chill zone grow dendritically in certain crystallographic directions, e.g. <100> in the case of cubic metals.

→ grow fastest and outgrow less favorably oriented neighbors

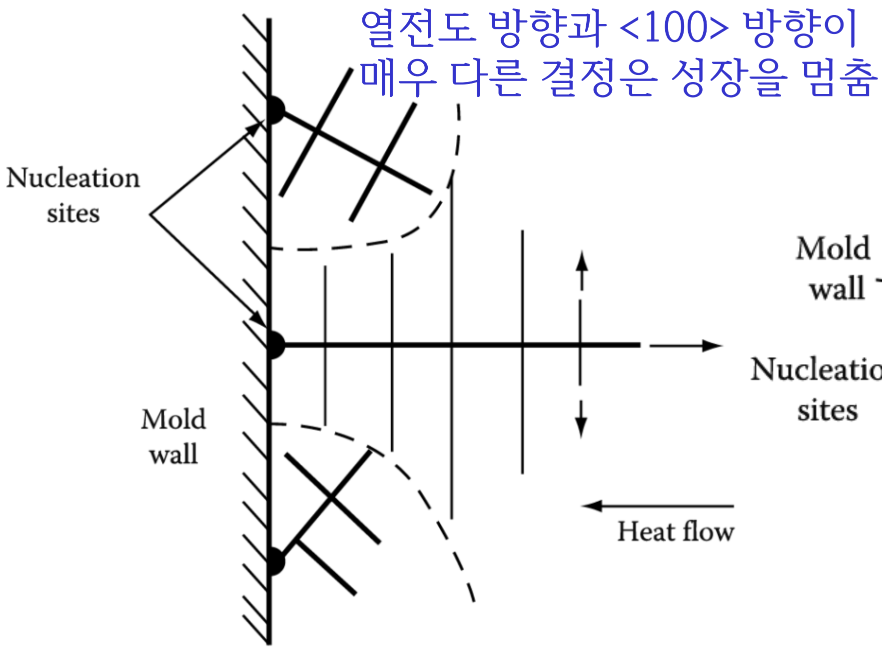

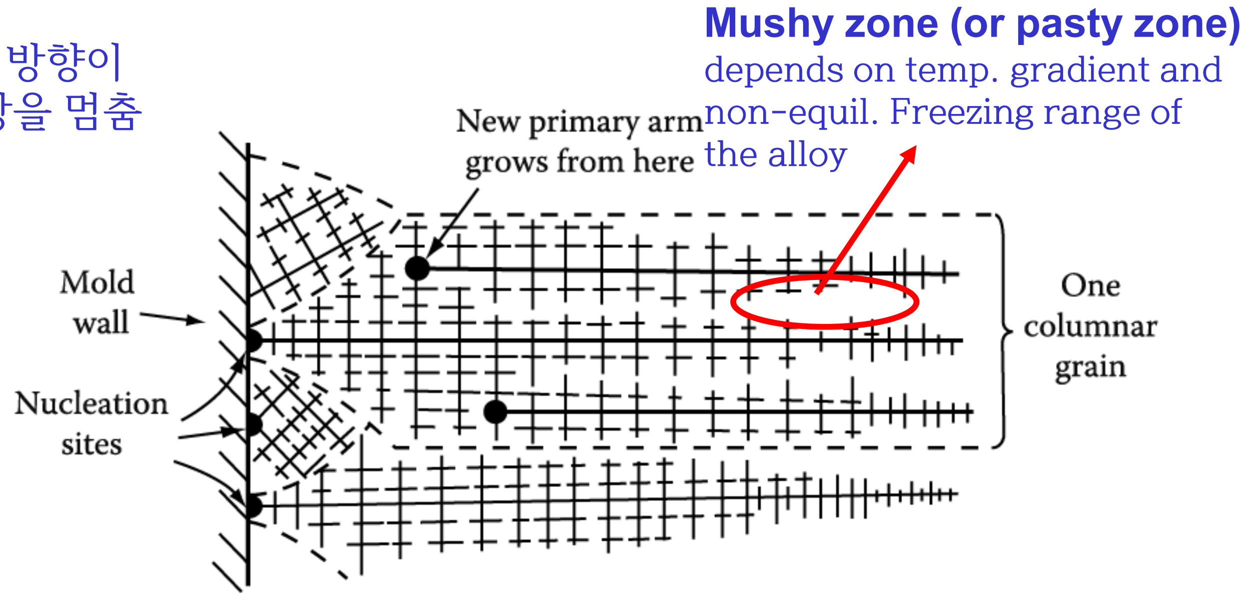

Fig. 4.44 Competitive growth soon after pouring. Dendrites with primary arms normal to the mould wall, i.e. parallel to the maximum temperature gradient, outgrow less favorably oriented neighbors.

Fig. 4.45 Favorably oriented dendrites develop into columnar grains. Each columnar grain originates from the same heterogeneous nucleation site, but can contain many primary dendrite arms.

1) In general, the secondary arms become coarser with distance behind the primary dendrite tips.

2) The primary and secondary dendrite arm spacing increase with increasing distance from the mold wall.
(∵ a corresponding decrease in the cooling rate with time after pouring)

⇨ **Mushy zone (or pasty zone)**
depends on temp. gradient and non-equil. freezing range of the alloy

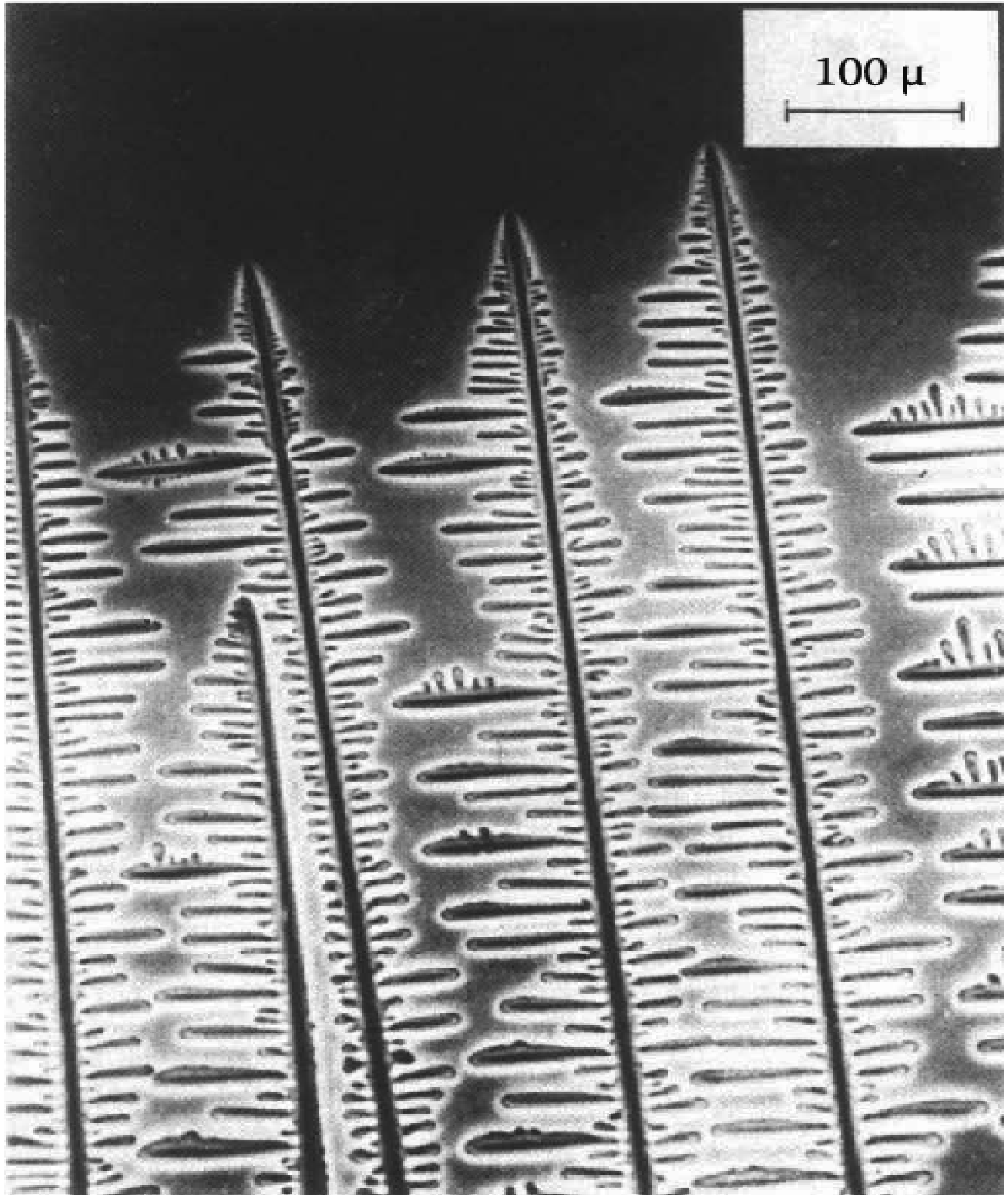

Fig. 4.28 Columnar dendrites in a transparent organic alloy.

(After K.A. Jackson in Solidification, American Society for Metals, 1971, p. 121.)

4.4.3 Equiaxed zone

The equiaxed zone consists of equiaxed grains randomly oriented in the centre of the ingot. An important origin of these grains is thought to be melted-off dendrite side-arms + convection current

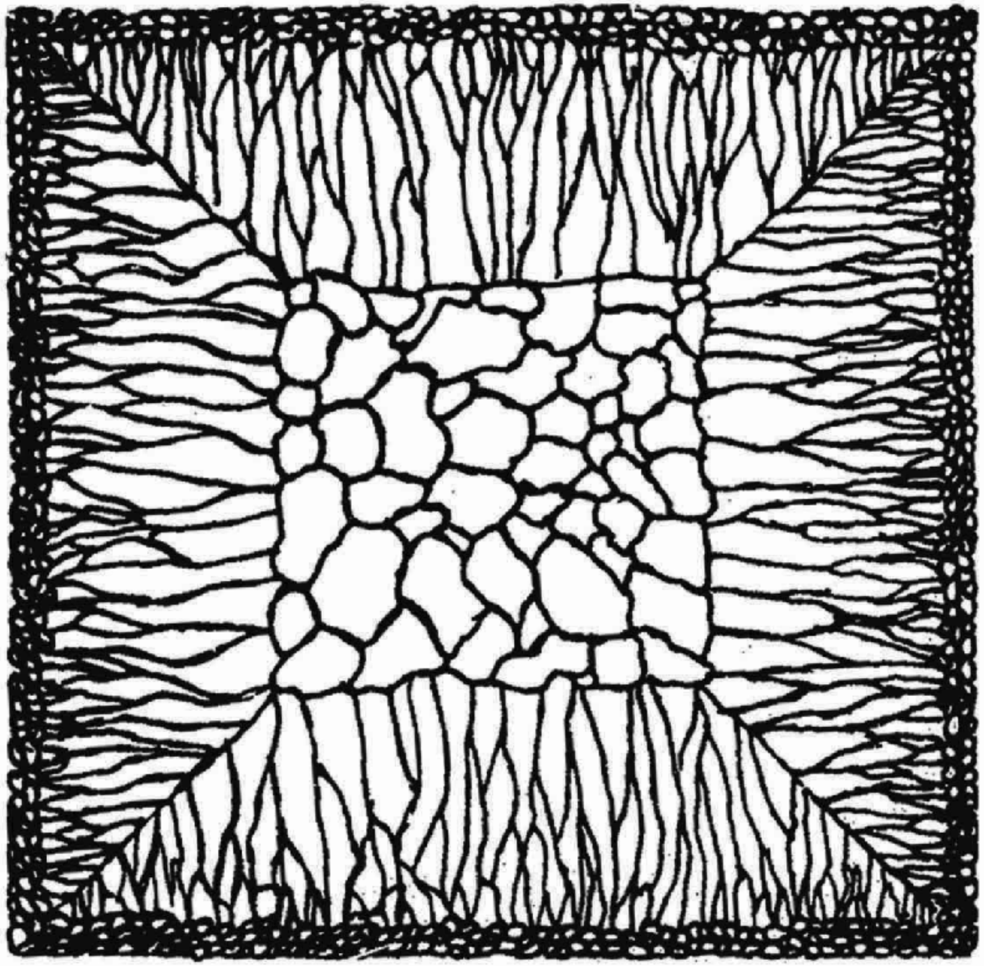

Fig. 4.43 Schematic cast grain structure.
(After M.C. Flemings, Solidification Processing, McGraw-Hill, New York, 1974.)

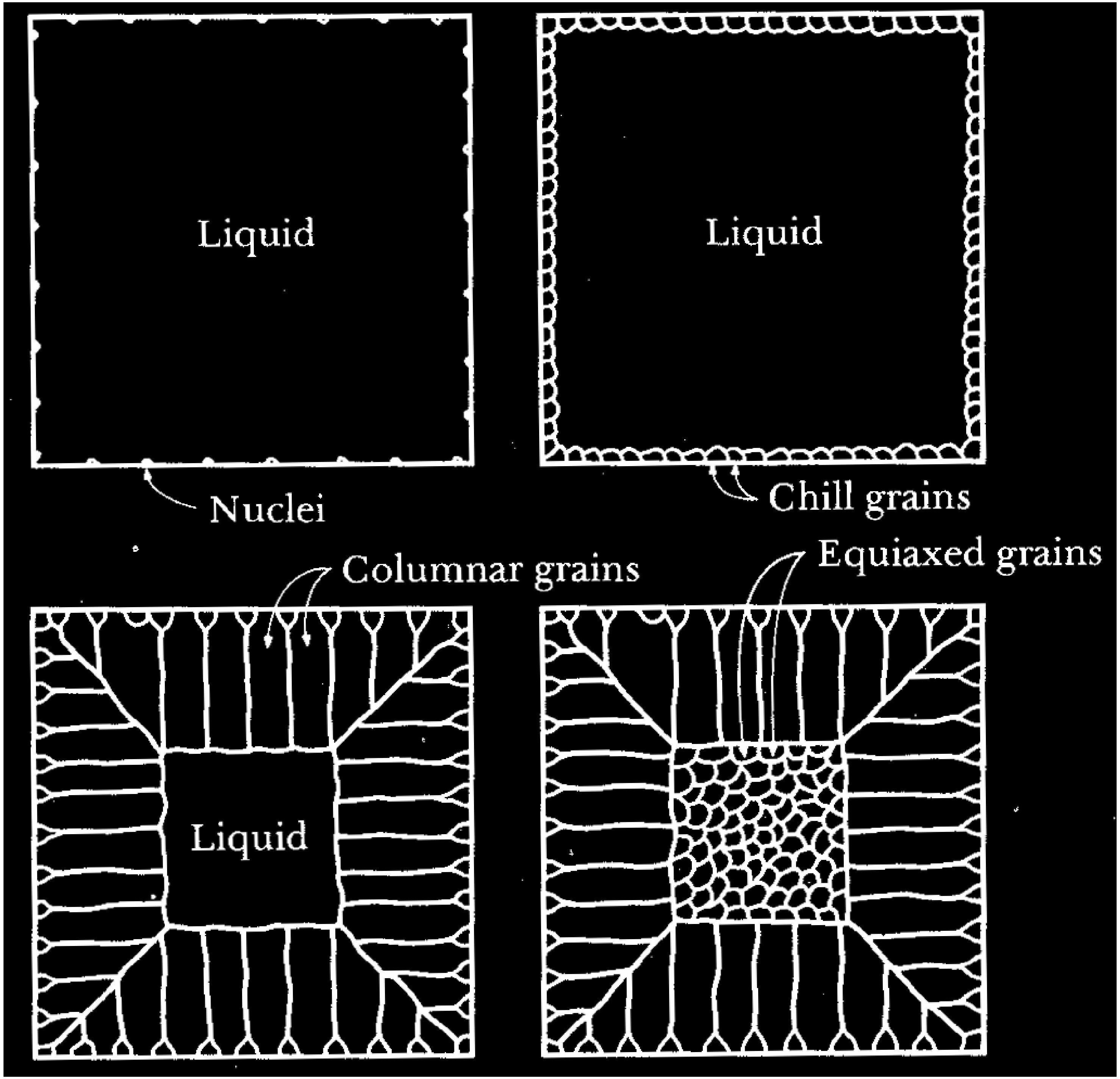

Liquid
Liquid
Nuclei
Chill grains
Columnar grains
Equiaxed grains
Liquid

Q: What kind of segregations exist?

* Segregation and Shrinkage in Ingots and Castings

(a) Segregation

- **Macrosegregation :** Large area
  composition changes over distances comparable to the size of the specimen.

- **Microsegregation :** In the secondary dendrite arm
  occur on the scale of the secondary dendrite arm spacing.

Four important factors that can lead to macrosegregation

a) **Shrinkage due to solidification and thermal contraction.**
b) **Density differences in the interdendritic liquid.**
c) **Density differences between the solid and liquid.**
d) **Convection currents driven by temperature-induced density differences in the liquid.**

Fig. Simulation of macrosegregation formation in a large steel casting, showing liquid velocity vectors during solidification (left) and final carbon macrosegregation pattern (right).

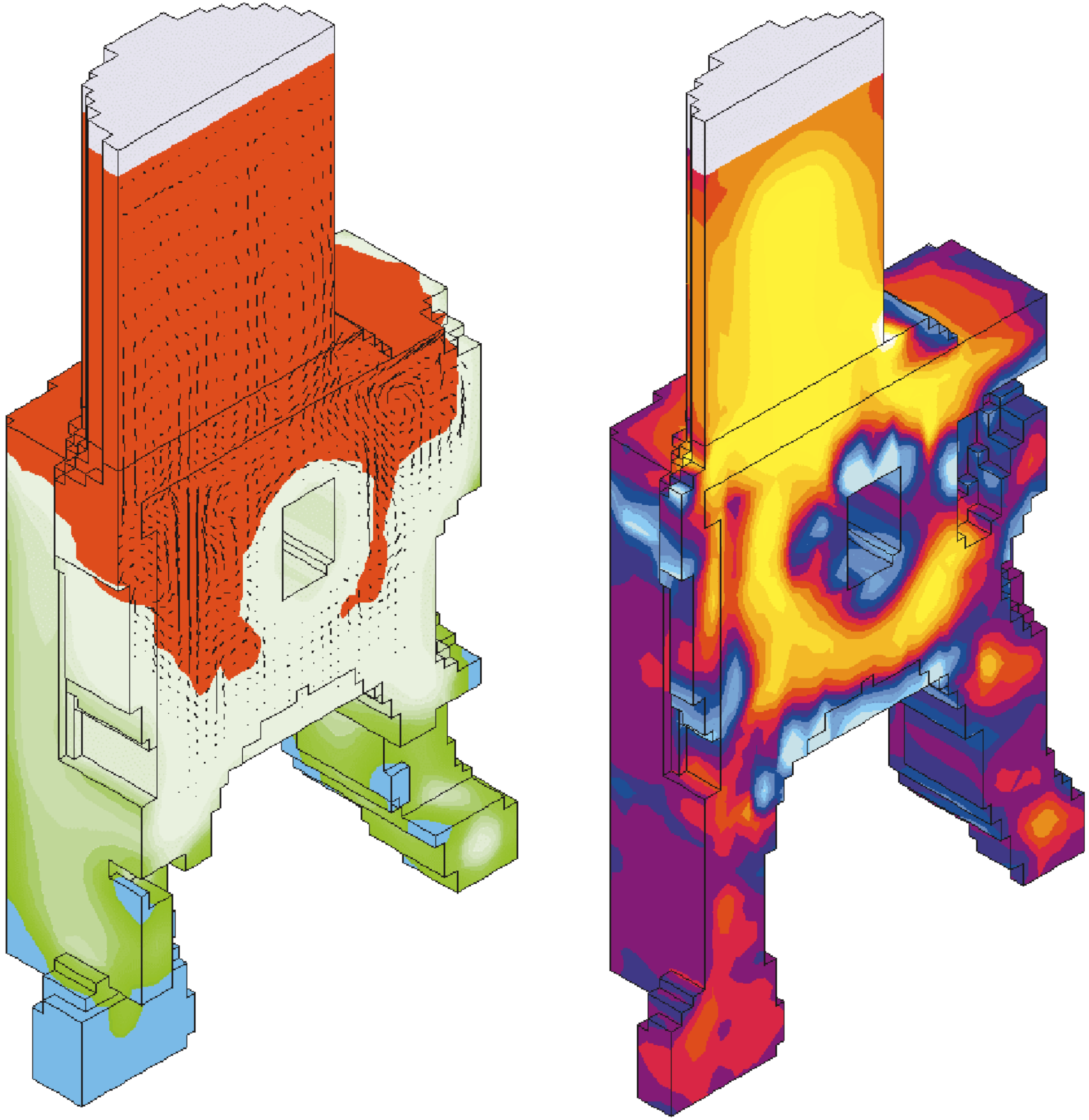

Fig.

Freckles in a single-crystal nickel-based superalloy prototype blade (left) and close-up of a single freckle (right) (courtesy of A. F. Giamei, United Technologies Research Center).

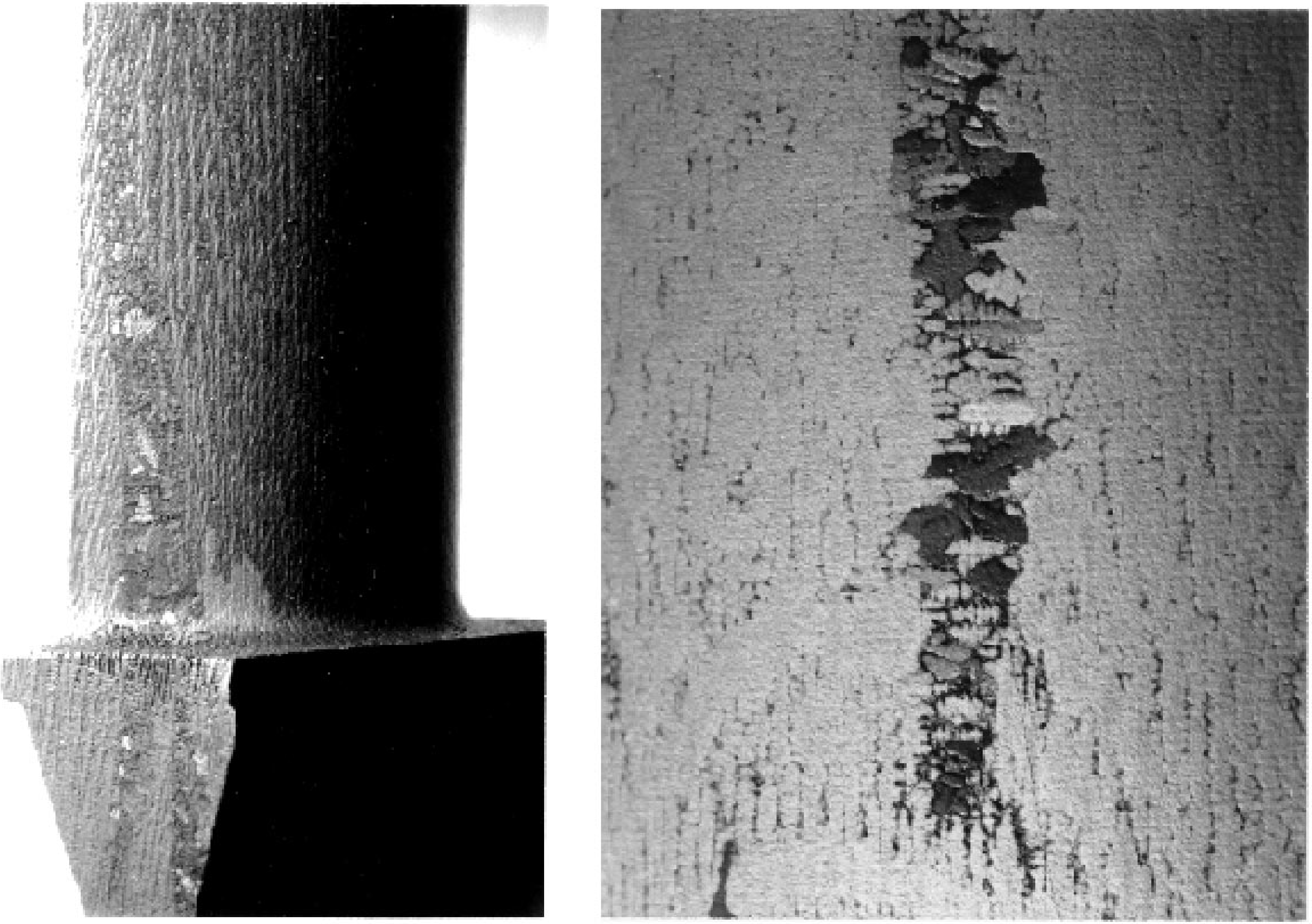

Fig.
Sulfur print showing centerline segregation in a continuously cast steel slab (courtesy of IPSCO Inc.).

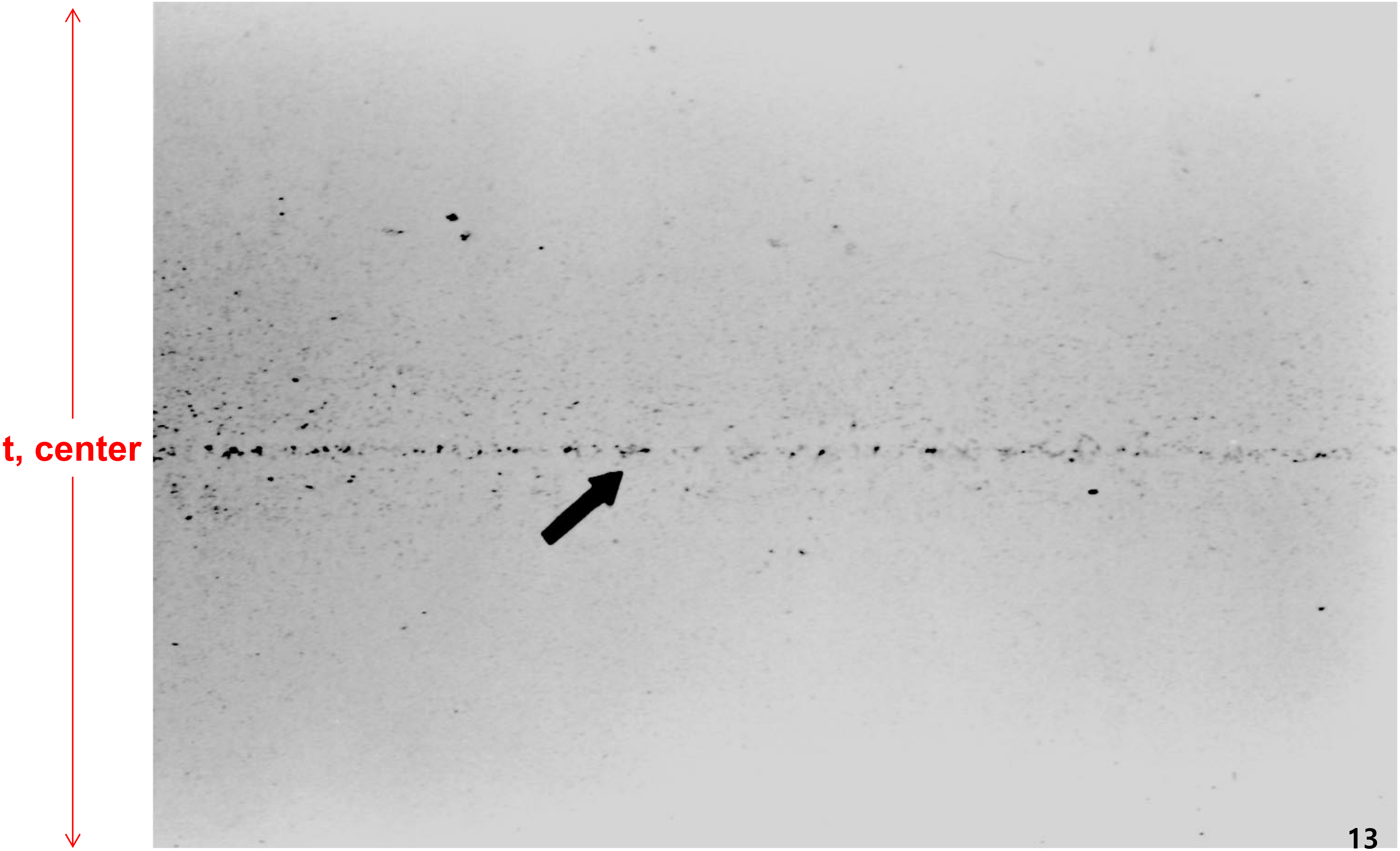

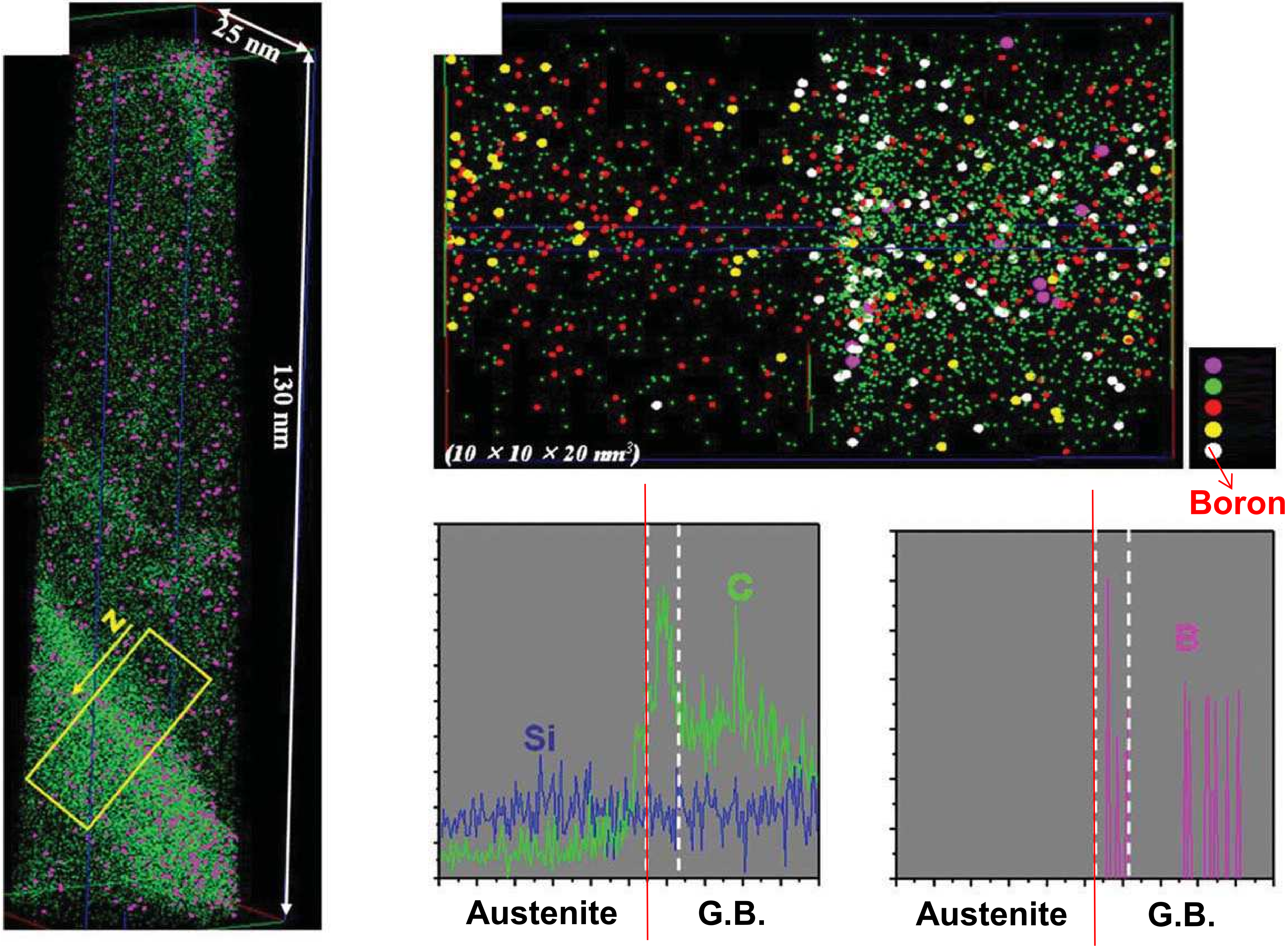

The result obtained by APT analysis. (a) 3D Atom map of **Boron steel containing 100 ppm Boron** and (b) composition profile showing **solute segregation within retained austenite and grain boundary**

Korean J. Microscopy Vol. 41, No. 2, 2011

* Segregation: undesiable ~ deleterious effects on mechanical properties

→ subsequent homogenization heat treatment, but diffusion in the solid far to slow

→ good control of the solidification process

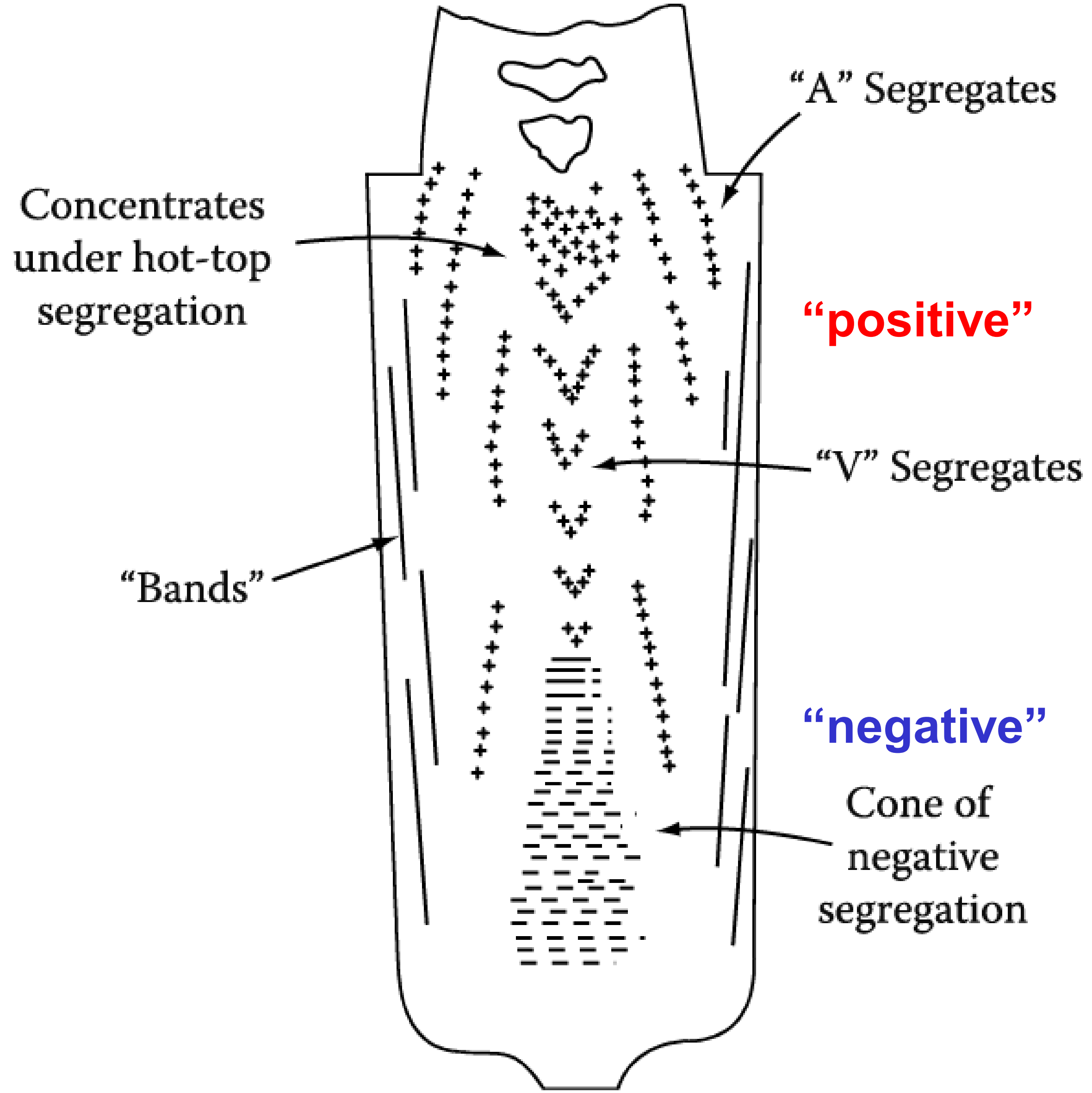

Inverse segregation (역편석): As the columnar dendrites thicken solute-rich liquid (assuming k<1) must flow back between the dendrites to compensate for (a) shrinkage and this raises the solute content of the outer parts of the ingot relative to the center.

EX) Al-Cu and Cu-Sn alloys with a wide freezing range (relatively low k)

Negative segregation: The solid is usually denser than the liquid and sinks carrying with it less solute (초기응고고상)than the bulk composition (assuming k<1). This can, therefore, lead to a region of negative segregation near the bottom of the ingot. ((b) Gravity effects)

Fig. 4.43 Segregation pattern in a large killed steel ingot. + positive, - negative segregation. (After M.C. Flemings, Scandinavian Journal of Metallurgy 5 (1976) 1.)

Q: Shrinkage in Solidification and Cooling?

(b) Shrinkage

Crystallization is Controlled by Thermodynamics

- Volume is high as a hot liquid
- Volume shrinks as liquid is cooled
- At the melting point, T_m, the liquid crystallizes to the thermodynamically stable crystalline phase
- More compact (generally) crystalline phase has a smaller volume
- The crystal then shrinks as it is further cooled to room temperature
- Slope of the cooling curve for liquid and solid is the thermal expansion coefficient, α

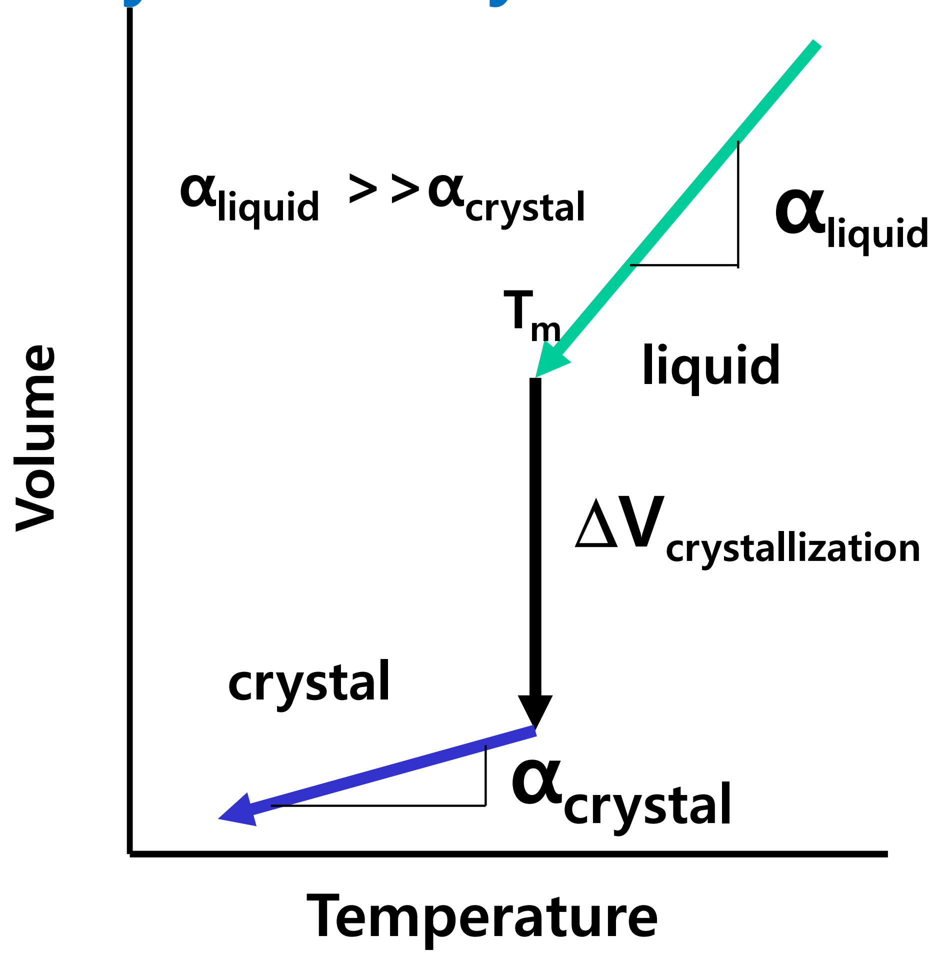

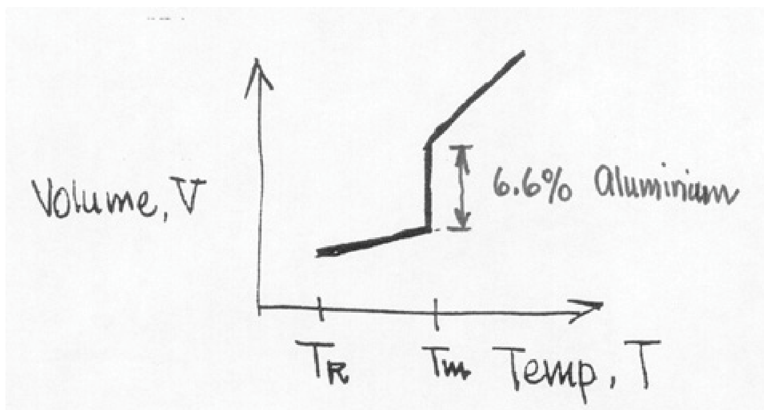

Shrinkage in Solidification and Cooling

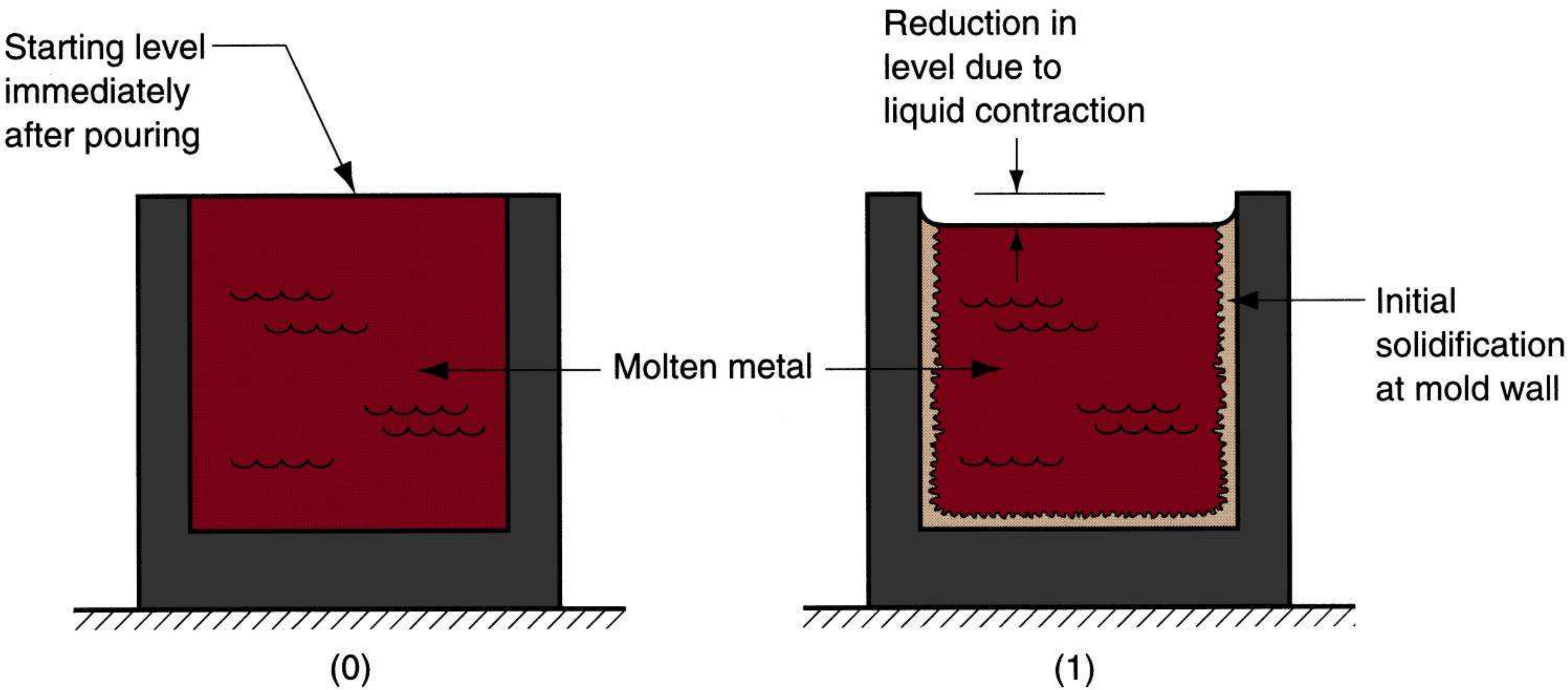

* Shrinkage of a cylindrical casting during solidification and cooling: (0) starting level of molten metal immediately after pouring; (1) reduction in level caused by liquid contraction during cooling (dimensional reductions are exaggerated for clarity).

Shrinkage in Solidification and Cooling

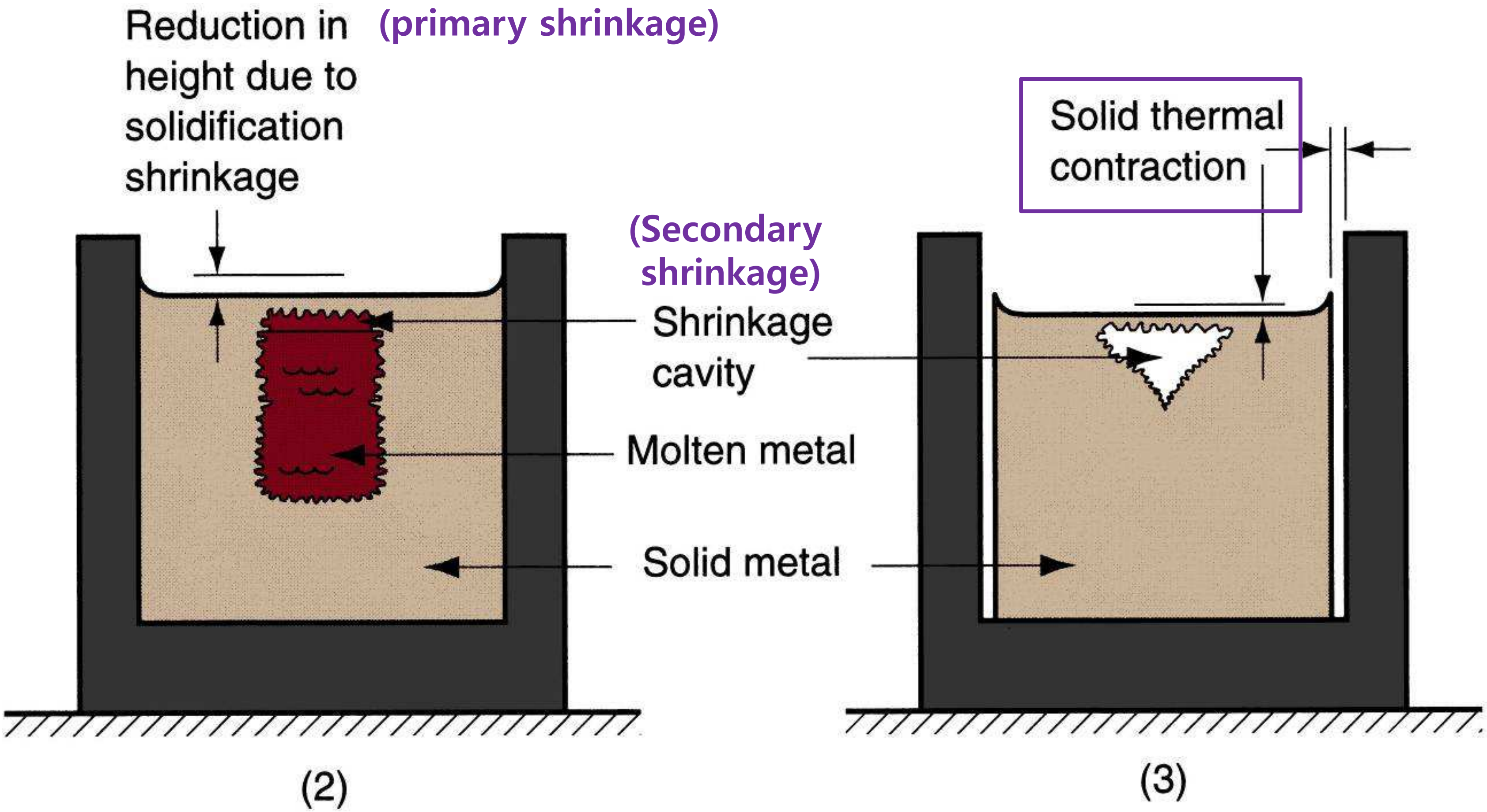

* (2) reduction in height and formation of shrinkage cavity caused by solidification shrinkage; (3) further reduction in height and diameter due to thermal contraction during cooling of solid metal (dimensional reductions are exaggerated for clarity).

Shrinkage effect

* Formation of Voids during solidification

Central shrinkage:
조성 변화가 크지 않은 주물의 응고 시 주로 응고수축, ΔV 에 의해 발생하는 주물 중심부에 발생

Dispersed Micro-Pore:
상당히 넓은 범위에 분산된 미소기공

외부수축 (몰드 주위) 및 1차수축공 (표면)을 제외하면, 이러한 수축공 결함은 주로 기포 결함임

기포 내에는 철합금에서는 CO, 질소, 산소, 수소 등이, 동합금에서는 수소, 산소, 알루미늄 합금에서는 수소 등의 가스가 존재

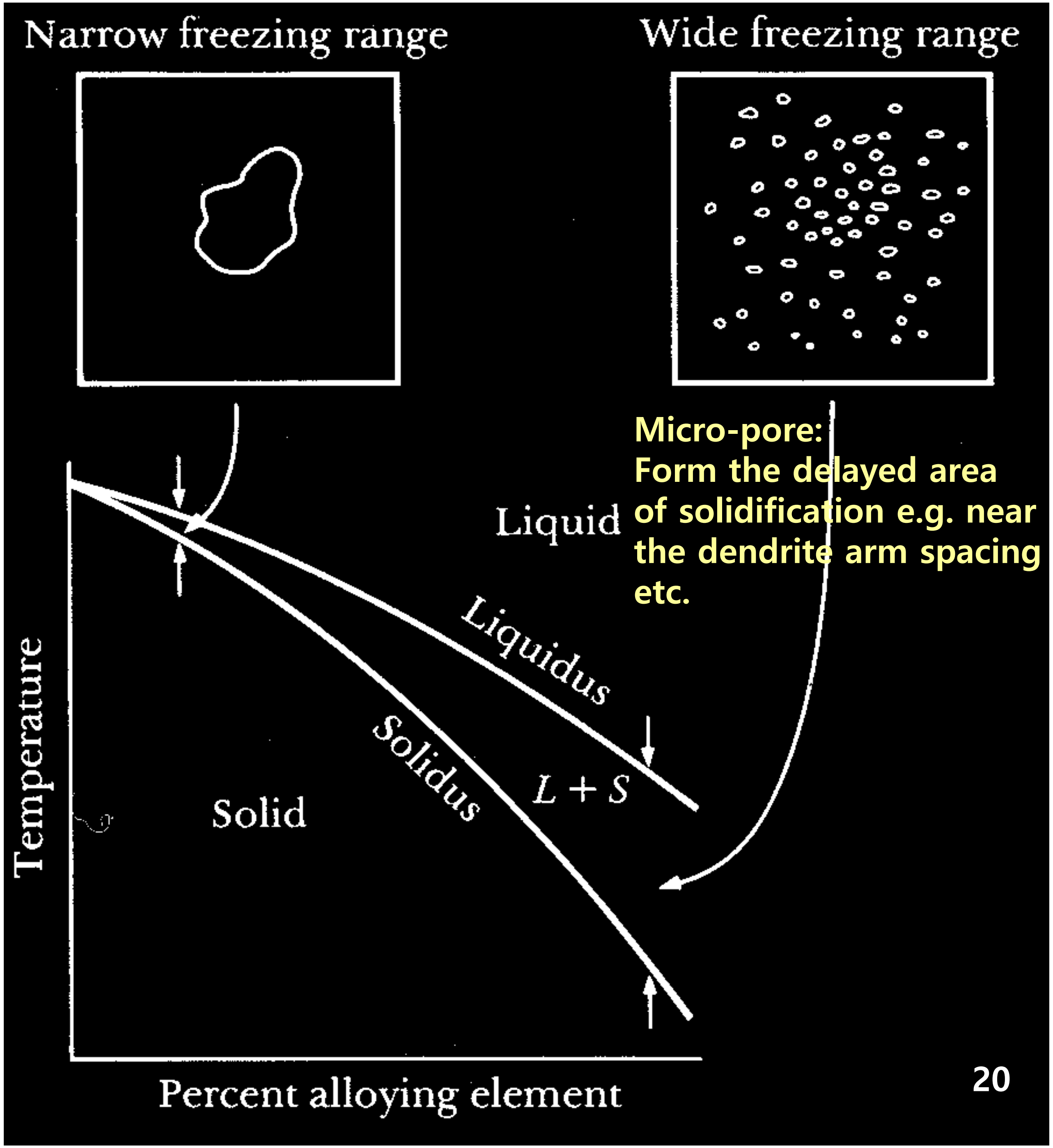

Shrinkage in Solidification and Cooling

- Can amount to 5-10% by volume
- Gray cast iron expands upon solidification due to phase changes
- Need to design part and mold to take this amount into consideration

TABLE 5.1

Metal or alloy	Volumetric solidification contraction (%)	Metal or alloy	Volumetric solidification contraction (%)
Aluminum	6.6	70%Cu–30%Zn	4.5
Al–4.5%Cu	6.3	90%Cu–10%Al	4
Al–12%Si	3.8	Gray iron	Expansion to 2.5
Carbon steel	2.5–3	Magnesium	4.2
1% carbon steel	4	White iron	4–5.5
Copper	4.9	Zinc	6.5

Source: After R. A. Flinn.

* Volumetric solidification expansion: H_2O (10%), Si (20%), Ge

ex) Al-Si eutectic alloy (casting alloy)→ volumetric solidification contraction of Al substitutes volumetric solidification expansion of Si.

Cast Iron: Fe + Carbon (~ 4%) + Si (~2%)

→ precipitation of graphite during solidification reduces shrinkage.

Q: What is continuous casting?

continuous casting: a number of dynamic industrial process

The molten metal is poured continuously into a water-cooled mold from which the solidified metal is continuously withdrawn in plate or rod form. (solid-liquid interface)

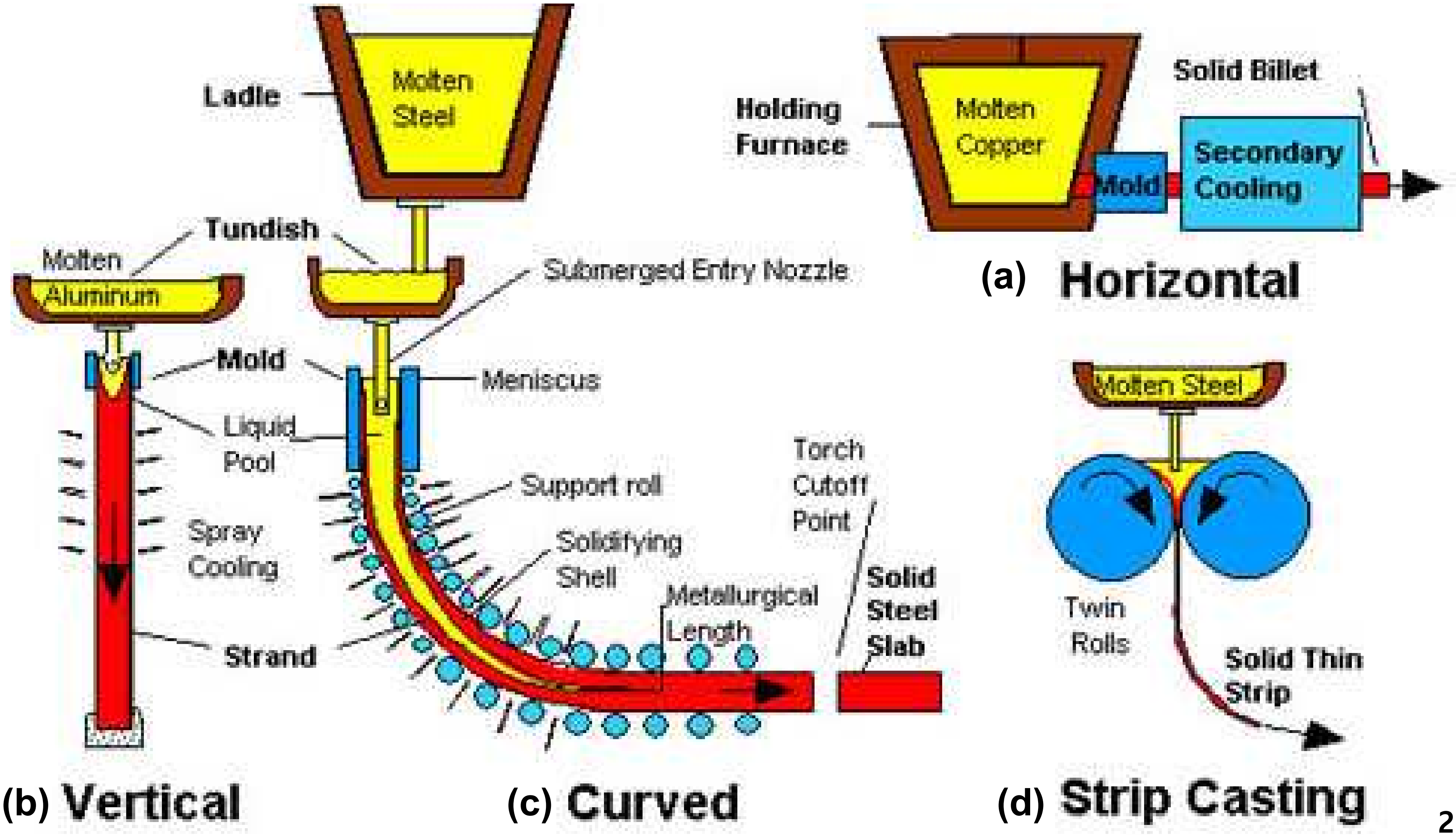

(a) Horizontal

(b) Vertical

(c) Curved

(d) Strip Casting

"Dynamic process: importance of isotherm distribution"

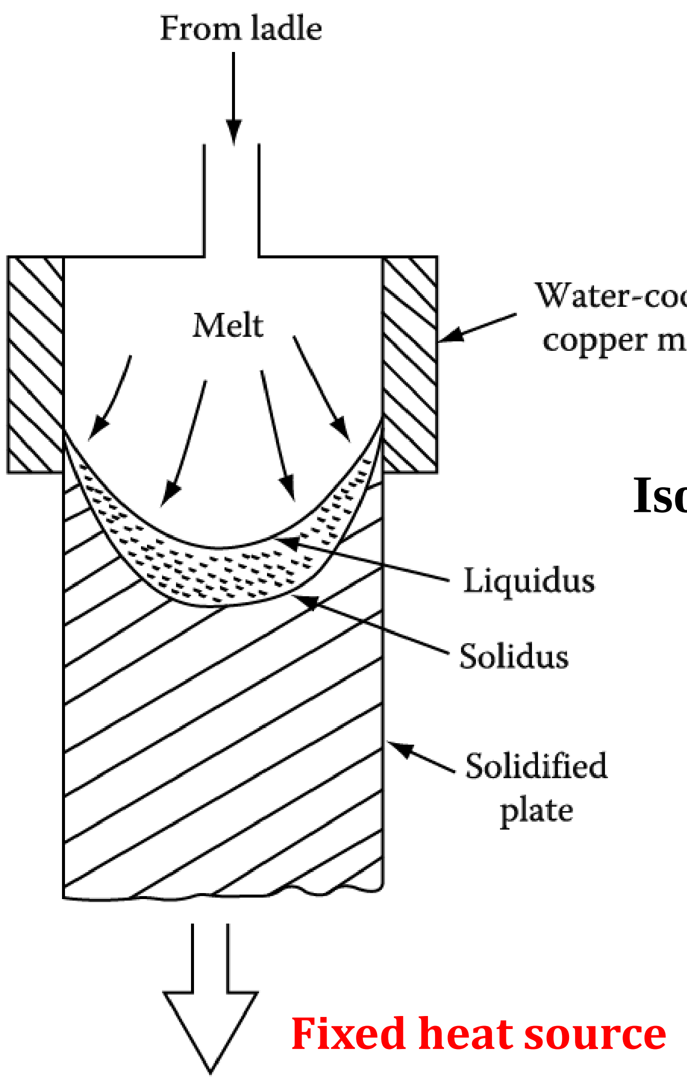

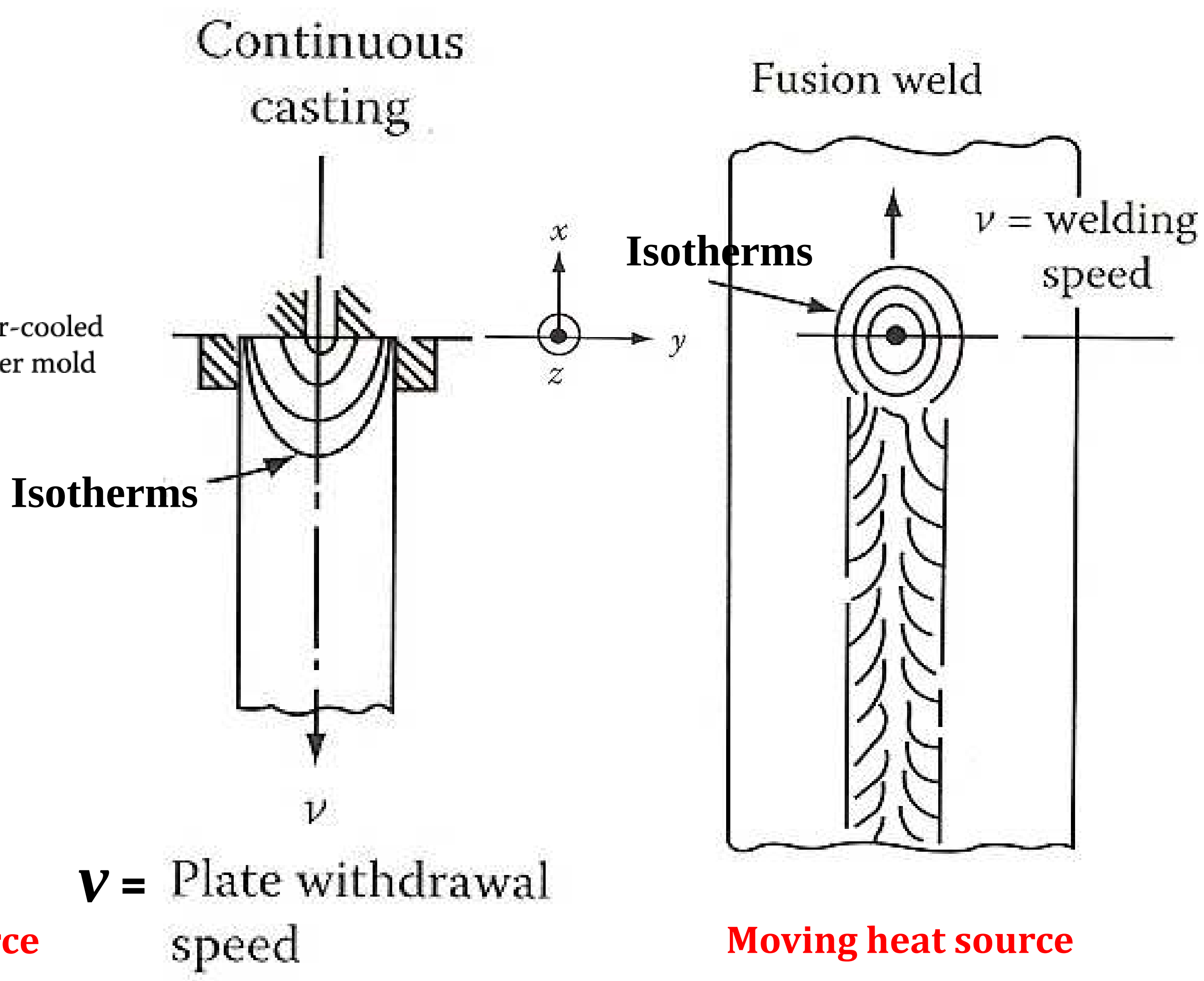

Fig. Schematic illustration of a continuous casting process

Fig. Illustrating the essential equivalence of isotherms about the heat sources in fusion welding and continuous casting


continuous casting

continuous casting

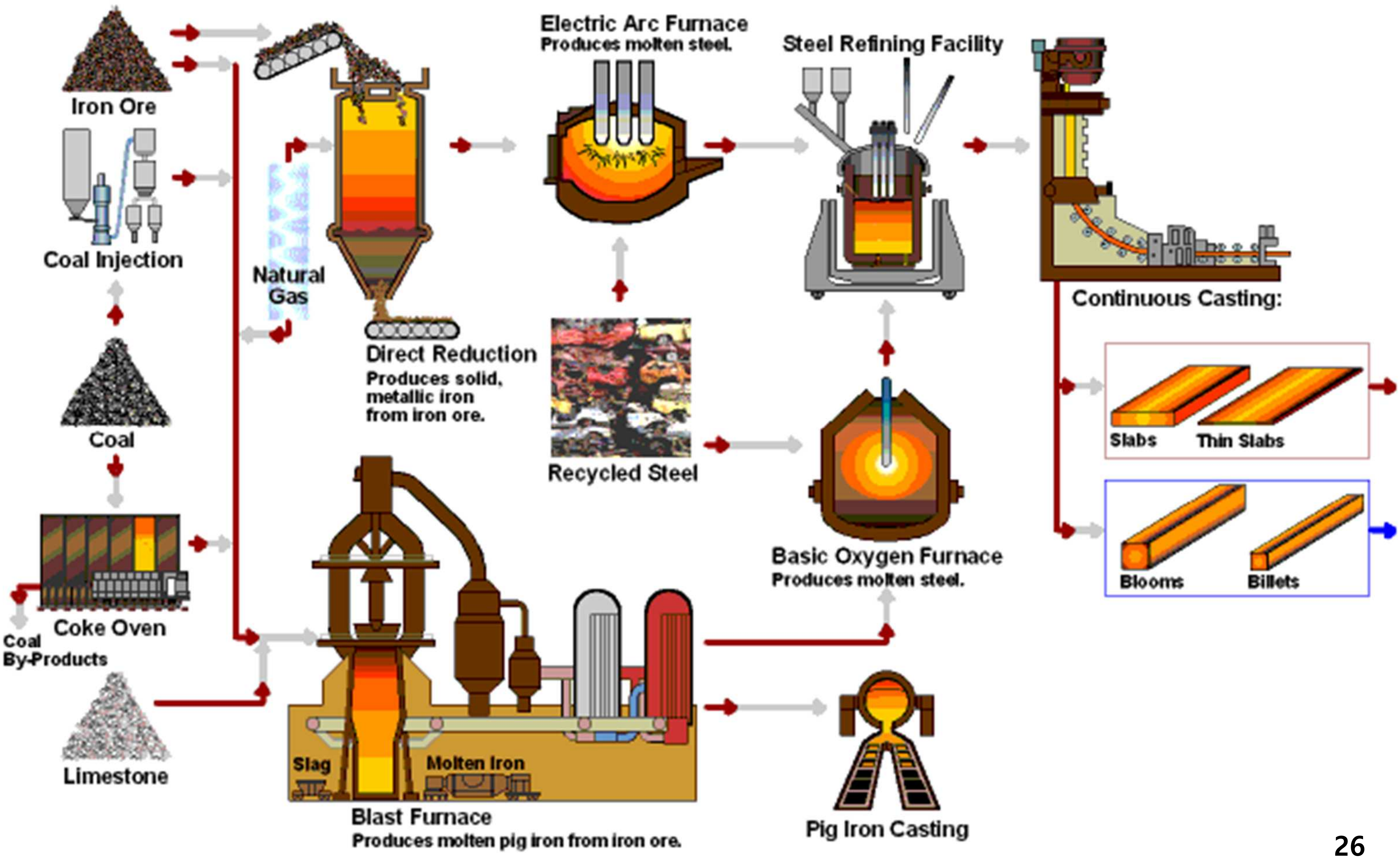

continuous casting

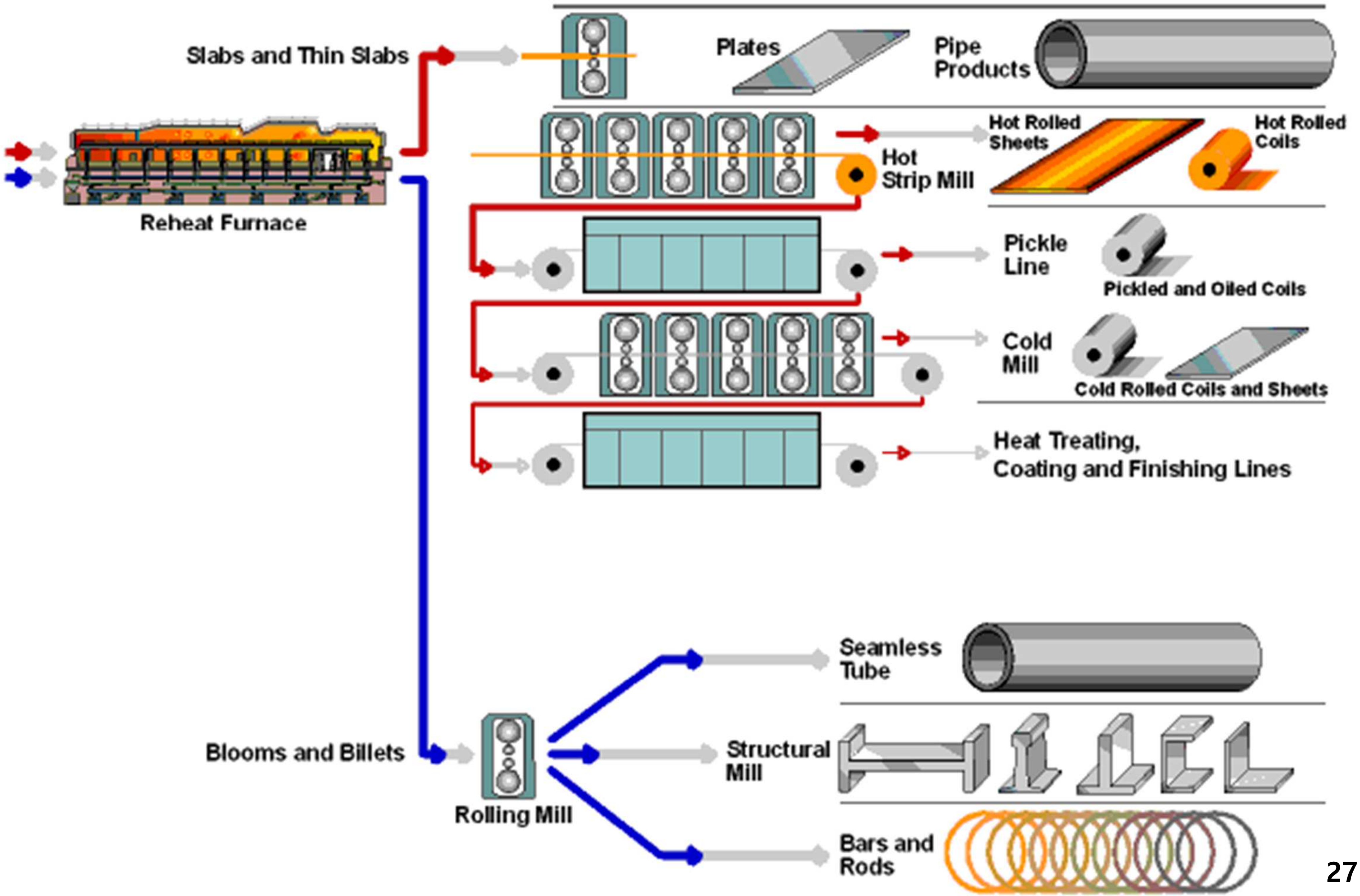

Q: Glass formation?

Time-Temperature-Transformation diagram

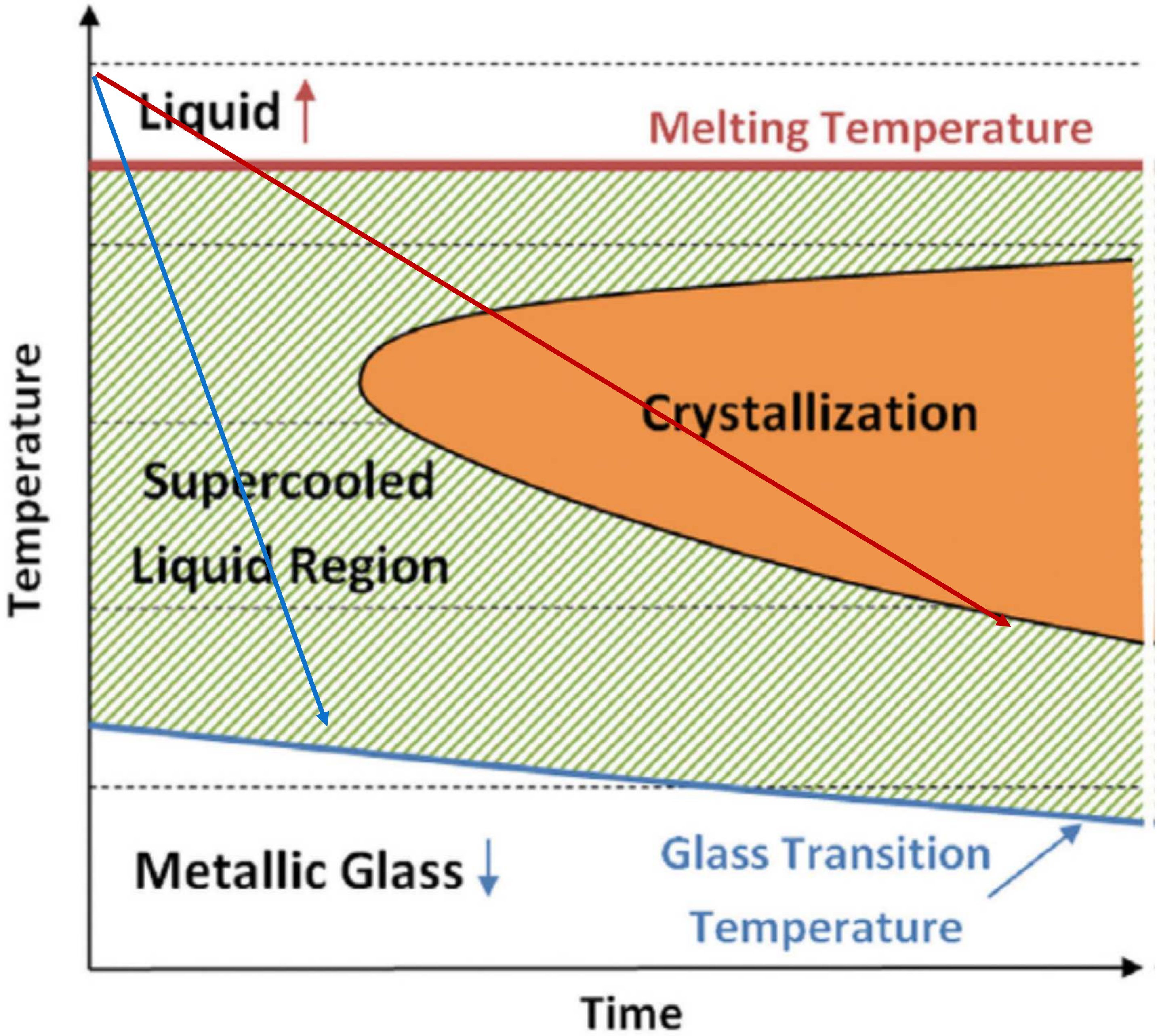

Electrostatic Levitation: cooling curve of Vitreloy 1 system

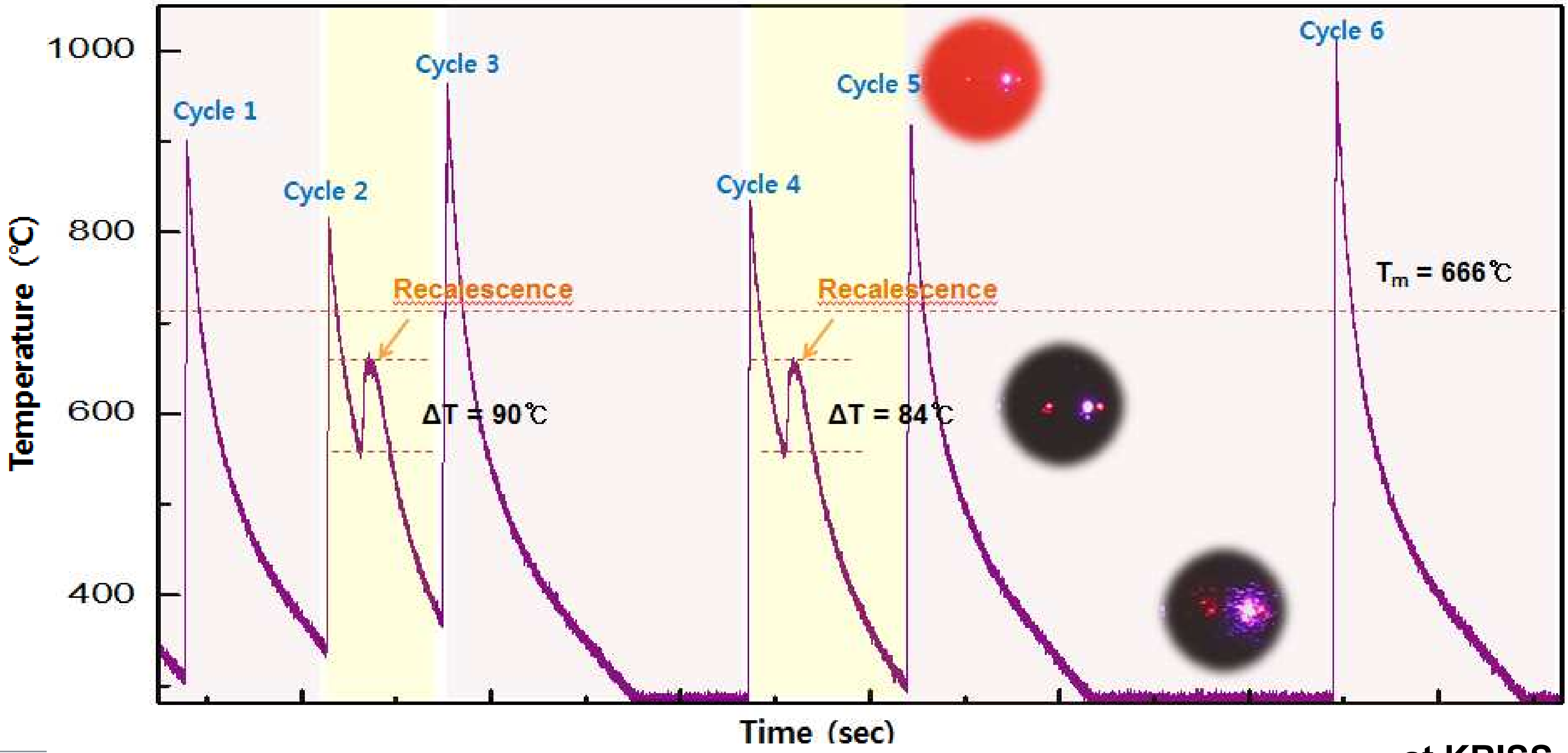

at KRISS

Structure of Crystals, Liquids and Glasses

Crystals

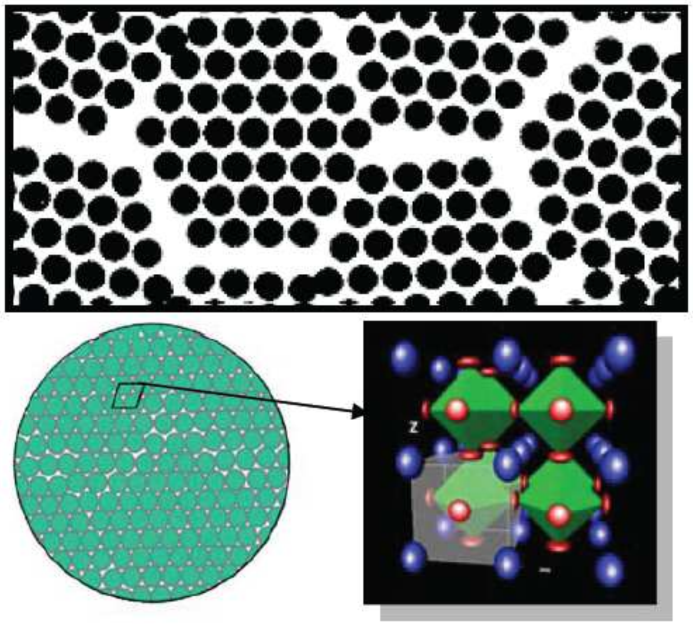

Liquids, glasses

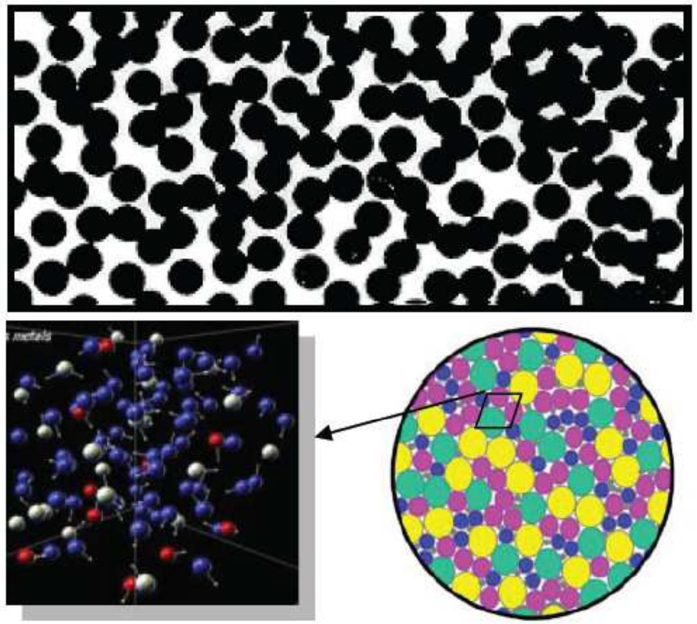

Building block: arranged in orderly, 3-dimensional, periodic array

nearly random = non-periodic

- **grain boundaries**

- **no grain boundaries**

Glass Formation is Controlled by Kinetics

- Glass forming liquids are those that are able to "by-pass" the melting point, T_m
- Liquid may have a high viscosity that makes it difficult for atoms of the liquid to diffuse (rearrange) into the crystalline structure
- Liquid maybe cooled so fast that it does not have enough time to crystallize
- Two time scales are present
  - "Internal" time scale controlled by the viscosity (bonding) of the liquid
  - "External" timescale controlled by the cooling rate of the liquid

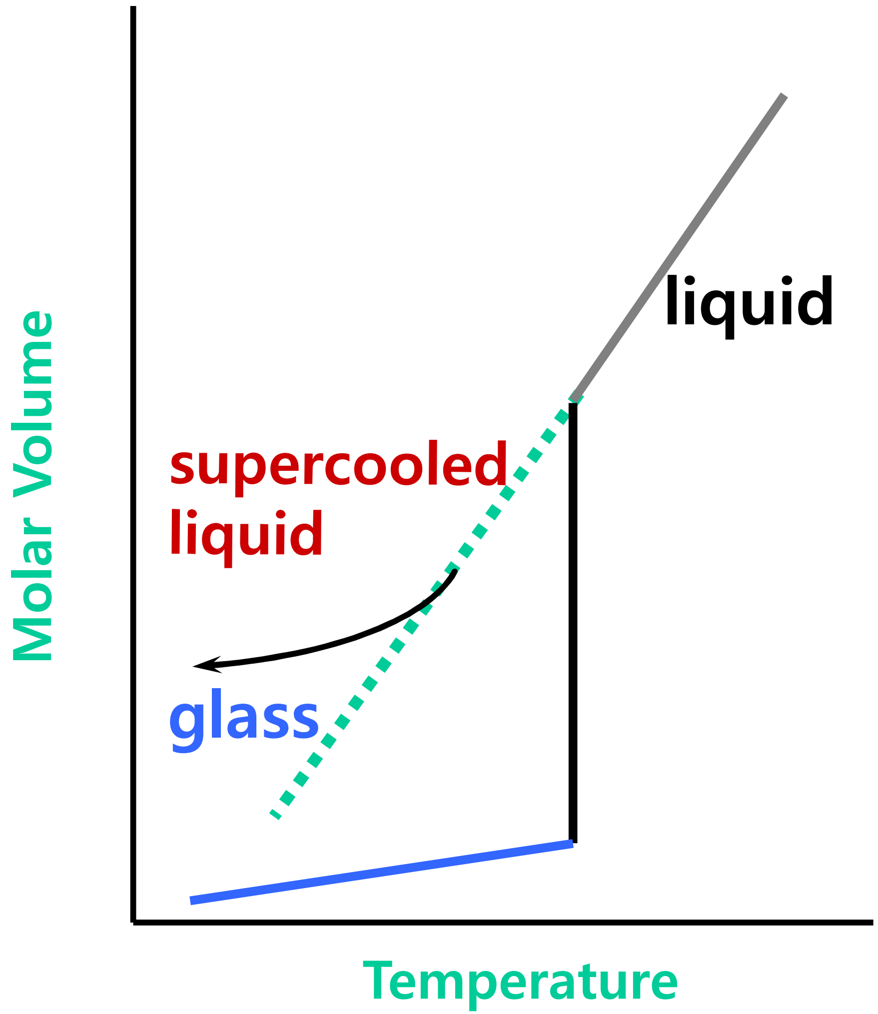

The Cooling Rate Affects the Properties of Glass

- Faster cooling freezes in the glass at a higher temperature
- The temperature is lowered so fast that the liquid does not have time to relax to the properties at the next lower temperature, glass is formed at a high temperature
- Slower cooling freezes in the glass at a lower temperature
- The temperature is lowered slowly enough that the liquids can relax to properties at lower and lower temperatures, glass is eventually formed at a lower temperature

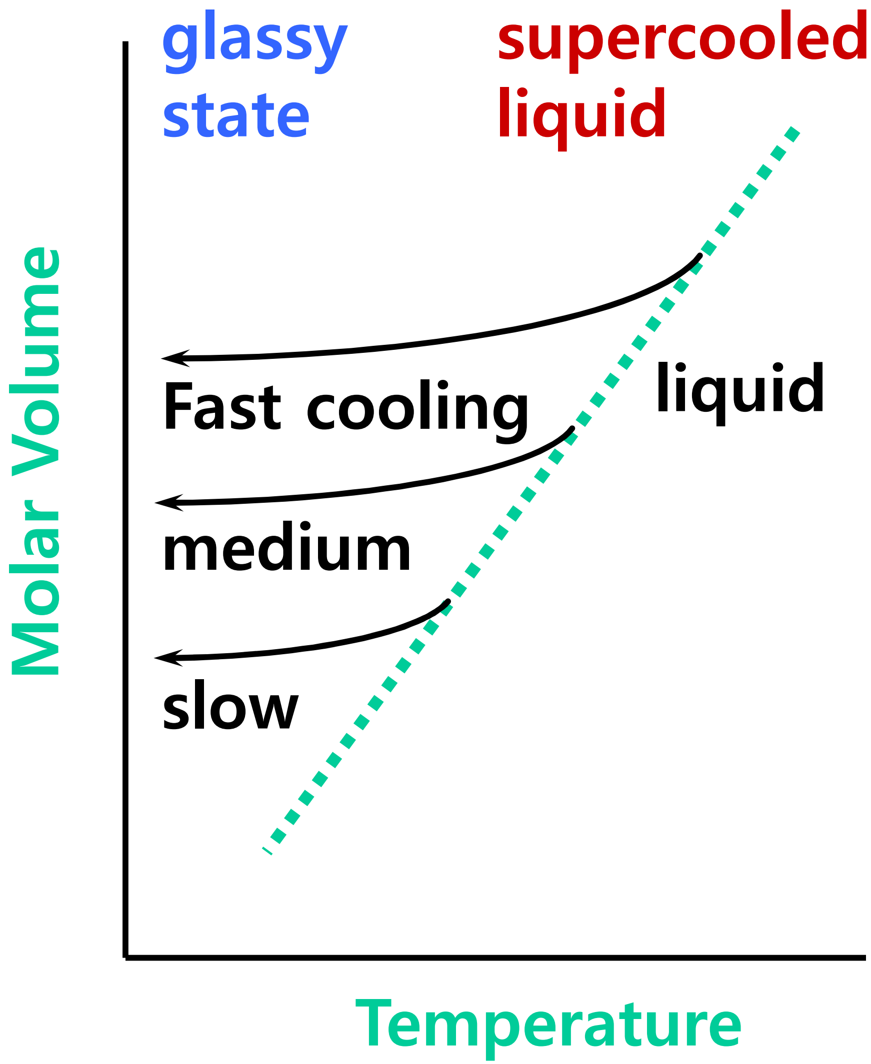

Fundamentals of the Glass Transition

- Melting and Crystallization are **Thermodynamic Transitions**

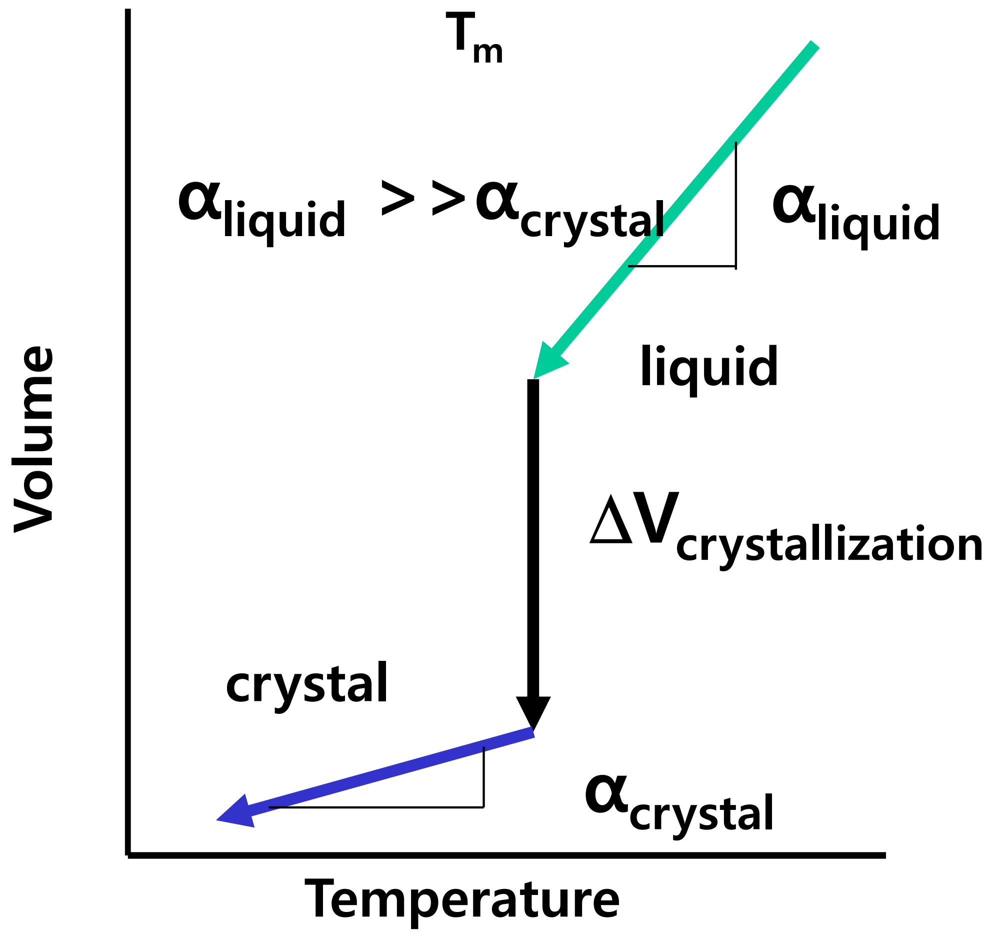

- The Glass Transition is a **Kinetic Transition**

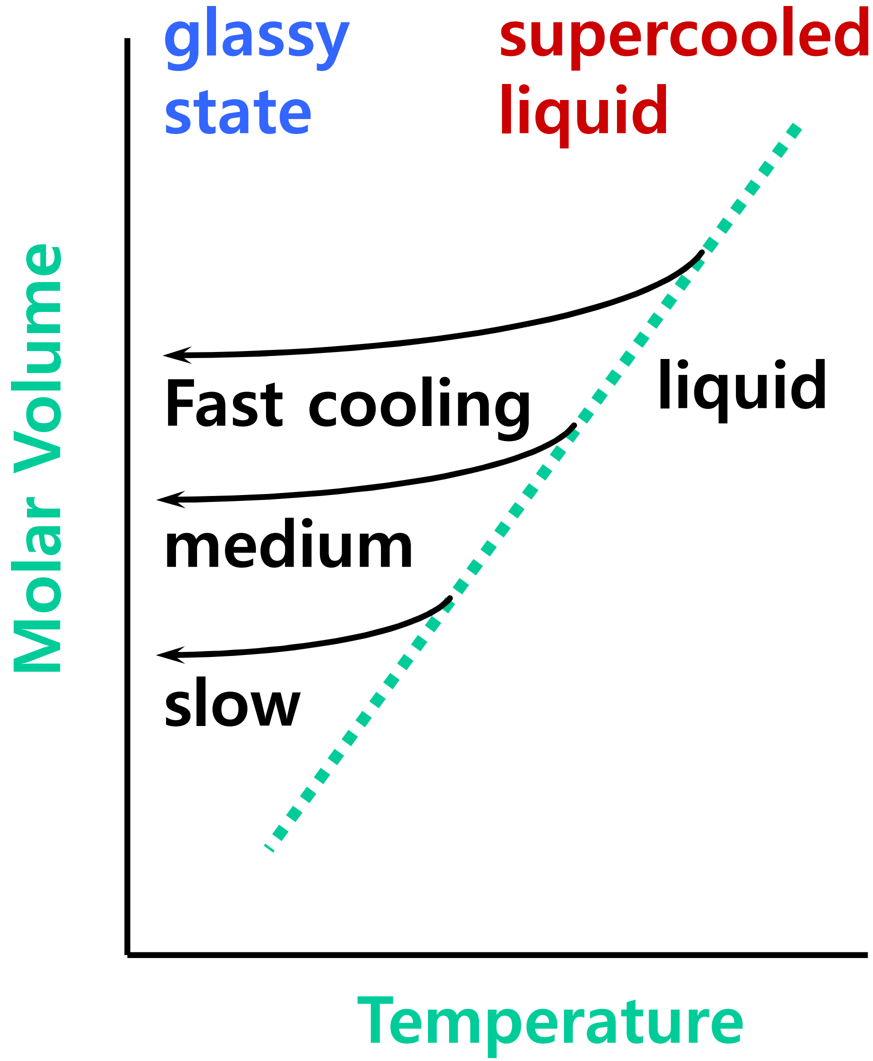

Schematic of the glass transition showing the effects of temperature on free energy

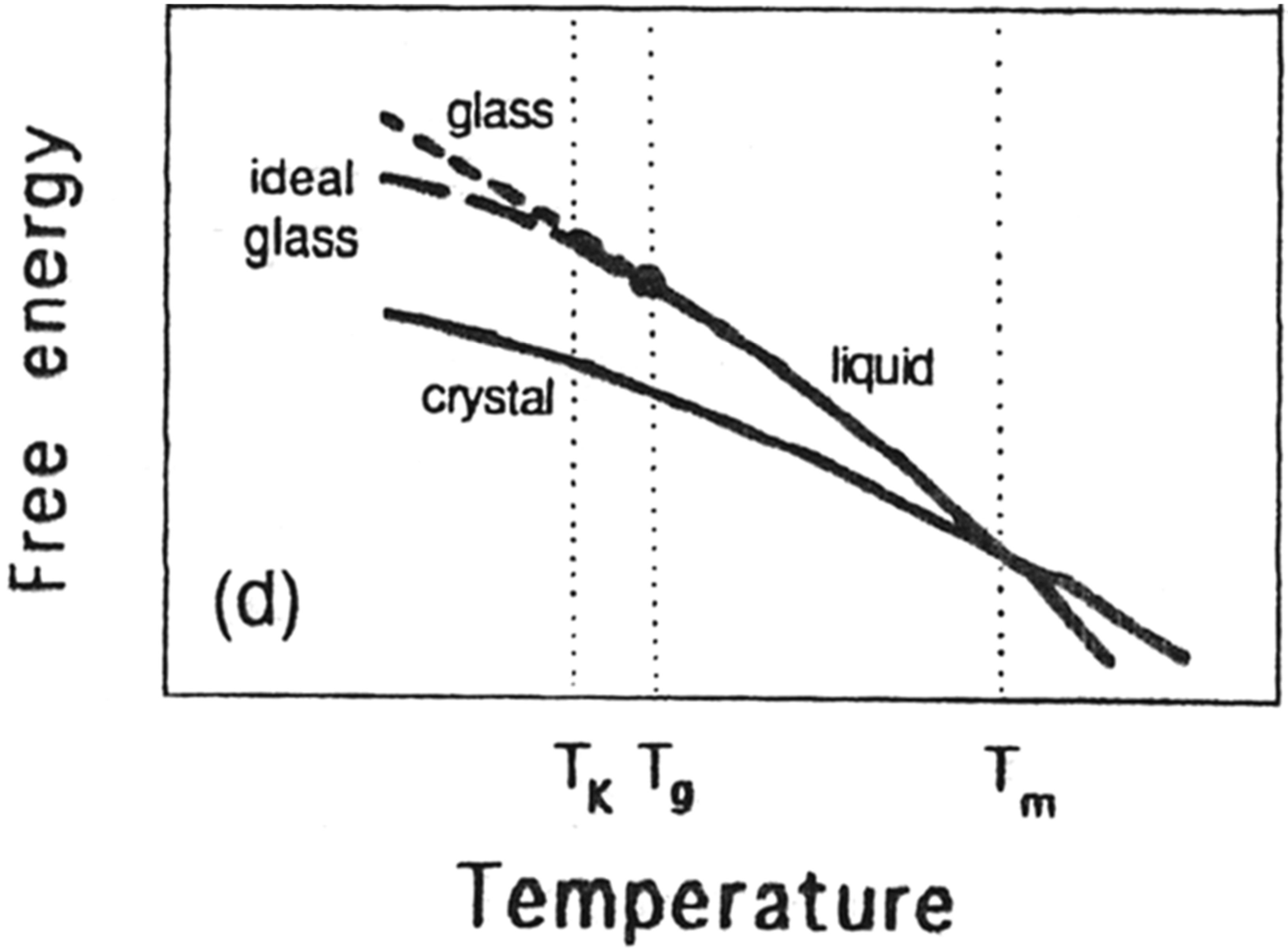

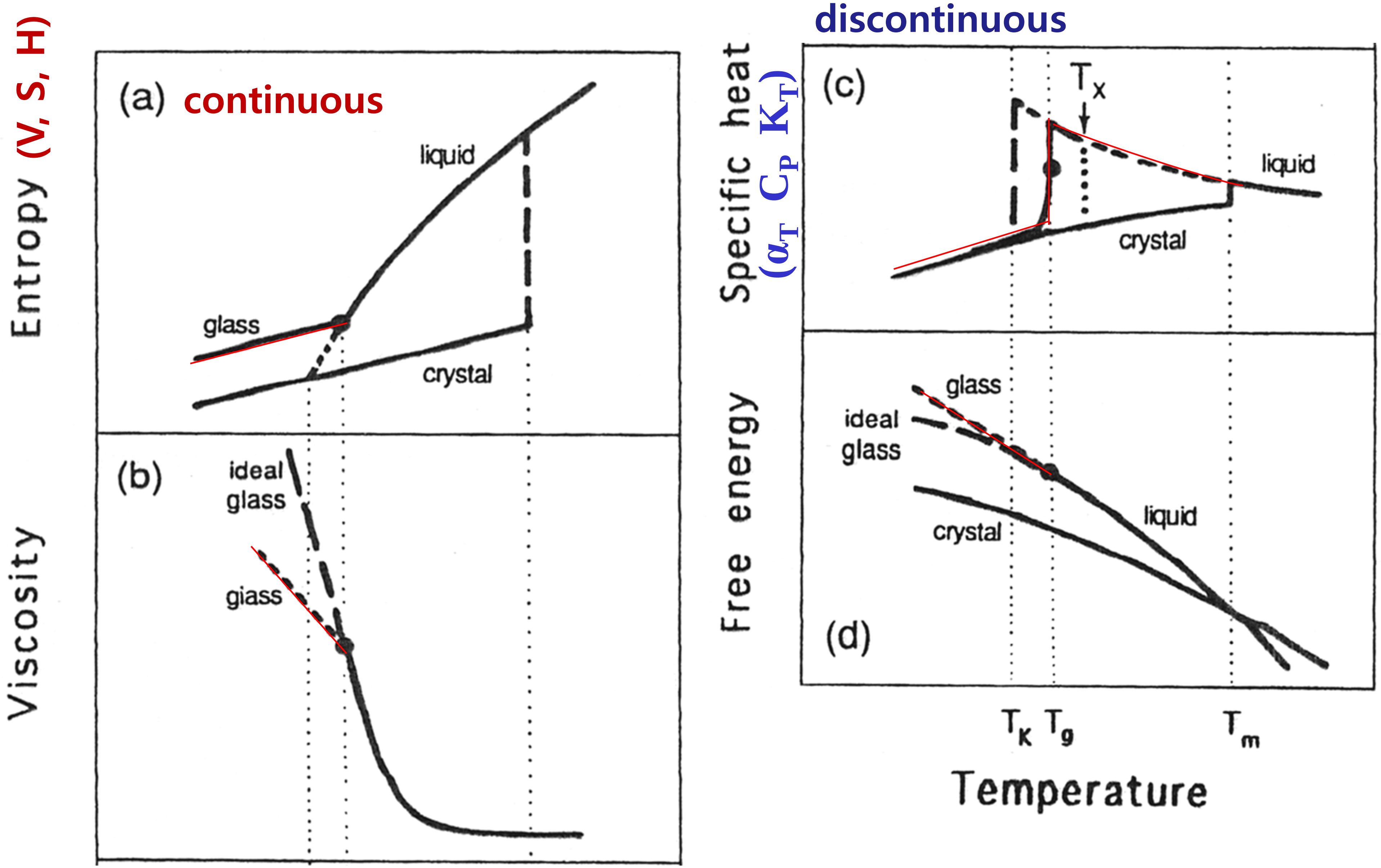

Schematic of the glass transition showing the effects of temperature on the entropy, viscosity, specific heat, and free energy. T_x is the crystallization onset temperature.

Glass formation : (1) Fast Cooling

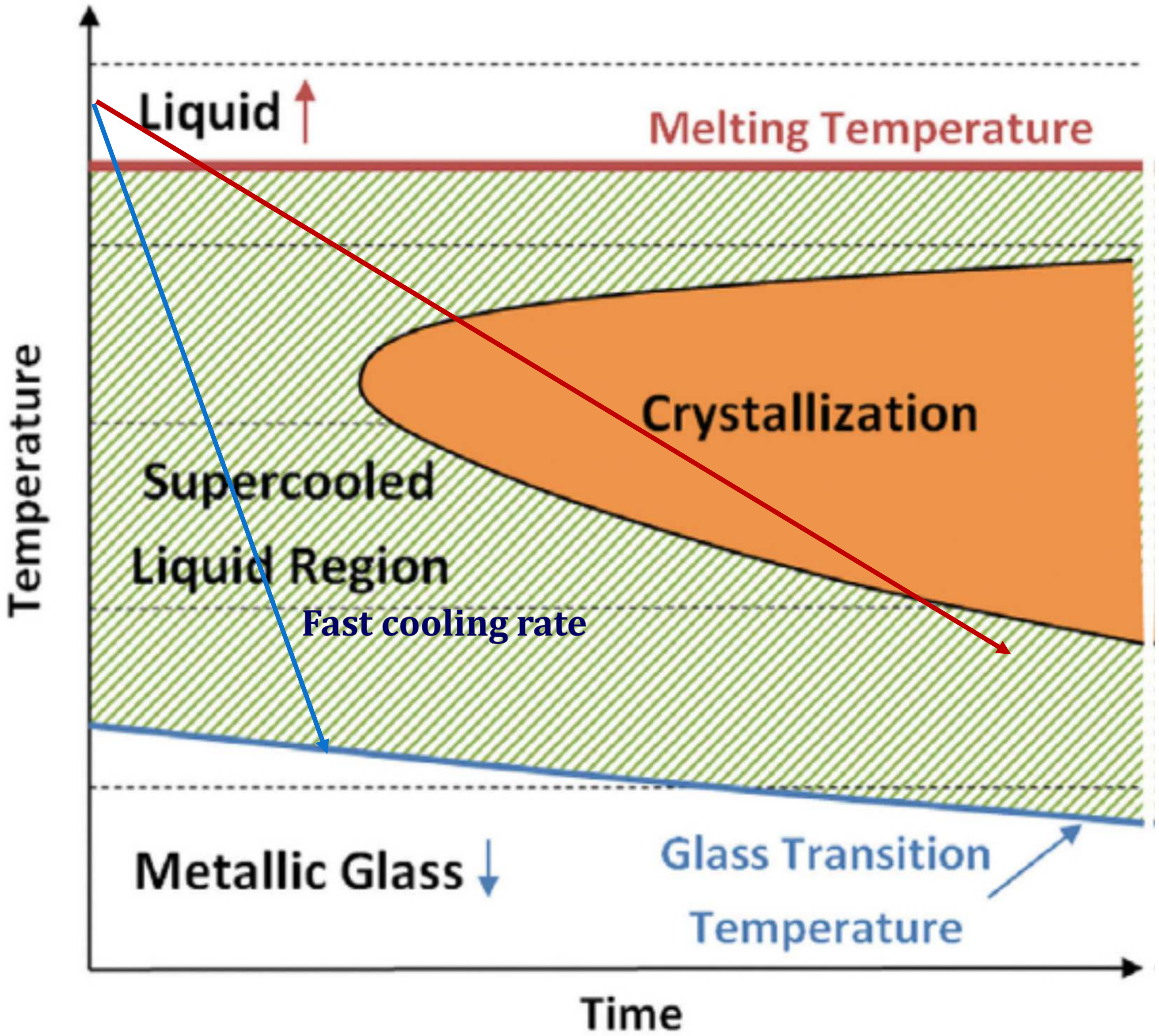

Glass formation : (2) Better Glass Former

GFA $R_c = \frac{\Delta T}{t_n}$ undercooled liquid → crystalline

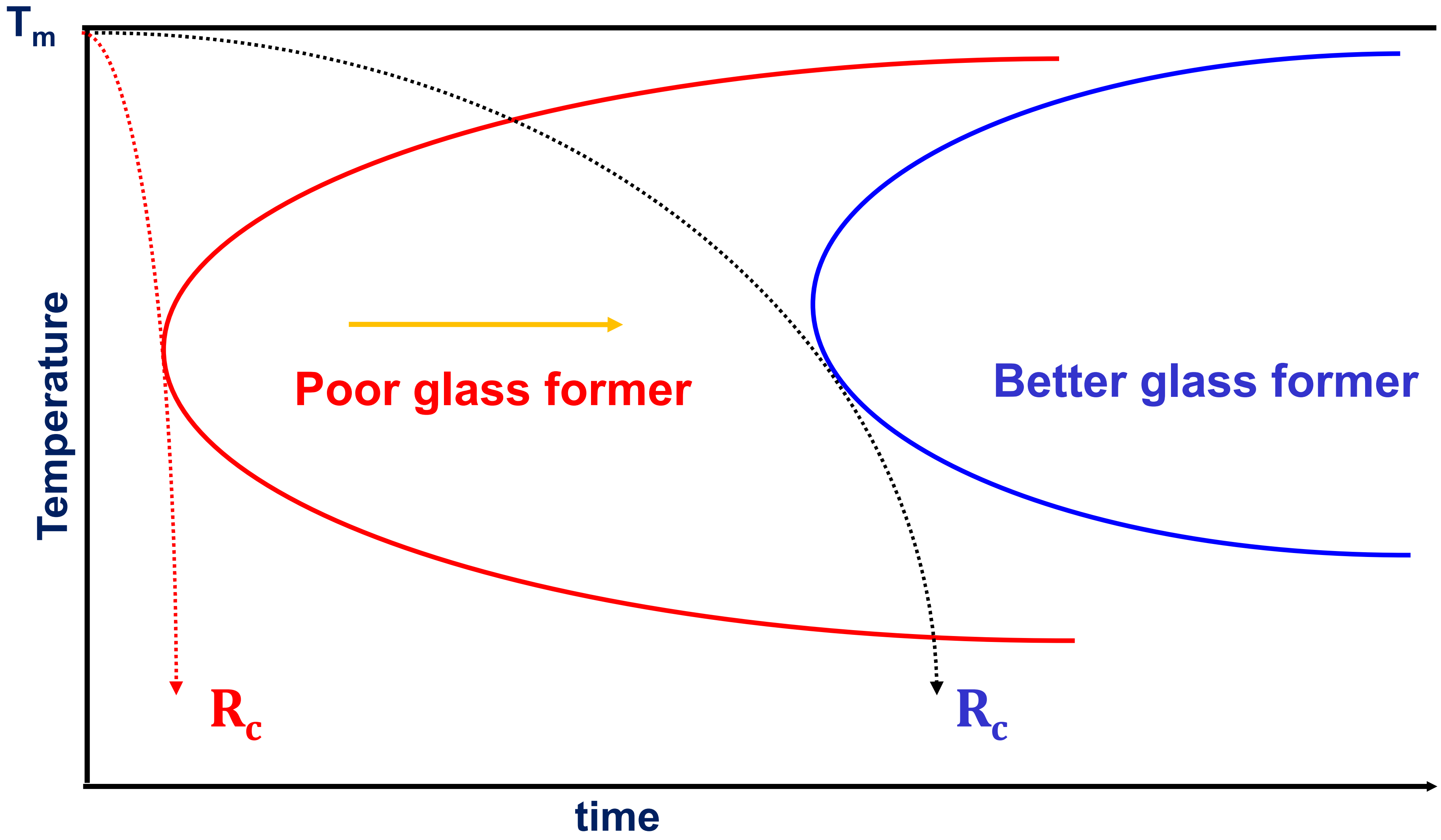

Glass formation : stabilizing the liquid phase

- First metallic glass ($Au_{80}Si_{20}$) produced by splat quenching at Caltech by Pol Duwez in 1960.

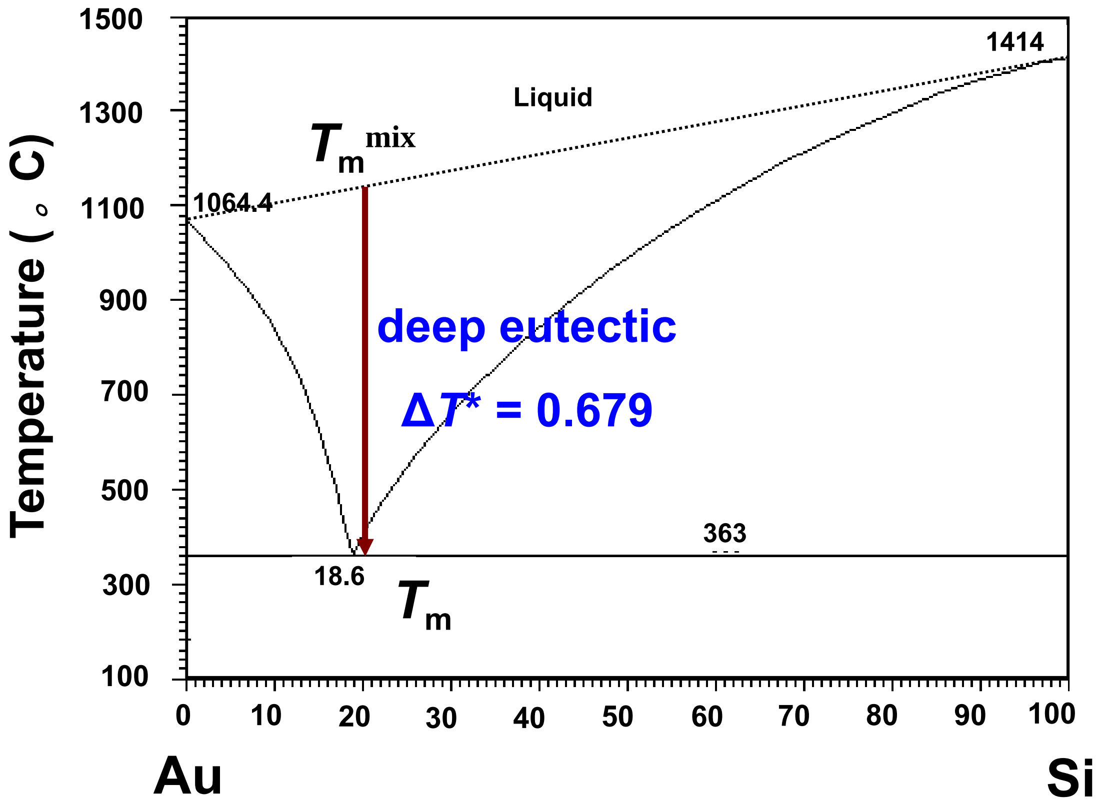

W. Klement, R.H. Willens, P. Duwez, Nature 1960; 187: 869.

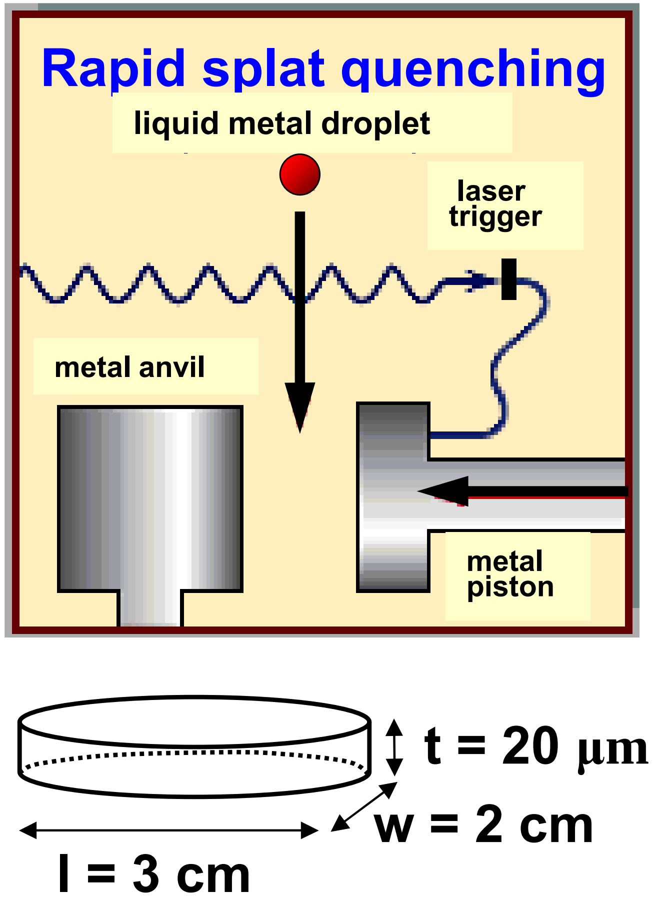

Glass formation: Rapid quenching (~$10^{5\text{-}6}$ K/s) of liquid phase

1969 Ribbon type with long length using melt spinner：FePC, FeNiPB alloy

Recent BMGs with critical size ≥ 10 mm

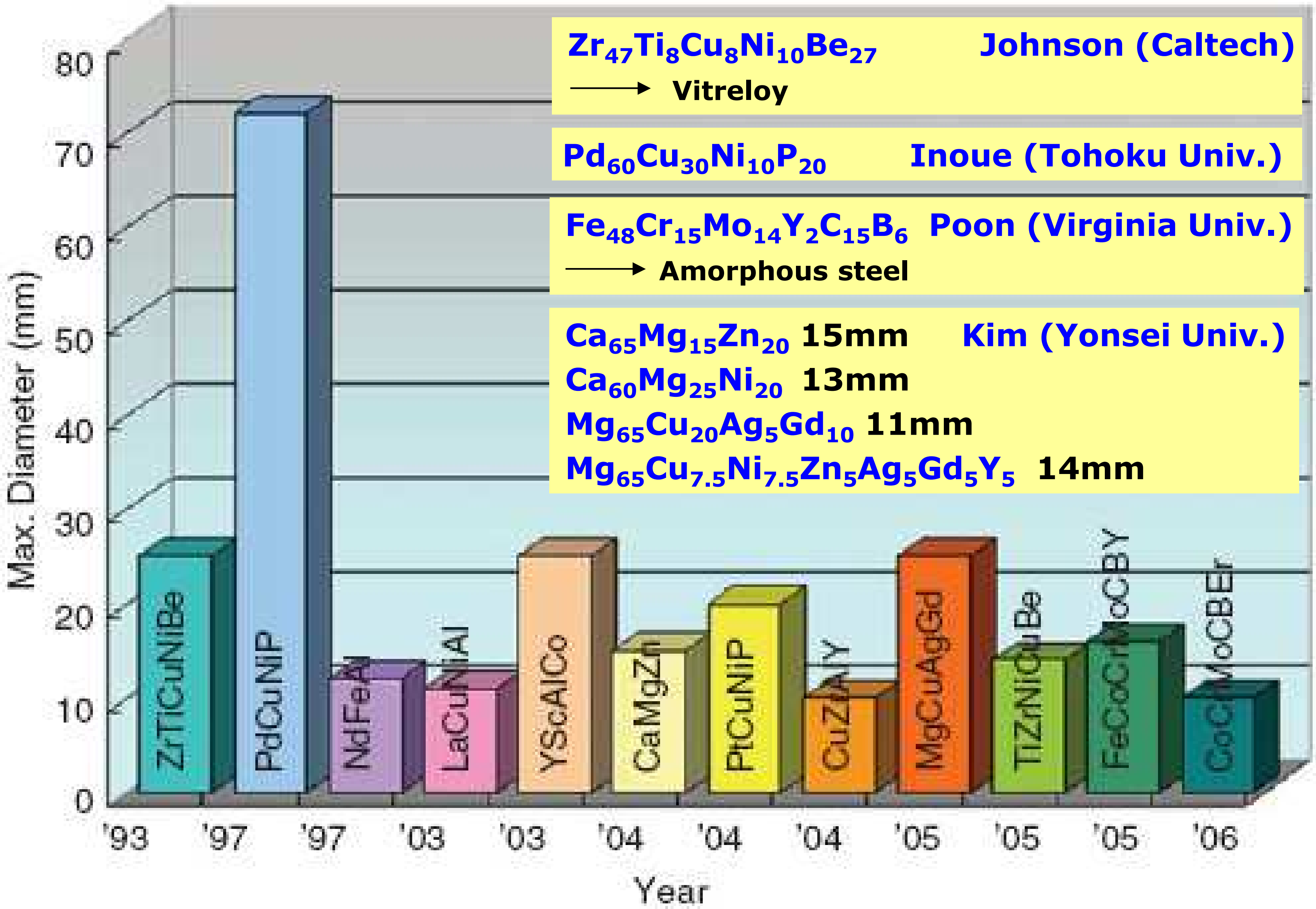

A.L. Greer, E. Ma, MRS Bulletin, 2007; 32: 612.

Bulk glass formation in the Pd-/Ni-/Cu-/Zr- element system

Massy Ingot Shape

(a) Pd-Cu-Ni-P

72ϕx 75 mm 80ϕx 85 mm

(b) Zr-Al-Ni-Cu

(c) Cu-Zr-Al-Ag

(d) Ni-Pd-P-B

Cylindrical Rods

(e) Pd-Cu-Ni-P

(f) Pt-Pd-Cu-P

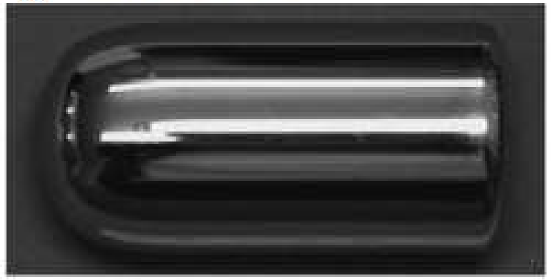

Hollow Pipes

(g) Pd-Cu-Ni-P

Recent BMGs with critical size ≥ 10 mm

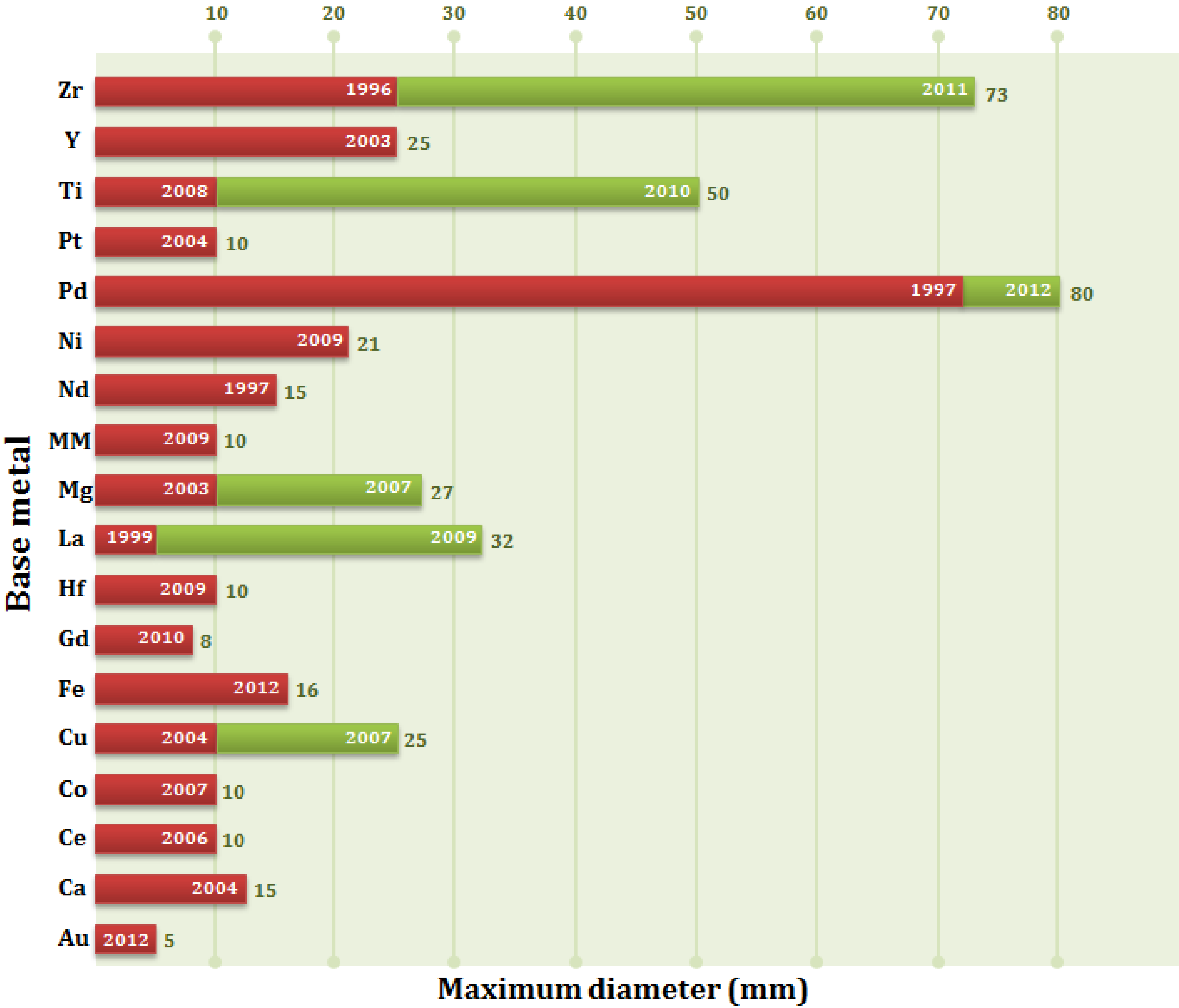

Q: BMG = The 3^{rd} Revolution in Materials?

The 3rd Revolution in Materials

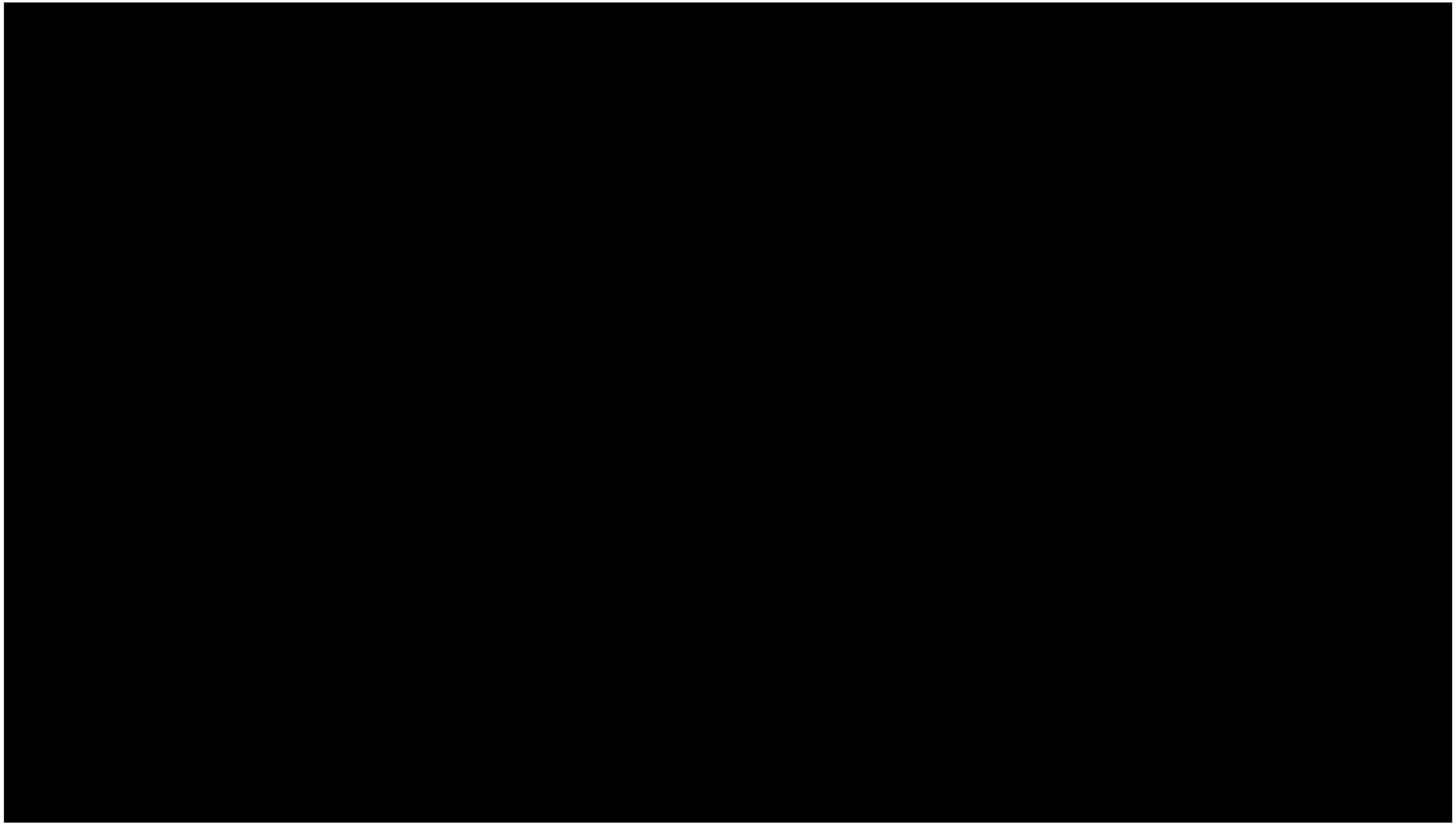

1. High strength of BMGs

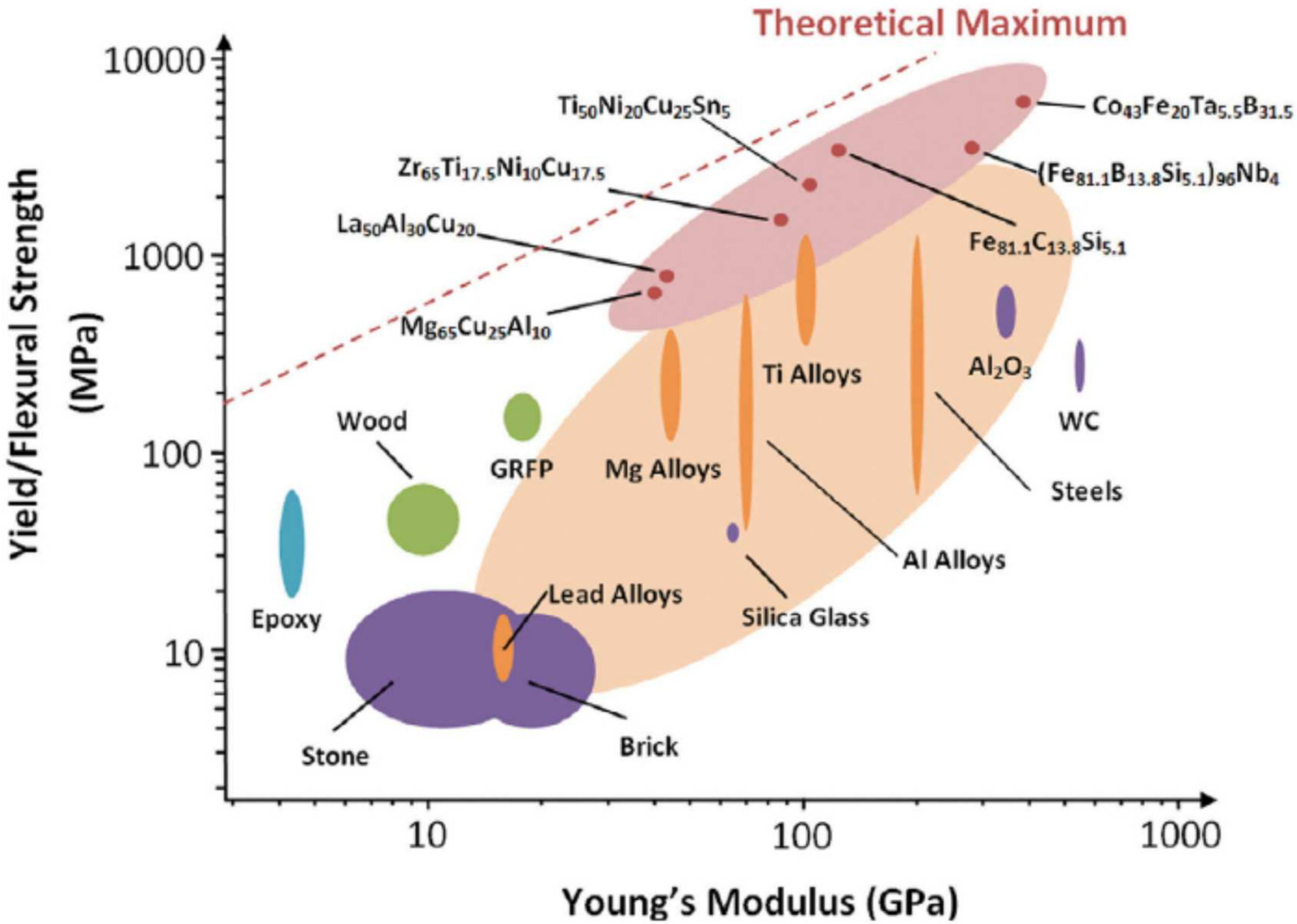

High fracture strength over 5 GPa in Fe-based BMGs

A.L. Greer, E. Ma, MRS Bulletin, 2007; 32: 612.

2. Large elastic strain limit of BMGs

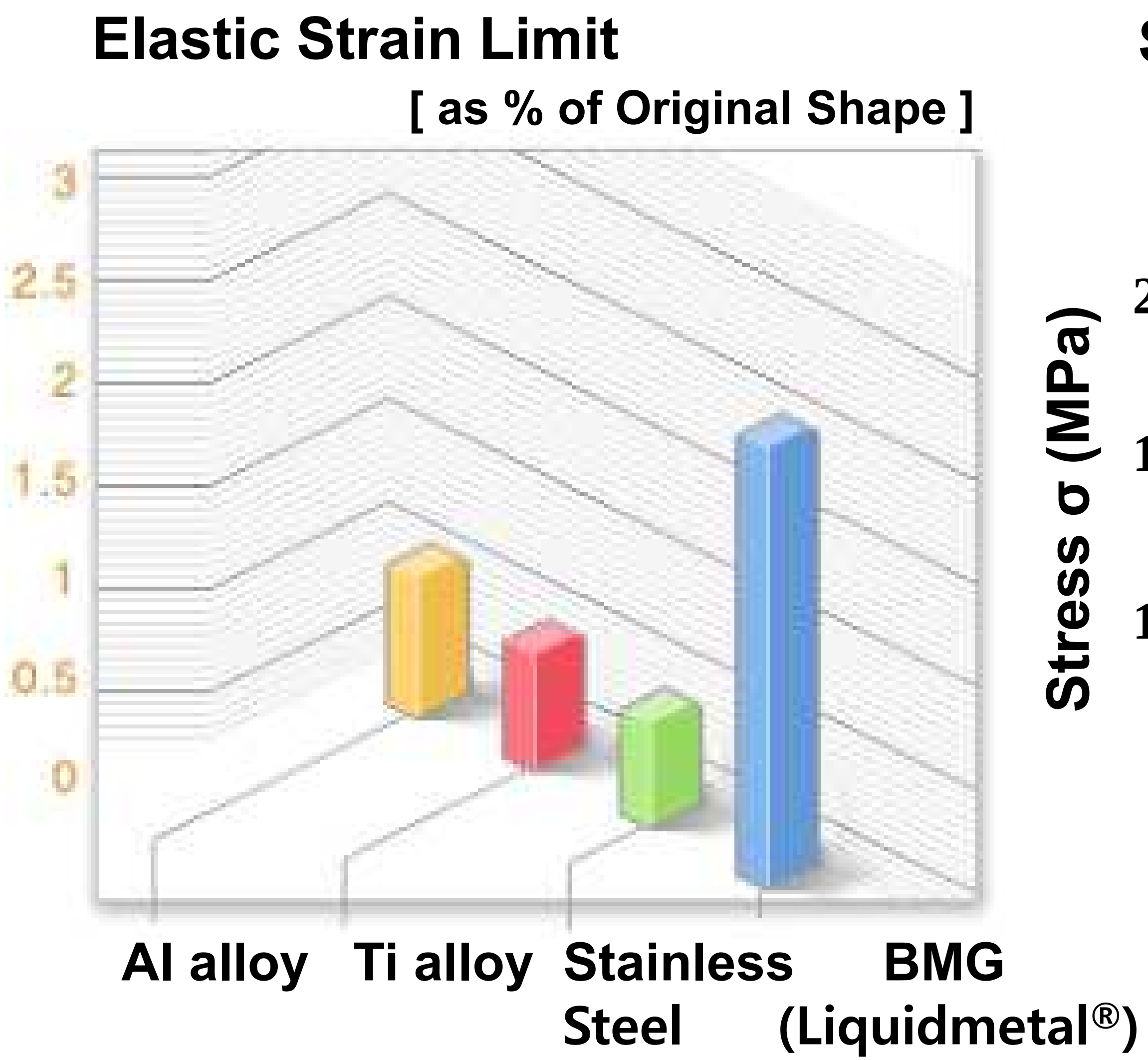

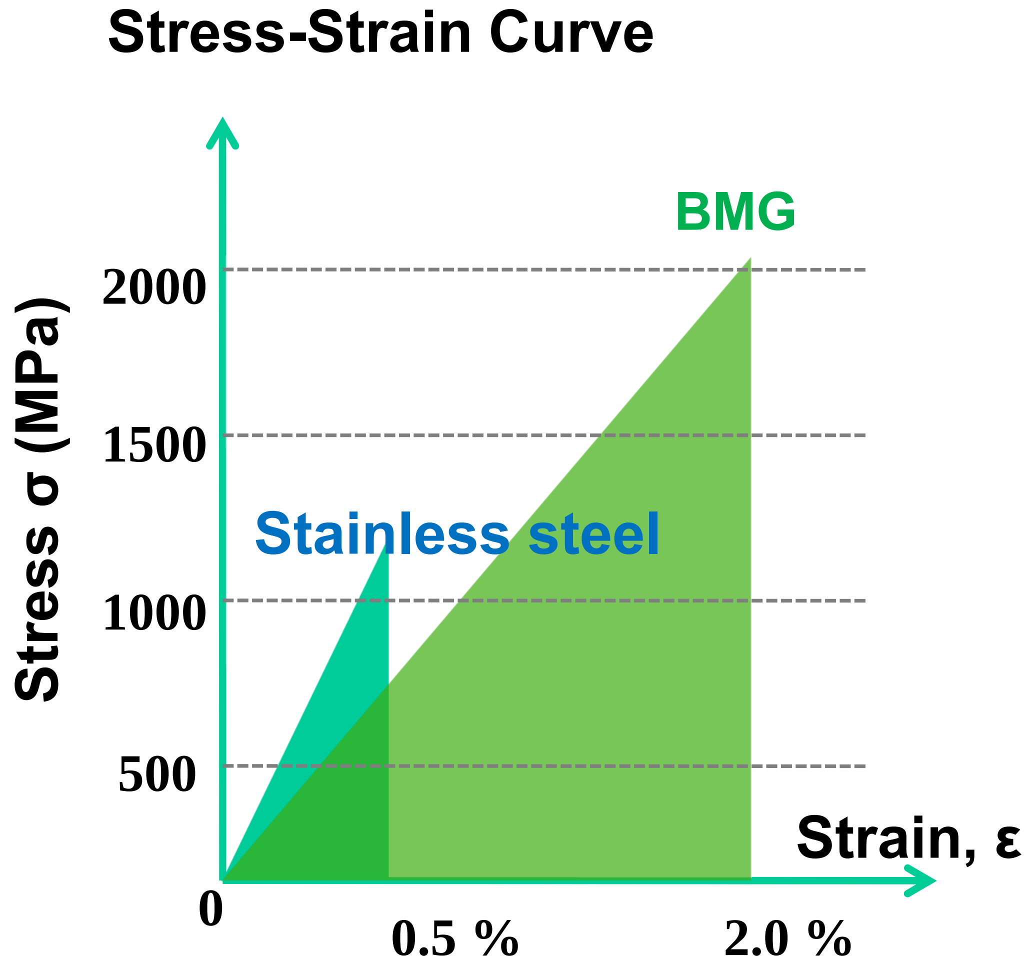

2. Large elastic strain limit of BMGs

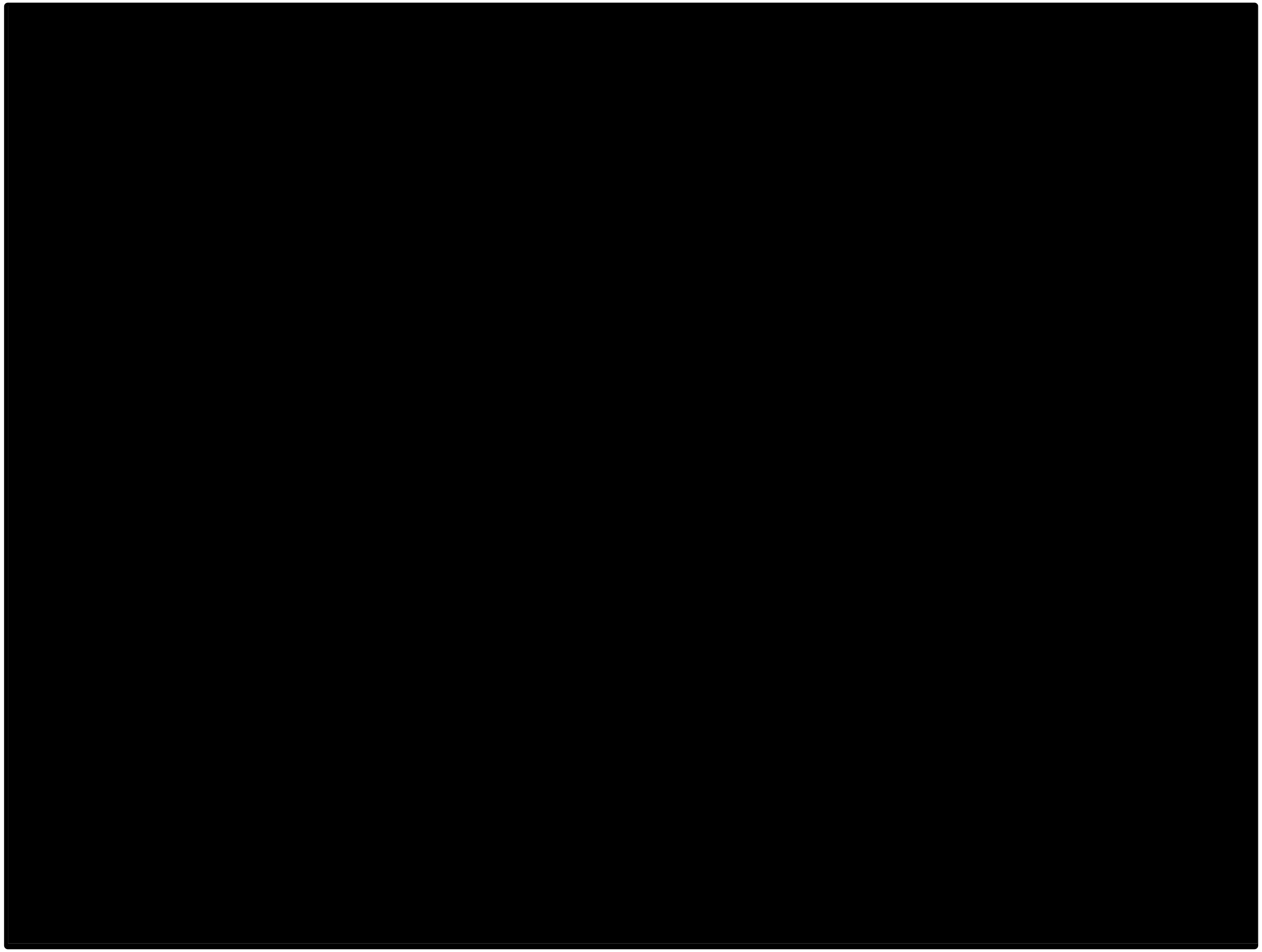

Metallic Glasses Offer

a Unique Combination of “High Strength” and “High Elastic Limit”

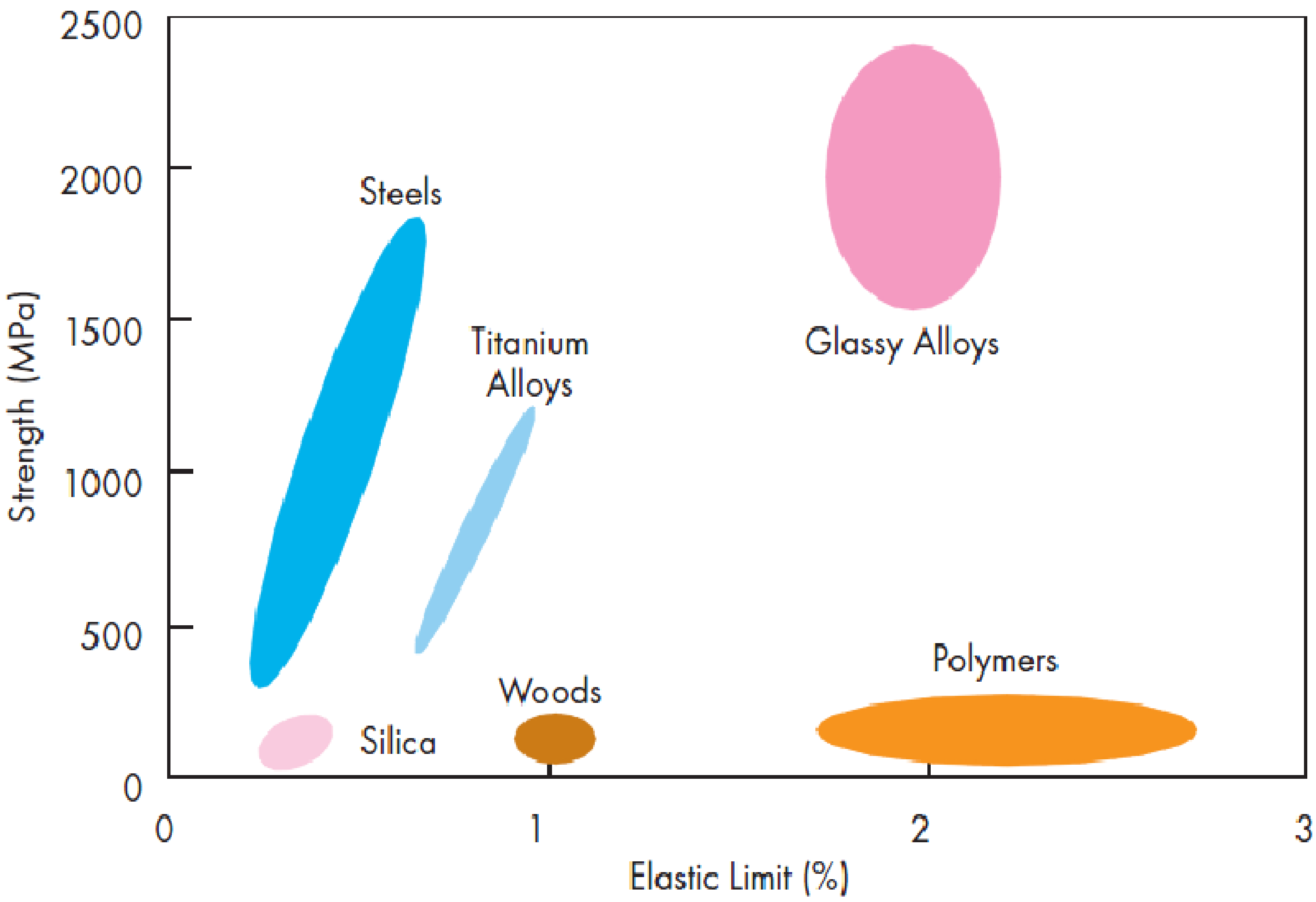

3. Processing metals as efficiently as plastics

* Thermoplastic forming in SCLR

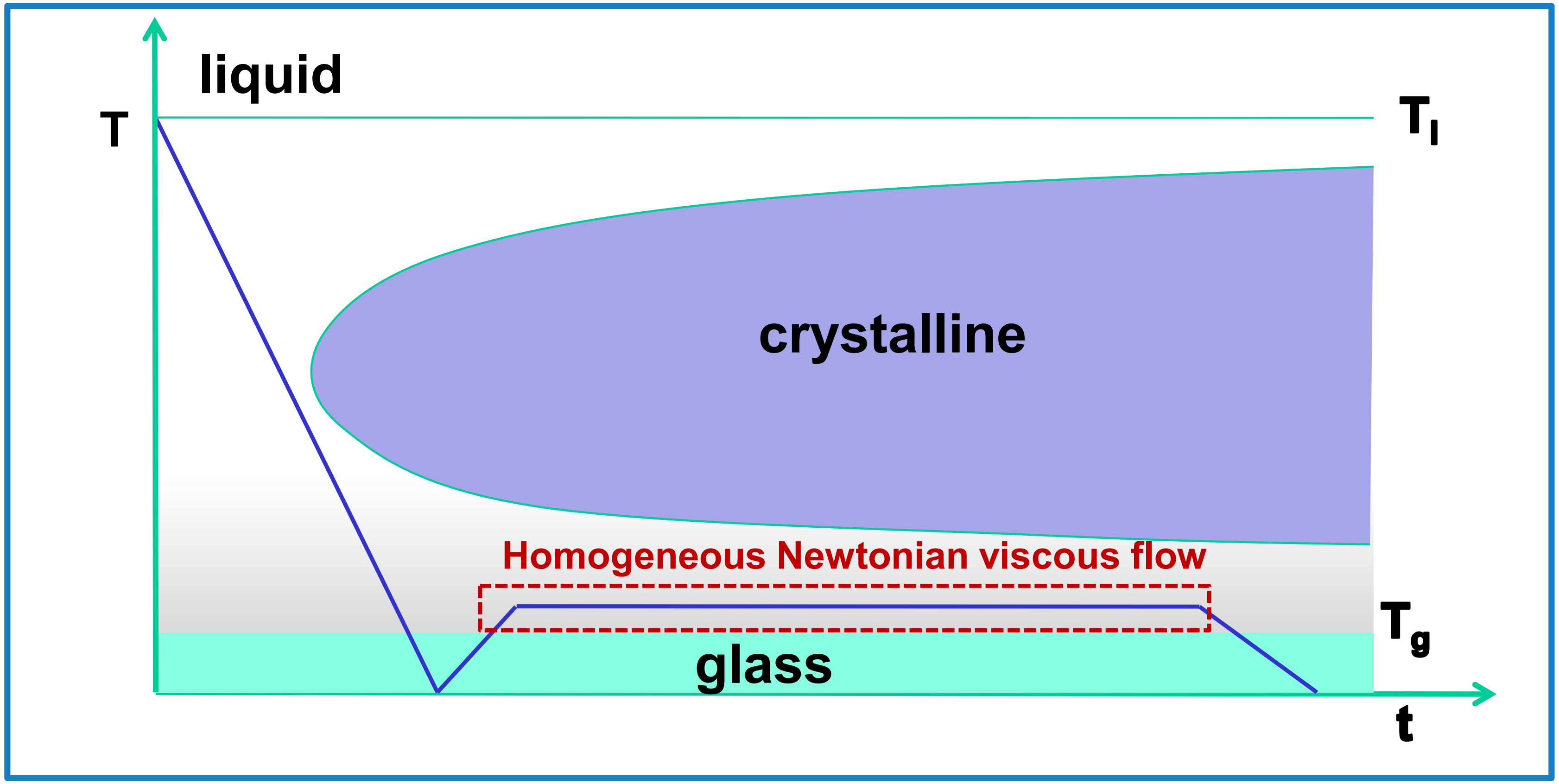

Metallic glass can be processed like plastics by homogeneous Newtonian viscous flow in supercooled liquid region (SCLR).

➡ **Possible to deform thin and uniform in SCLR**

3. Processing metals as efficiently as plastics

(a) Micro-casting

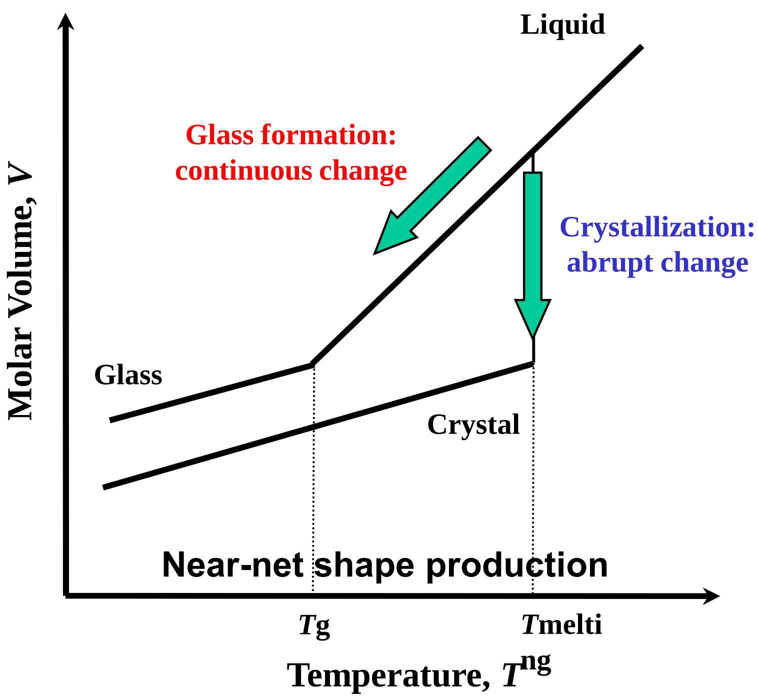

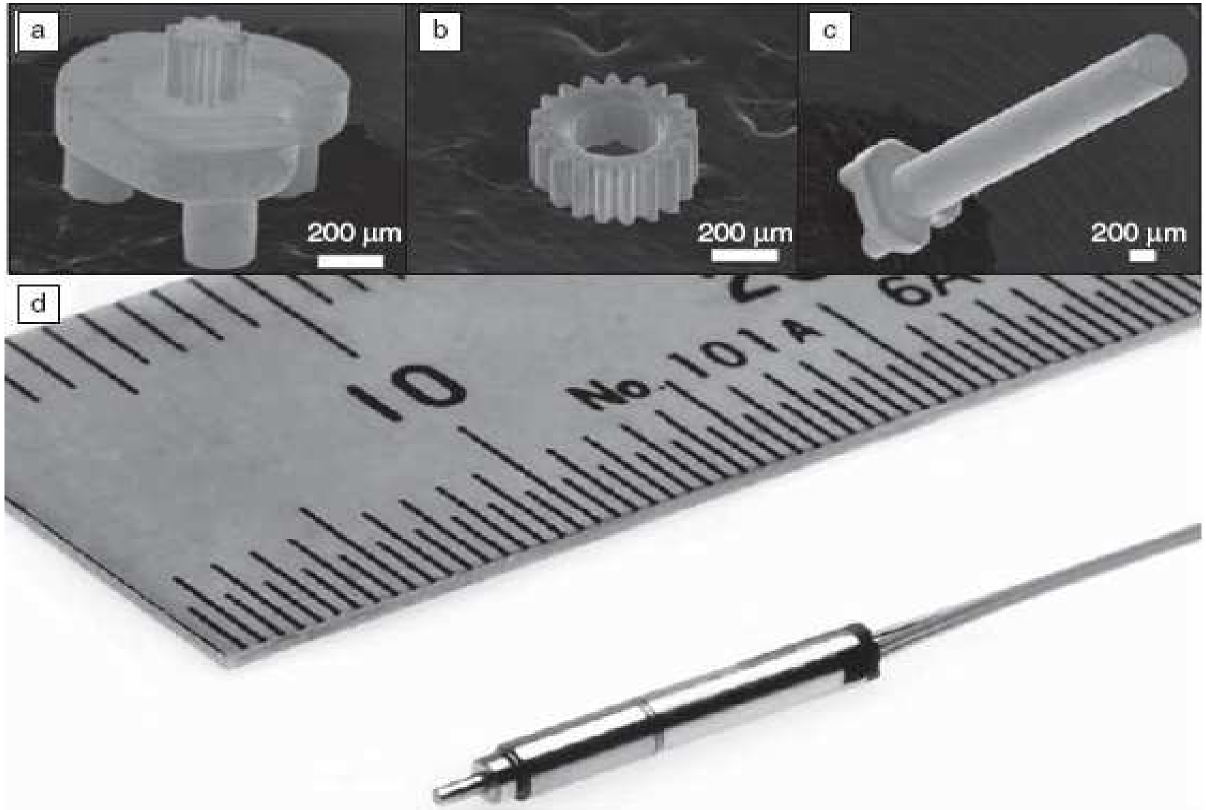

Precision Gears for Micro-motors

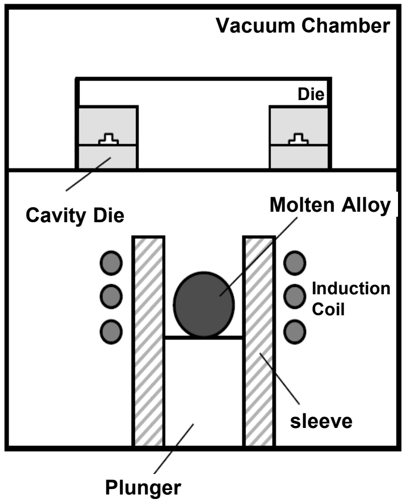

Precision die casting

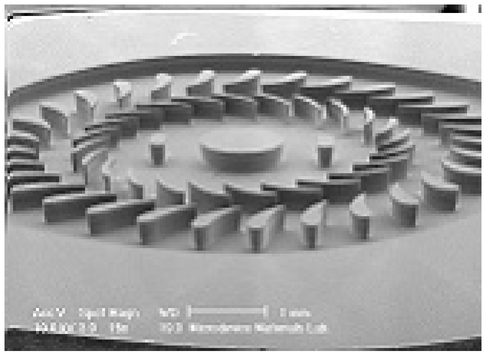

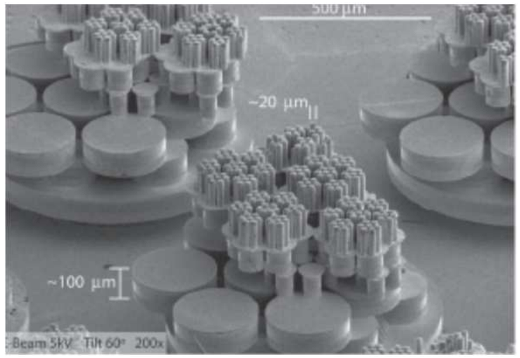

MRS BULLETIN ***32*** *(2007)654.*

3. Processing metals as efficiently as plastics

(b) Micro-forming

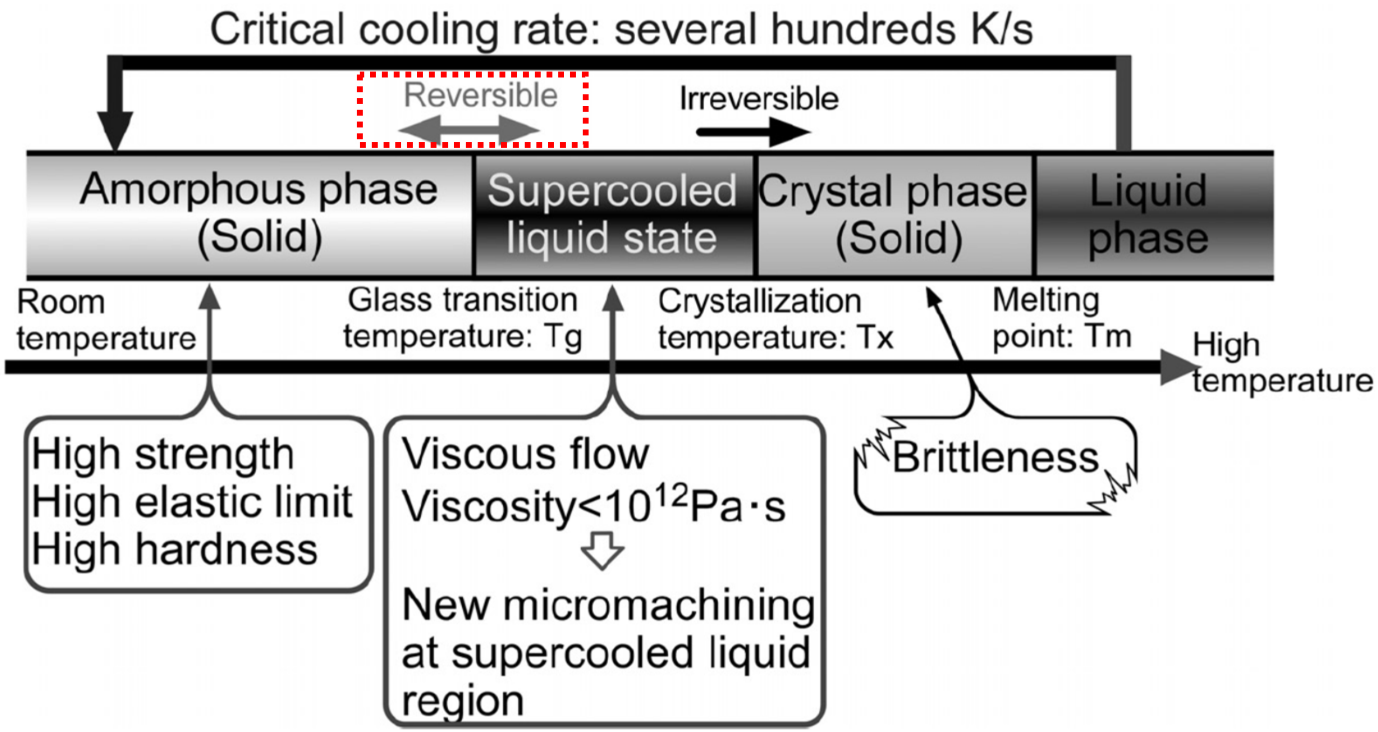

Micro-forming of three-dimensional microstructures from thin-film metallic glass

Micro-cantilever

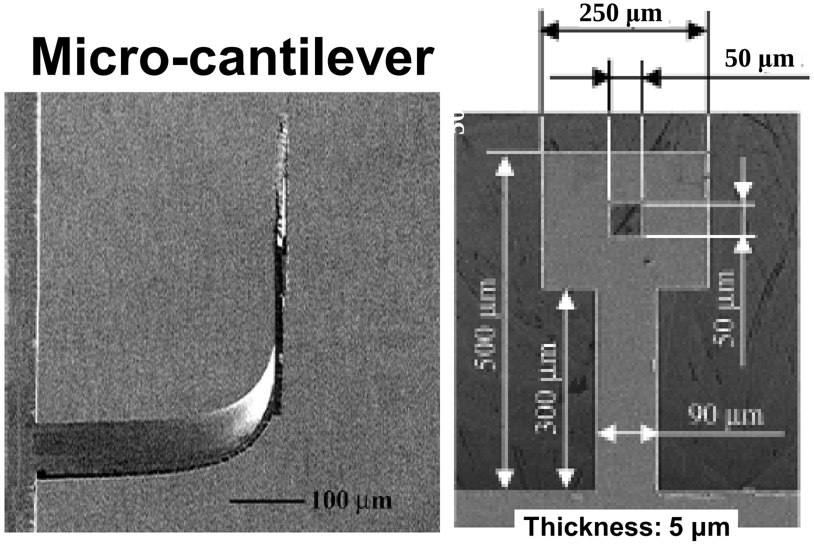

Integrated conical spring linear actuator

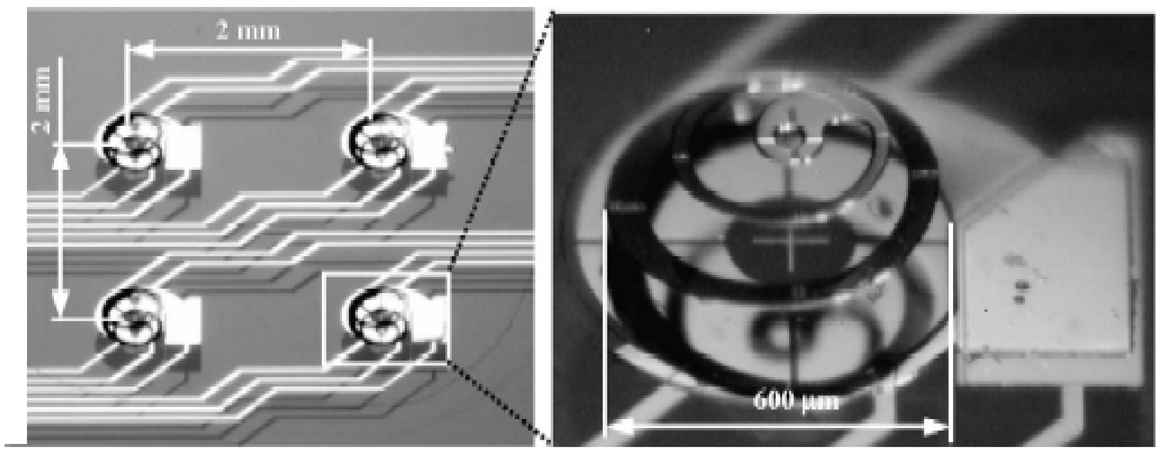

3. Processing metals as efficiently as plastics

* Thermoplastic forming in SCLR

$Mg_{65}Cu_{25}Gd_{10}$ metallic glass ribbon

‣ Drawing sample at 220°C ➡ Elongation over 1100%

3. Processing metals as efficiently as plastics

Seamaster Planet Ocean Liquidmetal® Limited Edition

- Superior thermo-plastic formability

  : possible to fabricate complex structure without joints

  ↳ **Multistep processing can be solved by simple casting**

  ↳ **Ideal for small expensive IT equipment manufacturing**

Materials Views
www.MaterialsViews.com

ADVANCED MATERIALS
www.advmat.de

Processing of Bulk Metallic Glass

Adv. Mater. **2009**, *21*, 1–32

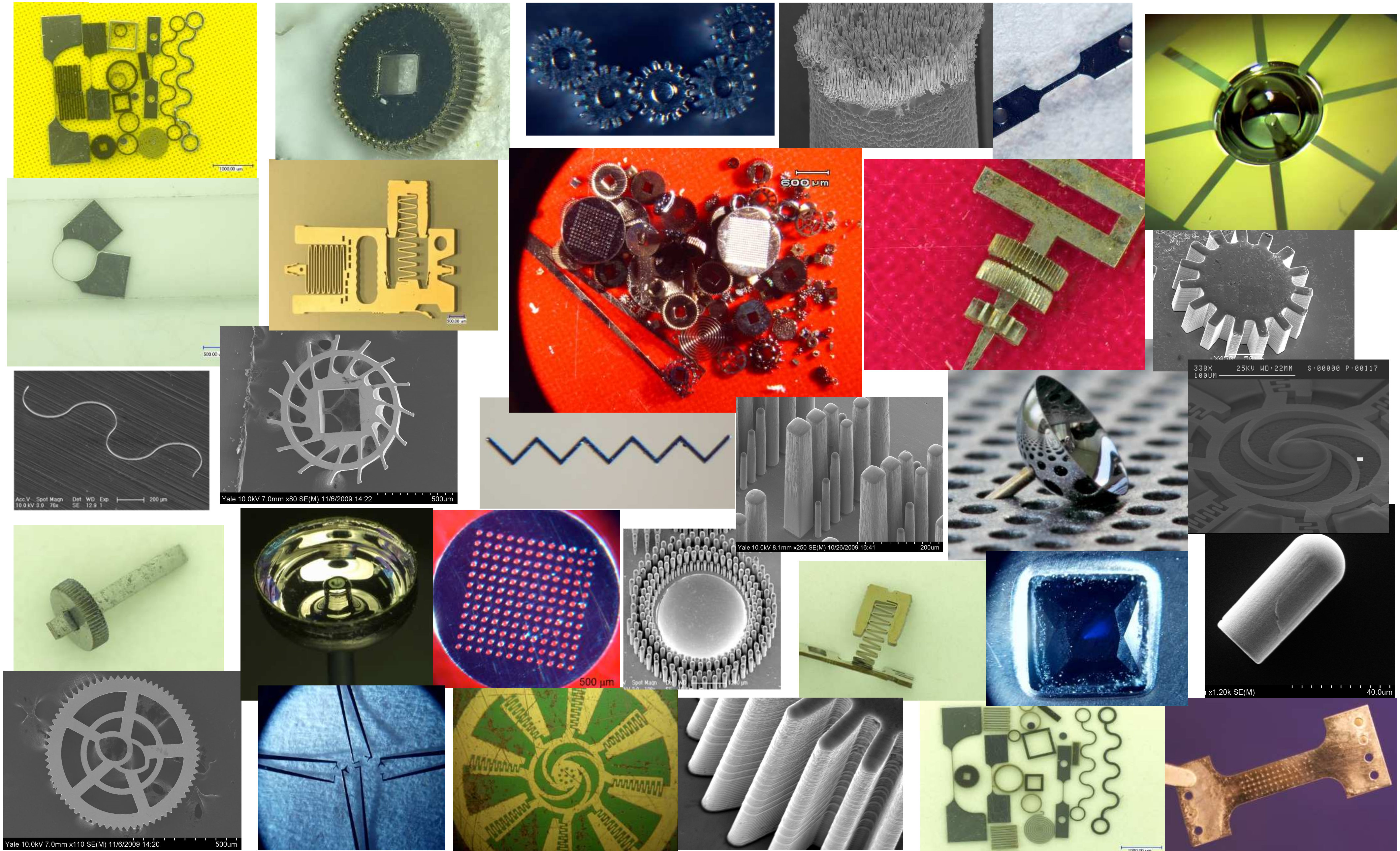

"Yale professor makes the case for Supercool Metals"

According to Yale researcher Jan Schroers, This material is 50 times harder than plastic, nearly 10 times harder than aluminum and almost three times the hardness of steel."

Apple buys exclusive right for Liquidmetal

Apple is using Liquidmetal for…

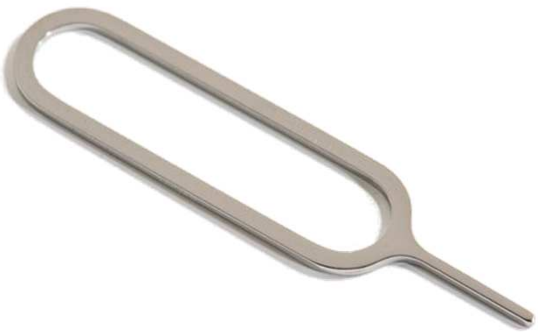

USIM ejector (iphone 4)

Enclosure / Antenna

Apple continuing work on Liquidmetal casting techniques…

October 29, 2015

Two New Liquid Metal Inventions Published Today Cover Every Current Apple Product and even Complete Car Panels

Liquidmetal™ in NEXT iPhone?

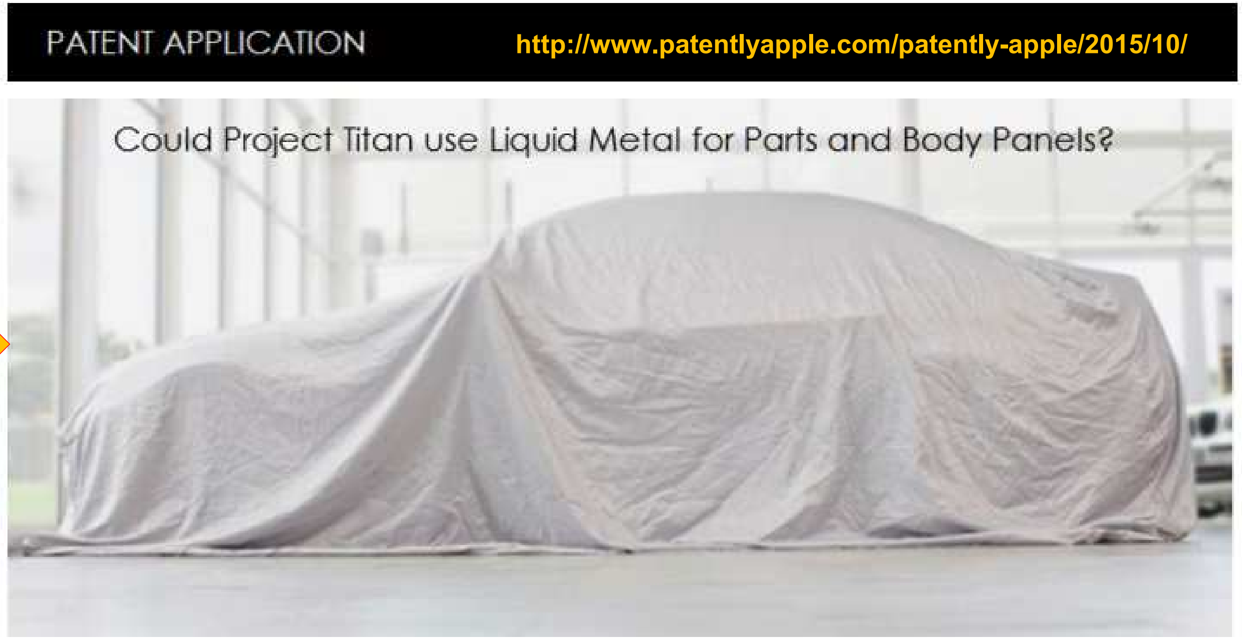

Apple's patents cover the use of liquid metal in <u>every imaginable Apple product</u> and even hints that the process described in these inventions could produce complete car panels. That makes you wonder if Apple's Project Titan will be able to take advantage of the liquid metal process for car parts and beyond.

First smart phone with BMG exterior

Turing phone
by Turing Robotics Industries (UK)

with

Metallic glass "Liquidmorphium™"

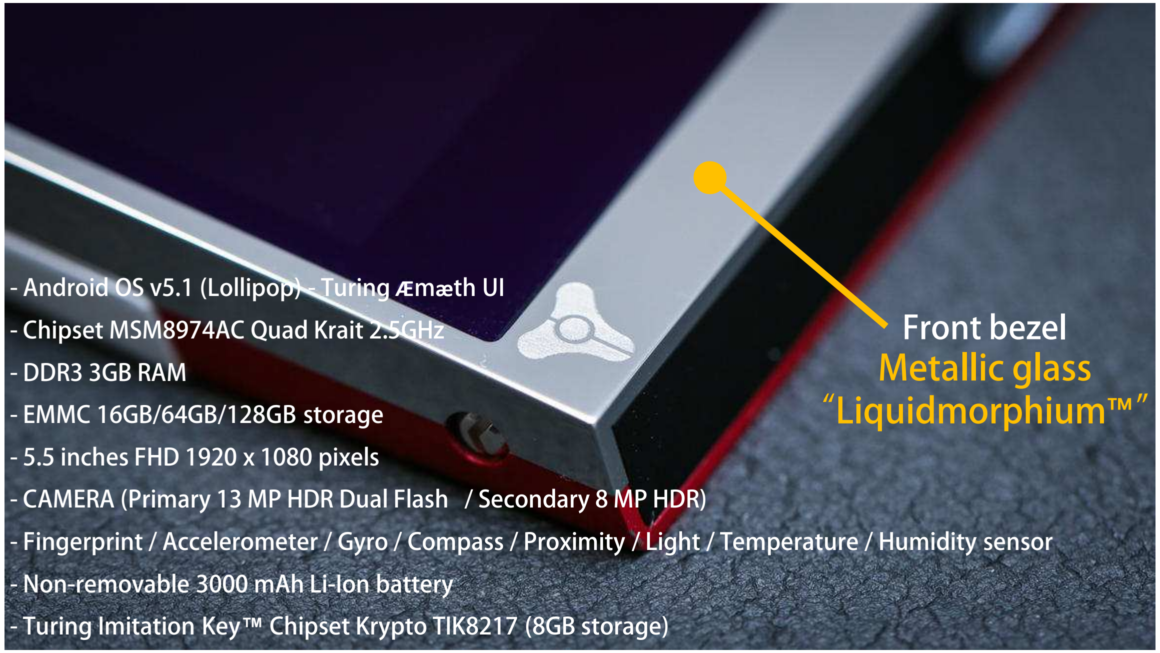

"Unhackable"
"Waterproof"
+
"Unbreakable"

The Turing Phone is built with a pioneering material called Liquidmorphium™, an amorphous "liquid metal" alloy tougher than either titanium or steel - so what's in your hand is as strong as your privacy protection.

from https://www.turingphone.com/

A new menu of engineering materials

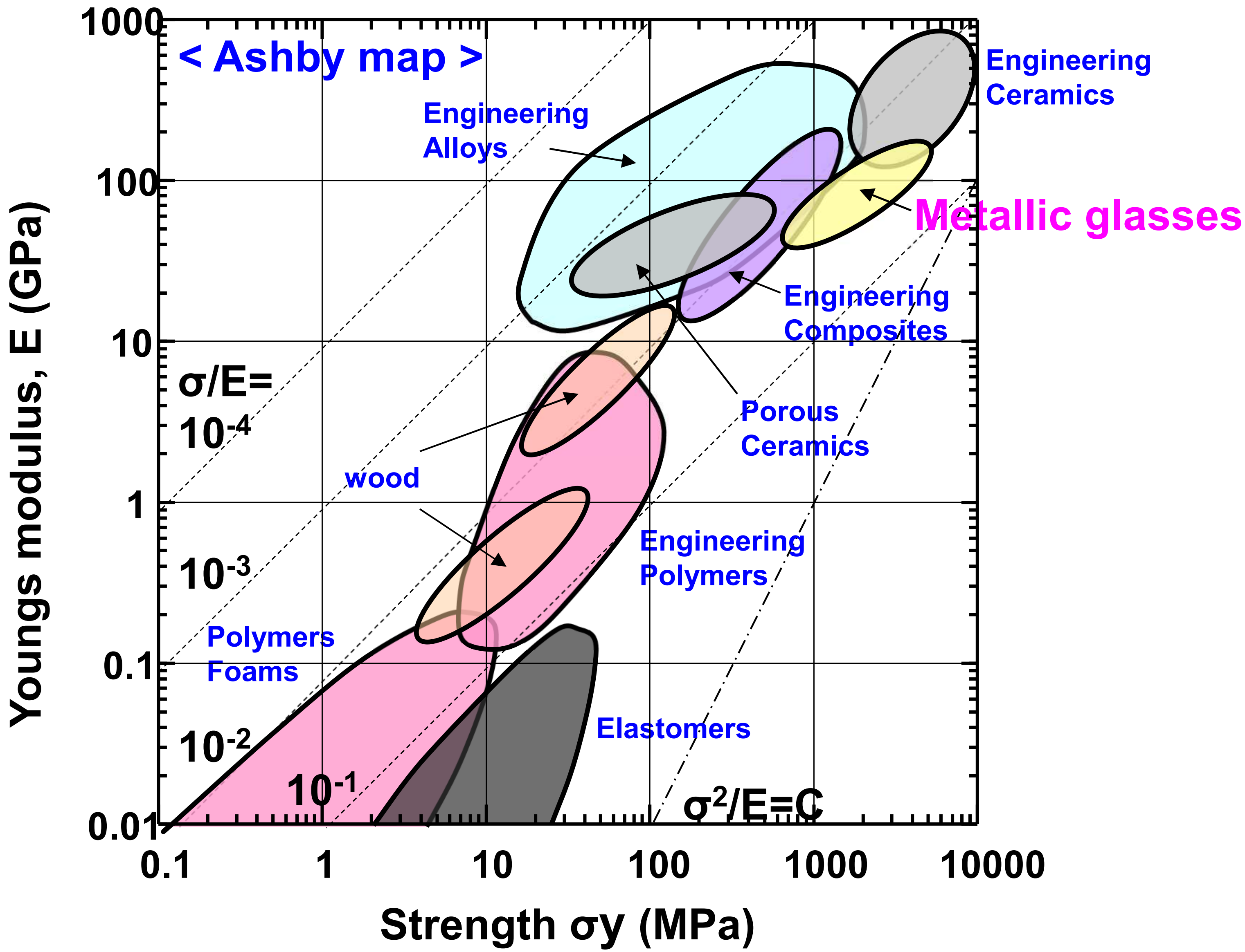

A new menu of engineering materials

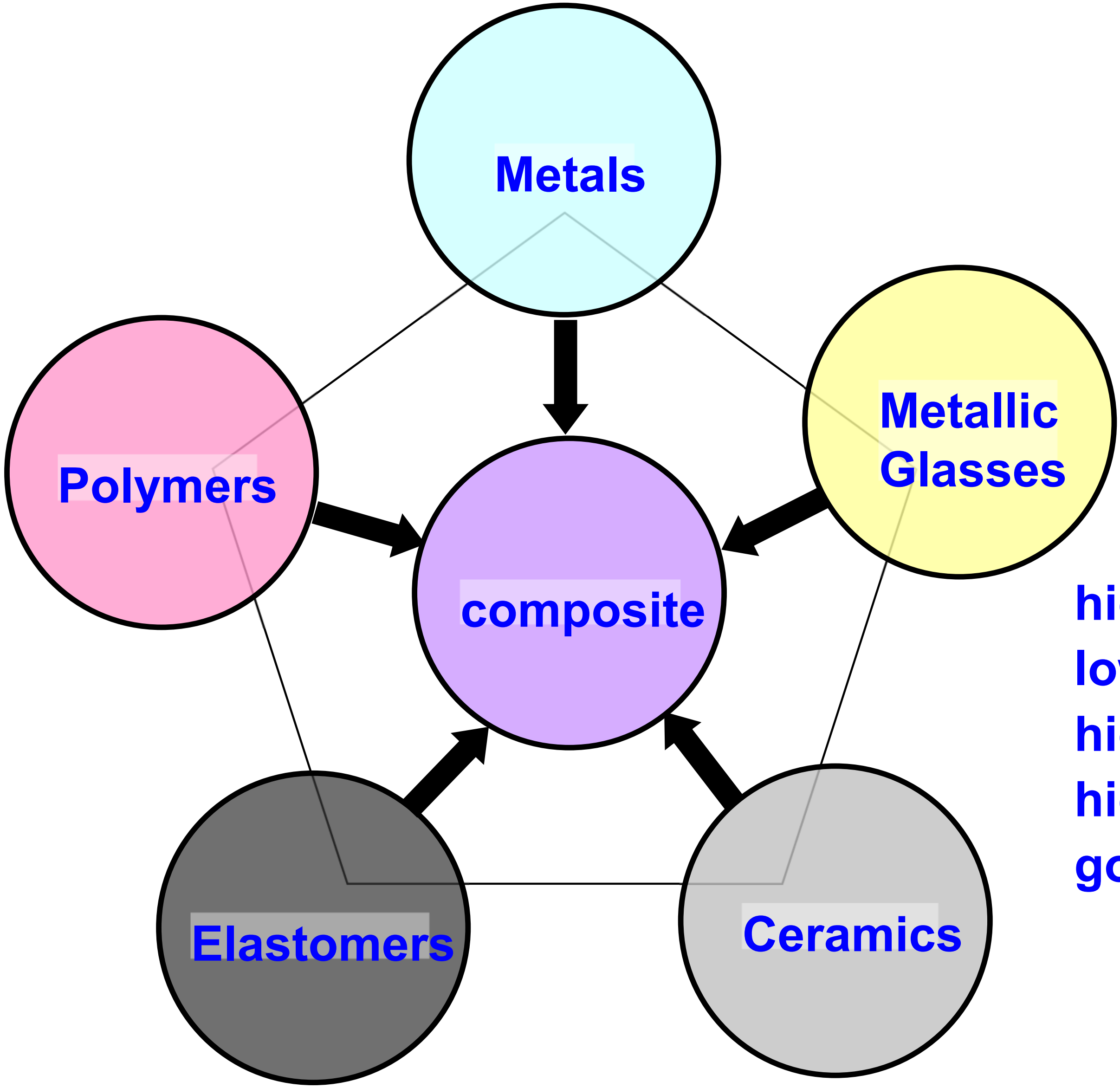

High GFA

High plasticity

higher strength
lower Young's modulus
high hardness
high corrosion resistance
good deformability
⋮

nature materials

NATURE MATERIALS | INTERVIEW

Is metallic glass poised to come of age?

Nature Materials **14**, 553–555 (2015) | doi:10.1038/nmat4297

Published online 20 May 2015

There have been a number of attempts to commercialize bulk metallic glass over the past 20 years. William L. Johnson, the Mettler Professor of Materials Science at California Institute of Technology, has been a prominent figure in these efforts and gives *Nature Materials* his perspective on the topic.

Bulk Metallic Glass_"초소형 고품위 부품소재 시장을 두드리다"

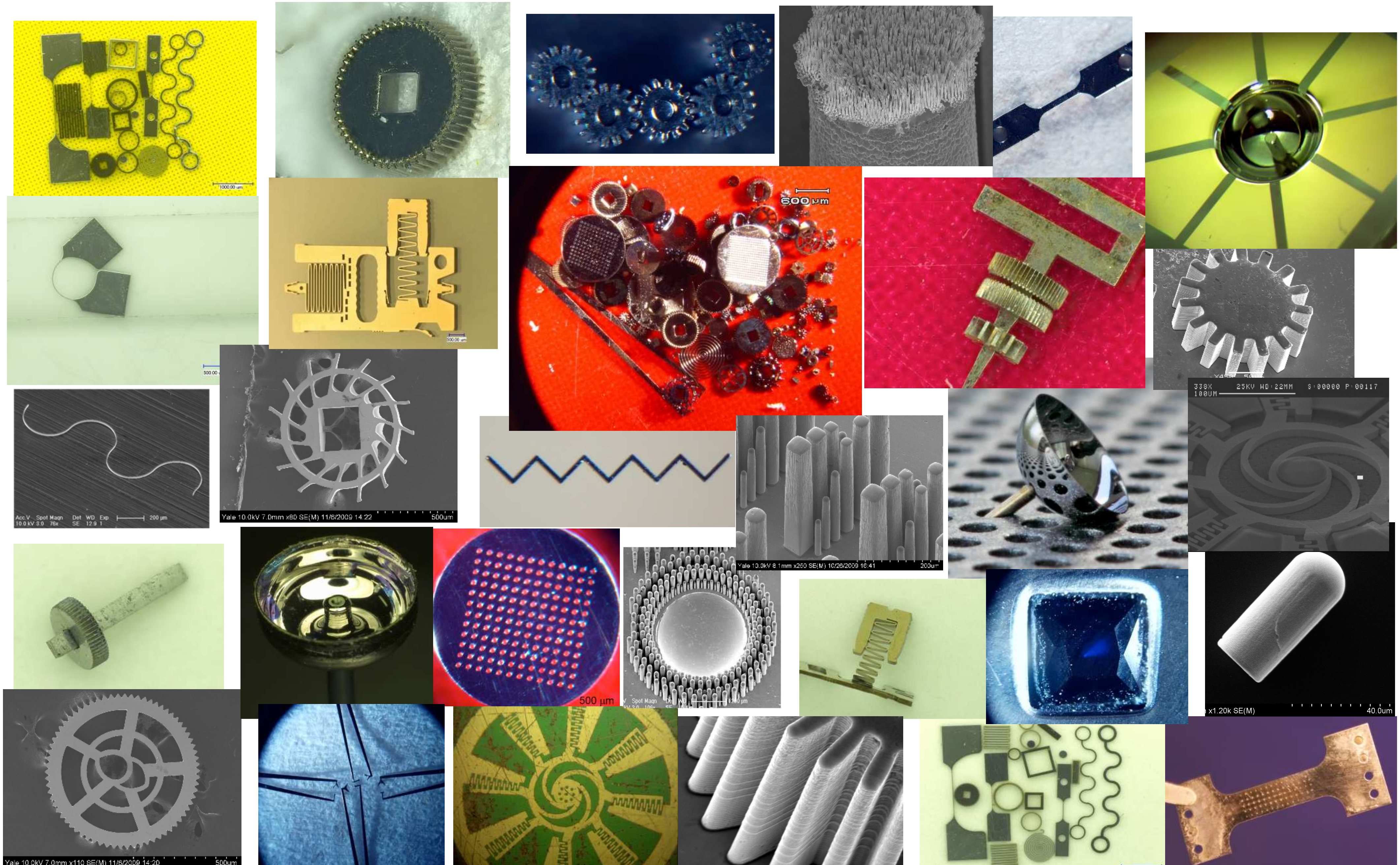

* Homework 4 : Exercises 4 (pages 258-260)

until 27th November

* Homework 5 : 수업시간에 Skip 한 section 4.5와 4.8을 PPT로 요약해서 27일까지 제출하시기 바랍니다. (10 pages 이내)

Good Luck!!